International Max Planck Research School for Maritime Affairs
at the University of Hamburg

Tatjana P. Ilyina

The Fat

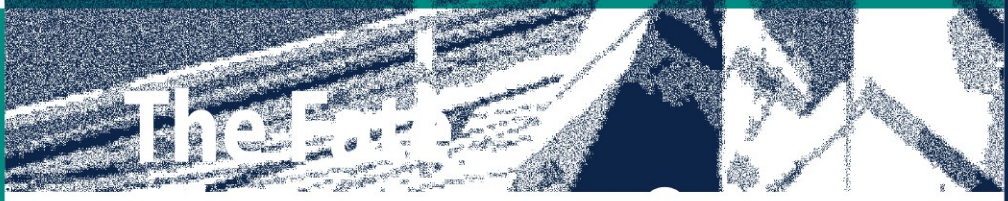

HAMBURG STUDIES ON MARITIME AFFAIRS 7

International Max Planck Research School (IMPRS)
for Maritime Affairs
at the University of Hamburg

Hamburg Studies on Maritime Affairs
Volume 7

Edited by

Jürgen Basedow
Peter Ehlers
Hartmut Graßl
Hans-Joachim Koch
Rainer Lagoni
Gerhard Lammel
Ulrich Magnus
Peter Mankowski
Marian Paschke
Jürgen Sündermann
Richard Tol
Rüdiger Wolfrum

Tatjana P. Ilyina

The Fate of Persistent Organic Pollutants in the North Sea

Multiple Year Model Simulations of γ-HCH, α-HCH and PCB 153

With 48 Figures and 13 Tables
Including 17 Color Figures

Springer

Dr. Tatjana P. Ilyina
University of Hawaii at Manoa
School of Ocean and Earth Science and Technology
Department of Oceanography
1000 Pope Road, MSB 524
Honolulu, HI 96822,
USA
ilyina@soest.hawaii.edu

Library of Congress Control Number: 2006939205

ISSN 1614-2462

ISBN 978-3-540-68162-5 Springer Berlin Heidelberg New York

This work is subject to copyright. All rights are reserved, whether the whole or part of the material is concerned, specifically the rights of translation, reprinting, reuse of illustrations, recitation, broadcasting, reproduction on microfilm or in any other way, and storage in data banks. Duplication of this publication or parts thereof is permitted only under the provisions of the German Copyright Law of September 9, 1965, in its current version, and permission for use must always be obtained from Springer. Violations are liable to prosecution under the German Copyright Law.

Springer is part of Springer Science+Business Media

springer.com

© Springer-Verlag Berlin Heidelberg 2007

The use of general descriptive names, registered names, trademarks, etc. in this publication does not imply, even in the absence of a specific statement, that such names are exempt from the relevant protective laws and regulations and therefore free for general use.

Production: LE-TEX Jelonek, Schmidt & Vöckler GbR, Leipzig
Cover-design: WMX Design GmbH, Heidelberg

SPIN 11948025 64/3100YL - 5 4 3 2 1 0 Printed on acid-free paper

Foreword

Within the last two decades the loading of the North Sea with pollutants such as nutrients, heavy metals and oil has been intensely investigated and, as a political consequence, gradually diminished. The main remaining challenges, both with respect to science and environmental policy, are understanding and handling the threat by organic contaminants, especially their spreading and fate. This task is ambitious, since the available data base (even for a well investigated area such as the North Sea) is poor and the biogeochemical processes involved are not sufficiently known. This situation is the background of the doctoral thesis of *Tatjana Ilyina* which presents an innovative model approach for investigating the spreading of three major persistent organic pollutants (POPs) in the North Sea.

The first really troublesome task was to compile appropriate observational data for validating the model, including spatial distributions within the North Sea and time series at single stations. As a second step a new Fate and Transport Ocean Model (FANTOM) for organic pollutants has been developed and tested. The validation against the field data turned out to be satisfactory. Remaining deviations could be understood by means of sensitivity studies as well as assessing the relative importance of different physical and chemical processes. The calibrated model has been used for simulating the real POPs loads in the North Sea within the period 1995–2001. Further, scenario calculations have been carried out for possible future states. The overall result is a new and comprehensive understanding of contaminant dynamics in the North Sea.

The findings represent the best scientific basis presently available for assessing and controlling the spreading and fate of organic pollutants in the North Sea. Such an approach provides a valuable decision aid for national and European marine environmental policy. Moreover, this approach can be applied to endangered shelf seas in other parts of the world.

The thesis forms a prototype of a targeted disciplinary contribution (in this case from marine physics and chemistry) applied to the more general interdisciplinary issue of environmental policy. It is an excellent fit, therefore, to the governing philosophy of the International Max Planck Research School on Maritime Affairs.

Hamburg, November 2006 *Jürgen Sündermann*

Preface

This book is based on a doctoral thesis submitted to the Faculty of Mathematics, Informatics and Natural Sciences of the University of Hamburg in 2006. It was accepted by the Faculty with the grade of *magna cum laude* in the same year.

First I would like to thank my academic advisor Professor Dr. *Jürgen Sündermann* and co-advisors P.D. Dr. *Gerhard Lammel* and P.D. Dr. *Thomas Pohlmann* for their constant support, for inspiring and teaching me, and for the interesting project they involved me in.

The International Max Planck Research School for Maritime Affairs and in particular Professor Dr. Dr. h.c. *Jürgen Basedow* and his co-directors are thanked for giving me the opportunity to perform this study in Hamburg.

Further, I would like to thank my colleagues at the Institute of Oceanography, in particular Dr. *W. Kühn*, Dr. *H. Lenhrat*, Dr. *A. Moll*, Dr. *J. Pätsch*, Dr. *I. Hamann*, *D. Hainbucher*, Dr. *P. Damm*, as well as Dr. *W. Puls*, Dr. *A. Aulinger* (GKSS Research Centre), Professor Dr. *H. Hühnerfuss* (Institute of Organic Chemistry), Professor Dr. *H. Schlünzen* (Meteorological Institute), Dr. *U. Brockmann* (Abteilung für Organomeereschemie at the University of Hamburg) for valuable discussions during my studies.

I would like to acknowledge Professor Dr. *Peter Ehlers* of Bundesamt für Seeschifffarht und Hydrographie (BSH) and Professor Dr. *Rainer Lagoni* of the Law of the Sea and Maritime Law Institute for providing excellent training opportunities throughout my studies. Dr. *Hartmut Nies* and Dr. *Norbert Theobald* of BSH are acknowledged for providing necessary data for this study.

Many thanks to my colleagues and friends *Philipp Weis* and *Stiig Wilkenskjeld* for all the fun at work and for reading the first version of this manuscript. I am also grateful to my other friends: *F. Guglielmo*, *Semeena*, *C. Röckmann*, *S. Kloster*, *M. Pfeffer*, *E. Marmer*, *A. Valdebenito*, *P. Wetzel* for encouraging me and the great time we had together.

I would like to thank Dr. *Robert W. Riddaway* of the Royal Meteorological Society for editing the final version of this manuscript.

Last but not the least many thanks to my husband *Mikhail Dobrynin* and my son *Alexej* for believing in me, for their patience, support and understanding.

This work has been funded by the International Max Planck Research School for Maritime Affairs.

Honolulu, October 2006 *Tatjana Ilyina*

Contents

Abbreviations

AMAP	Arctic Monitoring and Assessment Programme
BSH	Bundesamt für Seeschifffahrt und Hydrographie (Federal Maritime and Hydrographic Agency)
CLRTAP	Convention on Long-range Transboundary Air Pollution
DDT	Dichlorodiphenyltrichloroethane
DOD	Deutsche Ozeanographische Datenzentrum (German Oceanographic Data Centre)
DONAR	Dutch database with water-related monitoring data from the Directorate-General of Public Works and Water Management
ECMWF	European Centre for Medium range Weather Forecasting
EEZ	Exclusive Economic Zone
ELPOS	Environmental Long-range Transport and Persistence of Organic Substances Model
EMEP	Co-operative Programme for Monitoring and Evaluation of the Long Range Transmission of Air Pollutants in Europe
EQC model	Equilibrium Criterion model
ERA-40	ECMWF Re-Analysis
FANTOM	Fate and Transport Ocean Model
HAMSOM	Hamburg Shelf Ocean Model
HCH	Hexachlorocyclohexane
HELCOM	Helsinki Commission
HLC	Henry's Law Constant
IFCS	Intergovernmental Forum on Chemical Safety
IMO	International Maritime Organisation
LRT	Long-range transport
MEDPOL	The Programme for the Assessment and Control of Pollution in the Mediterranean region
NLÖ	Nidersächsisches Landesamt für Ökologie
OSPARCOM	Oslo-Paris Commission
PAHs	Polycyclic Aromatic Hydrocarbons
PCBs	Polychlorinated Biphenyls
POC	Particulate Organic Carbon
POPs	Persistent Organic Pollutants

PRISMA	Prozesse im Schadstoffkreislauf Meer-Atmosphäre
REACH	The European Union regulatory framework for the Registration, Evaluation and Authorisation of Chemicals
SPM	Suspended Particulate Matter
SRU	Der Sachverständigenrat für Umweltfragen (The German Advisory Council on the Environment)
SST	Sea Surface Temperature
TBT	Tributyltin
UNEP	United Nations Environment Programme
WFD	The European Union Water Framework Directive
WHO	World Health Organisation
WMO	World Meteorological Organisation
ZISCH	Zirkulation und Schadstoffumsatz in der Nordsee

Summary

Persistent organic pollutants (POPs) are harmful to human health and to the environment. Their fate in the marine environment is not yet fully understood. An ocean model (FANTOM) has been developed to investigate the fate of selected POPs in the North Sea. The main focus of the model is on quantifying the distribution of POPs and their aquatic pathways. Key processes are three-dimensional transport of POPs by ocean currents, diffusive air–sea exchange, wet and dry atmospheric depositions, phase partitioning, degradation, and net sedimentation in bottom sediments. This is the first time that a spatially-resolved, measurement-based ocean transport model has been used to study POP-like substances, at least on the regional scale. The model was applied for the southern North Sea and tested by studying the behaviour of γ-HCH, α-HCH and PCB 153 in sea water in the years 1995 to 2001.

Concentrations of γ-HCH, α-HCH and PCB 153 and their fluxes between the upper sediment, sea and atmosphere were modelled, based on discharge and emission estimates available through various monitoring programmes. Model results are evaluated against measurements. It is found that modelled concentrations of the three selected POPs in sea water are in good agreement with measurements. The spatial distribution and the downward trend of the two HCHs in the entire North Sea are reproduced during the simulation period.

The pathways of γ-HCH, α-HCH and PCB 153 in the North Sea were investigated and the results suggest that the temperature dependence of the air–sea exchange is important. Model results showed that for the North Sea as a whole the air–sea flux is depositional, whereas in the German Bight it can be net volatilisational. For PCB 153 a net volatilisational flux also occurred for the German Bight and for the whole North Sea. Model experiments suggest that the direction and magnitude of the flux is altered significantly by the temperature dependency of Henry's law constant; this could be responsible for more than 50% of the variability in the sea water concentrations of the studied POPs. Uptake by particulate matter in sea water was the most important for PCB 153 with up to 90% of the total concentration being on particles, whereas for the two HCHs this fraction was below 2% during the entire simulation period.

For the first time mass budgets of γ-HCH, α-HCH and PCB 153 in the North Sea and in the German Bight were calculated based on a modelling study. Calculated mass budgets show that γ-HCH and PCB 153 are controlled predominantly by the local sources, whereas for α-HCH transport from remote sources is probably the major contributor for the North Sea environment.

This model study proves that transport models, such as FANTOM, are capable of reproducing realistic multi-year temporal and spatial trends of selected POPs and can be used to address further scientific questions.

1 Introduction and Background

Awareness about persistent organic pollutants (POPs) began in the 1960s with the publication of Rachel Carson's book "Silent Spring" where evidence of harmful effects of DDT (dichlorodiphenyltrichloroethane) on marine mammals and birds was documented.

The fate and behaviour of POPs in the environment has attracted considerable scientific and political interest arising from concern over human exposure to these chemicals and their discovery in pristine environments far from their source regions (Sect. 1.1). The ability of certain POPs to undergo long-range transport has resulted in international actions to reduce and eliminate releases of these chemicals and to reduce the risks to regional and global environments (Sect. 1.2). International protocols require criteria for assessing the environmental risk posed by POPs based on sound scientific knowledge and models of their environmental behaviour (Sect. 1.3).

Knowledge of processes and pathways that POPs undergo in the aquatic environment is particularly important as the hydrosphere is where many POPs resist degradation and are more prone to bioaccumulation; thus they are more hazardous to living organisms (AMAP 1998). However, present knowledge of the processes which control the distribution and fate of POPs in the aquatic environment in general and in the North Sea in particular is clearly insufficient (Sect. 1.4).

These issues motivated the present study which aimed at advancing our knowledge about the fate of POPs in shelf seas by modelling their environmental behaviour and identifying the driving mechanisms of their cycling in sea water (Sect. 1.5).

1.1 Persistent organic pollutants (POPs): occurrence and effects

Persistent organic pollutants (POPs) are synthetic organic chemical compounds which are environmentally persistent, bioaccumulative and toxic. They are released into the environment through a range of processes including release during industrial production, release during use (e.g. pesticides in agriculture), or release during combustion (e.g. dioxins). POPs have a particular combination of physical and chemical properties which ensures that once they have been released into the environment they remain intact for exceptionally long periods. Although POPs are mostly produced by anthropogenic processes, natural sources can also be signifi-

cant for some compounds. For example, emission of polycyclic aromatic hydrocarbons (PAHs) into the atmosphere can occur from forests fires and volcanic eruptions.

POPs migrate between the different environmental compartments (e.g. atmosphere, soil and water) and are able to undergo long-range transport by natural processes in both the atmosphere and in the ocean, thus becoming ubiquitous global contaminants. High levels of some POPs were detected in the Arctic far from regions where they were released (AMAP 1998).

Historically, the chemicals that have provoked the greatest concern are the chlorinated hydrocarbons due to their hazardous effects on the marine environment. They include such well known substances as the pesticide DDT and the PCBs (the polychlorinated biphenyls widely used in electrical devices). Hexachlorocyclohexane (HCH) used in agriculture is the most abundant organochlorine pollutant in both the atmosphere and oceans.

Although there are many hundreds of different chemicals under the heading of chlorinated hydrocarbons (PCBs alone may consist of up to 209 distinct chemicals) many of them share a number of important properties. In particular, they are generally fairly toxic, persistent in the environment, and bioaccumulative.

Bioaccumulation and biomagnification are two important processes affecting the concentration of pollutants in organisms.

(a) *Bioaccumulation* (increase in concentration of a pollutant from the environment to the first organism in a food chain) refers to how pollutants enter a food chain.

(b) *Biomagnification* (increase in concentration of a pollutant from one link in a food chain to another) refers to the tendency of pollutants to concentrate as they move from one trophic level to the next.

Together these processes can cause even small concentrations of chemicals in the environment to find their way into organisms in high enough dosages to pose a danger. In order for biomagnification to occur, the pollutant must be long-lived (persistent[1]), mobile (long-range transport[2]), soluble in fats and biologically active

[1] A persistent substance resists physical, biological and chemical degradation. A measure of a substance's persistence can be determined from laboratory tests and from measurements in the environment. Source: http://www.eurochlor.org (last visited 5 January 2006).

[2] Long-range transport is dependent on a substance's volatility, water solubility, and its longevity in air and water, usually expressed as the half-life. For some chemicals the potential for long-range transport can be predicted from its intrinsic properties, but monitoring provides the most reliable evidence. Long-range transport may also occur through a successive migration of short-range leap frog movements. Source: http://www.eurochlor.org (last visited 5 January 2006).

(bioaccumulation[3]). If a pollutant is short-lived, it will be broken down before it can become dangerous. If it is not mobile, it will stay in one place and is unlikely to be taken up by organisms. If the pollutant is soluble in water it will be excreted by an organism.

Wildlife exposure to POPs is mainly attributed to the food chain (AMAP 1998). Contamination of food may occur through environmental pollution of air, water and soil, or through the previous use of organochlorine pesticides on food crops, some of which may be unauthorized. Episodes of massive food contamination have been reported. Some chlorinated hydrocarbon insecticides have been known to cause serious, acute poisonings. Humans can be exposed to POPs through diet, occupation, accidents and the environment, including the indoor environment. It is believed that exposure to certain POPs can have the potential for a significant impact on human health either in the short or long term (WHO 2003). High (over) exposures at the point of use of some POPs can lead to acute effects, including death, while at lower exposure levels long-term effects can occur. In general, exposure to POPs, either acute or chronic, can be associated with a wide range of adverse health effects, including cancer, damage to the central and peripheral nervous systems, diseases of the immune system, reproductive disorders, and interference with infant and child development. However the effects resulting from low-level chronic exposure have yet to be understood. Human health impacts may be felt most acutely in populations that consume large amounts of fish (e.g. subsistence fishermen), since fish have a high fat content and thus they can contain high concentrations of POPs.

Shifting from POPs to chemical and non-chemical alternatives is the key issue in reducing their impact. A high priority is finding alternatives to hazardous chemicals for insect control. POPs can be produced cheaply compared to most other industrial chemicals. There are many safer chemical and non-chemical alternatives, but their development and use will require time, money, and training. For example, replacing DDT (widely used to control malarial mosquitoes) with less hazardous forms of insect control requires time to plan effective actions (e.g. integrated pest management systems, consisting of the sparing use of pest-specific pesticides and biological control methods).

1.2 Legal instruments and measures to control POPs

The first publication where toxic effects of POPs were addressed appeared in 1970 (Prest et al. 1970). However it was only in 1995 that an international working

[3] A bioaccumulative substance builds up in tissues of living organisms as a result of direct exposure to polluted water, air or soil, or through consumption of contaminated food. A measure of the ability to bioaccumulate is expressed as a ratio of the substance's concentration in the organism and the medium to which it is exposed, termed the bioaccumulation factor.
Source: http://www.eurochlor.org (last visited 5 January 2006).

group was convened by the UNEP[4] Governing Council to develop assessments of twelve POPs, thus recognising the threat posed by these chemicals as a global problem which has to be dealt with at an international level.

Political interest in the fate and behaviour of POPs in the environment arises from concern over human exposure to these chemicals and to their discovery in pristine environments far from source regions (UNEP 2003). The UNEP Stockholm Convention (POPs Convention)[5], a global treaty to protect human health and the environment from POPs, was open for signature/ratification in May 2001. It is based on the precautionary principle, which seeks to guarantee the safe elimination of these substances as well as reductions in their production and use.

The Convention targets an initial 12 priority chemicals (POPs) for phase out and lays out a process for adding new chemicals that meet agreed criteria for persistence, bioaccumulation and transportability. The eventual long-term objective is to cover many other substances. These twelve POPs covered by the treaty are aldrin, chlordane, dichlorodiphenyltrichlorethane (DDT), dieldrin, endrin, heptachlor, mirex, toxaphene, polychlorobiphenyls (PCBs), hexachlorobenzene, dioxins and furanes. The Convention entered into force in May 2005 and most of the twelve POPs currently addressed in international negotiations have been banned or subjected to severe restrictions in many countries for more than 20 years. Many of them, however, are still in use in many countries, and stockpiles of obsolete POPs exist in many parts of the world.

The Rotterdam Convention on the Prior Informed Consent Procedure for Certain Hazardous Chemicals and Pesticides in International Trade (PIC Convention) is an important companion treaty of the Stockholm Convention. The Rotterdam Convention was developed to reduce international trade of dangerous chemicals, and entered into force in February 2004. The Convention "enables the world to monitor and control the trade in certain hazardous chemicals and it is not a recommendation to ban the global trade or use of specific chemicals it is rather an instrument to provide importing Parties with the power to make informed decisions on which of these chemicals they want to receive and to exclude those they cannot manage safely."[6]

The Protocol to the 1979 Convention on Long-Range Transboundary Air Pollution for POPs (POPs Protocol to LRTAP)[7], another POPs-related international agreement, entered into force in October 2003. It focuses on a list of 16 substances that have been singled out according to agreed risk criteria. The ultimate objective is to eliminate any discharges, emissions and losses of POPs. The Protocol bans the production and use of some products outright (aldrin, chlordane, chlordecone, dieldrin, endrin, hexabromobiphenyl, mirex and toxaphene). Others are scheduled

---

[4] United Nations Environment Programme: http://www.chem.unep.ch/pops/ (last visited 25 January 2006).

[5] Stockholm Convention on Persistent Organic Pollutants: http://www.pops.int/ (last visited 23 December 2005).

[6] The Rotterdam Convention: http://www.pic.int/ (last visited 25 January 2006).

[7] Convention on Long-range Transboundary Air Pollution of the UNECE: http://www.unece.org/env/lrtap/welcome.html (last visited 25 January 2006).

for elimination at a later stage (DDT, heptachlor, hexaclorobenzene, PCBs). Finally, the Protocol severely restricts the use of DDT, HCH (including lindane) and PCBs. The Protocol includes provisions for dealing with the wastes of products that will be banned. It also obliges Parties to reduce their emissions of dioxins, furans, PAHs and HCB below their levels in 1990 (or an alternative year between 1985 and 1995). For the incineration of municipal, hazardous and medical waste, it lays down specific limit values[8].

In summary, both the POPs Convention and POPs Protocol to LRTAP establish strict international regimes for initial lists of POPs (16 in the UNECE Protocol and 12 in the Stockholm Convention). Both instruments also contain provisions for including additional chemicals into these lists. This provision helps to ensure that the treaty remains dynamic and responsive. They lay down the following control measures[9]:

(a) Prohibition or severe restriction of the production and use of intentionally produced POPs.

(b) Restrictions on export and import of the intentionally produced POPs (Stockholm Convention).

(c) Provisions on the safe handling of stockpiles (Stockholm Convention).

(d) Provisions on the environmentally sound disposal of wastes containing POPs.

(e) Provisions on the reduction of emissions of unintentionally produced POPs (e.g. dioxins and furans).

UNEP has also initiated actions on sharing information, evaluating and monitoring implementation strategies, identifying alternatives to POPs, preparing inventories of PCBs, assessing available destruction capacity, and other issues. Also UNEP and the Intergovernmental Forum on Chemical Safety (IFCS) are convening awareness-raising workshops in developing countries and countries with economies in transition. International agreements (i.e. Stockholm Convention and the CLRTAP) require assessment criteria of the environmental risks posed by POPs based on sound scientific knowledge and models of their behaviour.

Investigation of the environmental contamination by POPs involves determining emission patterns, making field measurements and modelling. However, there are still many important problems and open questions that need to be addressed. These are primarily connected with there being only poor information about sources and pathways of POPs in different media. Although reporting of emission is required by some international conventions (e.g. Stockholm Convention or CLRTAP), for the majority of POPs it is difficult to obtain information about their sources into the environment that covers a time scale reflective of their persistence, which may be as large as several decades. Information on the release of

[8] http://www.unece.org/env/lrtap/pops_h1.htm (last visited 25 January 2006).

[9] See also http://ec.europa.eu/environment/pops/index_en.htm (last visited 25 January 2006).

POPs is therefore fragmentary and is available only for some parts of the world (e.g. North America and Europe).

In the European region the monitoring of some POP-like chemicals is included in different national and international programmes (e.g. HELCOM[10], AMAP[11], OSPARCOM[12], WFD[13], EMEP[14] and MEDPOL[15]). Under the OSPAR monitoring programme, measurement of organic compounds is only mandatory for γ-HCH, while measurement of PCBs is recommended. In 1990, the Ministers of the North Sea countries signed an agreement to reduce inputs of certain toxic substances between 50% and 70% by 2020. The International Maritime Organisation has agreed to a global ban on new use of TBT (a widely used organotin antifoulant) on ship hulls from 1 January 2003. After 2008, TBT-based antifouling paints must be removed from ship hulls or encapsulated with an impermeable paint which stops leakage to the environment.

The activities on the preparation of protocols for emission reductions of POPs under UNECE/CLRTAP have put a focus on the current state of knowledge about atmospheric and oceanic transport and deposition of these compounds.

Within the European Union (EU), a proposed strategy for acidifying pollutants is currently being discussed with even more far-reaching restrictions on emissions of sulphur, nitrogen and other hazardous substances. By the end of 2006, the EU is expected to adopt REACH, a proposal that would "require manufacturers to test industrial chemicals used in the manufacturing process to gather health and safety data". The EU regulatory framework REACH[16] aims at improving the protection of human health and the environment through the better and earlier identification of the properties of chemical substances. Under REACH certain classes of industrial chemicals regarded as of Very High Concern would have to be registered, evaluated and authorized before they could be marketed. They are:

(a) Carcinogens, mutagens, and reprotoxins which are either known or very likely to be toxic to humans.

---

[10] Helsinki Commission: http://www.helcom.fi/ (last visited 23 December 2005).

[11] Arctic Monitoring and Assessment Programme: http://www.amap.no/ (last visited 23 December 2005).

[12] Oslo-Paris Commission: http://www.ospar.org/ (last visited 23 December 2005).

[13] The EU Water Framework Directive: http://www.ospar.org/ (last visited 23 December 2005).

[14] Co-operative Programme for Monitoring and Evaluation of the Long-Range Transmission of Air pollutants in Europe: http://www.emep.int/ (last visited 23 December 2005).

[15] The Programme for the Assessment and Control of Pollution in the Mediterranean region.

[16] The EU regulatory framework for the Registration, Evaluation and Authorisation of Chemicals: http://europa.eu.int/comm/environment/chemicals/reach.htm (last visited 25 January 2006).

(b) Chemicals that can become widely disseminated in the environment, and which are persistent, bioaccumulative and toxic, particularly persistent organic pollutants.

(c) Chemicals that are very persistent and very bioaccumulative in humans and wildlife for which toxicity data is still unavailable.

All these actions have increased the scientific activity at national and international levels, and various programmes are under way for dealing with emissions, measurements and transport modelling. Significant contributions in summarising the scientific status in this area and identifying knowledge gaps have been made at the UN-ECE/EMEP Workshops in Durham, USA in 1993 (EMEP 1993), Beekbergen, the Netherlands in 1994 (de Leeuw 1994) and Moscow, Russian Federation in 1996 (WMO 1997).

For many organic contaminants it is still hard to draw conclusions about whether the existing actions and measures are sufficient. There is already a widespread restriction on production and use of DDT and PCBs, although levels in the environment suggest that there are still problems. Therefore, their sources should be identified and adequate strategies developed to prevent these pollutants from entering the environment.

1.3 Approaches in POPs modelling

Field measurements of POPs are difficult to conduct and costly. Therefore, models investigating the environmental fate of POPs are helpful tools for testing hypotheses and studying systems which are not fully accessible. However, there are serious constraints due to insufficient knowledge about POPs: their processes, their release and their amount in the environment. There are two main approaches in modelling the environmental fate of POPs. These are multimedia box models and models based on transport models of the atmosphere and the ocean.

(a) *Box models* are simpler to construct and use, yet they have only low spatial and temporal resolution.

(b) *Transport models* adequately represent transport patterns and are spatially resolved, but they also require high computational effort and more detailed input data.

Multimedia box models (i.e. those with several environmental compartments) are based on mass-balance equations that balance the input and output of a chemical in each environmental compartment. Models constructed that way have been widely used for various purposes and scales. There are several established multimedia box models including: SimpleBox (van de Meent 1995), ELPOS (Beyer and Matthies 2001), Chemrange (Scheringer 1997), EQC (Mackay et al. 1996) and GloboPOP (Wania and Mackay 1995). The main advantage of these models is that they are relatively easy to construct and use, and the computational effort required

for the model solution is relatively low. The spatial resolution of these models is very low (i.e. a single box represents an area of thousands square kilometres). In most cases the validation of these models has shown that their results are far from reality.

Spatially-resolved transport models of the ocean and atmosphere have been developed and used for simulating the transport and deposition of pollutants such as NOx, aerosol particles in the atmosphere, heavy metals or suspended particulate matter (SPM), and microorganisms in the ocean. The spatial and temporal resolution of such models is relatively high. Transport models can be adapted for the modelling of POPs by incorporating the additional processes which capture their cycling. Because of the geo-referencing and the ability to resolve environmental conditions and processes, spatially-resolved transport models are typically applied for a specific period. They can be validated if measurements are available. The background concentrations in the different media at the beginning of a particular model simulation have to be incorporated into the initial conditions. Calculations with transport models have so far mostly concentrated on the hexachlorocyclohexane (HCH) isomers because these chemicals have the most reliable, spatially-resolved emission inventories. Several transport models have been developed to describe the atmospheric transport of POPs on regional (van Jaarsveld et al. 1997; Ma et al. 2003), hemispheric (Hansen et al. 2004; Malanichev et al. 2004) and global scales (Semeena and Lammel 2003; Koziol and Pudykiewicz 2001). The majority of the existing models take into account the behaviour of POPs in several environmental compartments. The main environmental compartments included in the models are the atmosphere, soil and water. Some models also take into account vegetation, sediments or the cryosphere.

Though both types of models are based on the same principle (i.e. mass conservation) they are constructed for different purposes and accordingly have different advantages and limitations. Box models are easier to understand and use, whereas transport models require a large number of model parameters and are more complex. However, box model results are hard to compare with measurements while transport model results can easily be used to make such comparisons. Furthermore, due to simplifications of the dynamical environmental processes, box models may fail to reproduce the transport and spatial variability of the cycling of POPs in the environment. For example, using a complex model of the global fate of chemicals in the atmosphere, Semeena and Lammel (2005) demonstrated that under certain atmospheric conditions DDT may reach the stratosphere, whereas such a conclusion is not possible if simplified modelling approaches are used.

Models have been used for the quantification of the atmospheric input of POPs to receptor areas versus the input via other pathways or for calculating the deposition of POP on a European scale (Baart et al. 1995; Jacobs and van Pul 1996; van Jaarsveld et al. 1997). The models used in these studies were originally designed for other air pollutants but have been extended by including the soil and sea water compartments.

Research on modelling the long-range transport and deposition levels of POPs is also encouraged within the framework of CLRTAP (Sect. 1.2). Furthermore, Jones and de Voogt (1999) conclude that progress in models supplemented by

comprehensive geographical coverage of chemical concentration and flux data requires active research over the next few years.

1.4 POPs fate in the aquatic environment

In the 1970s it was predicted that the oceans may be recipients of most of the persistent pesticides used globally (Goldberg 1975). Observations (Bidleman et al. 1995) and global budget calculations (Strand and Hov 1996) show that the oceans are a major store of HCH pesticides. Oceans are traditionally thought to be a global reservoir and ultimate sink of many POPs (Iwata et al. 1993; Dachs et al. 2002) and may be a slow but significant medium for their long-range transport (UNEP 2003; Wania and Mackay 1999).

POPs are distributed throughout the world's oceans as a consequence of atmospheric deposition and direct introduction into aquatic systems. Oceanic biogeochemical processes may play a critical role in controlling the global dynamics and the capacity of the oceans to store or release POPs. The physical and biogeochemical characteristics affecting the ocean's capacity to retain POPs show important spatial and temporal variability. They have not been studied in detail so far.

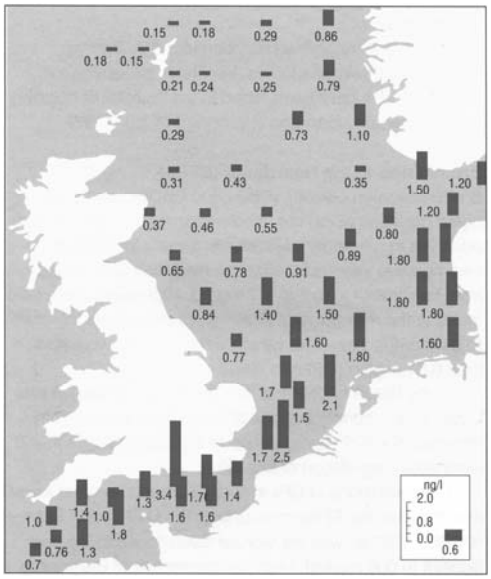

Fig. 1.1. Geographical distribution of γ-HCH concentrations (ng l^{-1}) in surface water (at a depth of 7 m) based on field measurement campaigns carried out in 1995. Source: OSPAR (2000).

Temperature, phytoplankton biomass and mixed layer depth influence the potential reservoir of POPs in the oceans. Jurado et al. (2004) suggest that settling fluxes will keep the surface oceanic reservoir of PCBs well below its maximum capacity, especially for the more hydrophobic compounds. The strong seasonal and latitudinal variability of the storage capacity of the surface ocean plays an important role in the global cycles controlling the ultimate sink of POPs.

Shelf and coastal seas such as the North Sea are important components of the global ocean. They contribute much of the biological production, and are crucial for an accurate quantification of POPs in global budgets. The shelf and coastal seas are highly dynamic systems usually characterised by strong physical-chemical gradients, enhanced biological activity, and intense sedimentation and re-suspension. These areas are also subject to tidal forcing which leads to an increased residence time of the fresh water in the estuarine mixing zones and the generation of a turbidity maximum.

The fate of POPs in the shelf and coastal seas is different from that in the oceans for several reasons. For the global ocean, the main contributor of POPs is the atmosphere. The coastal areas receive large amounts of POPs via river input, which in some cases can exceed the atmospheric deposition. Furthermore, for most of the POPs the air concentrations over the coastal waters are expected to be higher than those over the open ocean waters. The higher concentrations of some organic pollutants in the coastal waters (e.g. γ-HCH, Fig. 1.1) will contribute to their capacity to release these chemical to the atmosphere via volatilisation. In fact, Hornbuckle et al. (1993) showed that for PCBs the water masses in lakes may sometimes act as sources to the atmosphere. Furthermore, in the deep ocean, the water temperature is fairly low and the sun cannot penetrate through the deeper water. Thus persistence of POPs increases making the global ocean one of the most accumulative compartments. In shelf areas the sinking particles carrying POPs down to the bottom sediments may enter the water column again via re-suspension and even reach the surface. Therefore, as primary pollutant sources are reduced, remobilisation from previous repositories, such as water bodies, can act as secondary sources to the atmosphere (Jaward et al. 2004).

The environmental fate of some POPs in the Baltic Sea has been studied using box models within the POPCYCLING-Baltic project during the years 1996–1999. The long-term behaviour of the pesticide components α-HCH and γ-HCH in the Baltic Sea environment was addressed (Pacyna et al. 1999). In addition there have been some studies on POPs in open ocean and shelf seas (Iwata et al. 1993; Schulz-Bull et al. 1998; Lakaschus et al. 2002; Jaward et al. 2004). These were very limited in temporal and spatial terms because of practical or analytical constraints. Thus, it is still debatable whether the shelf seas are a net source or sink of POPs. Furthermore, the cycling of POPs in the marine environment has not yet been addressed using an ocean transport model, and studies on the impact of climate variability on the environmental fate of POPs have not been conducted. A complex, spatially-resolved ocean modelling study will significantly contribute to the understanding of the role of the shelf and shallow seas in the cycling of POPs.

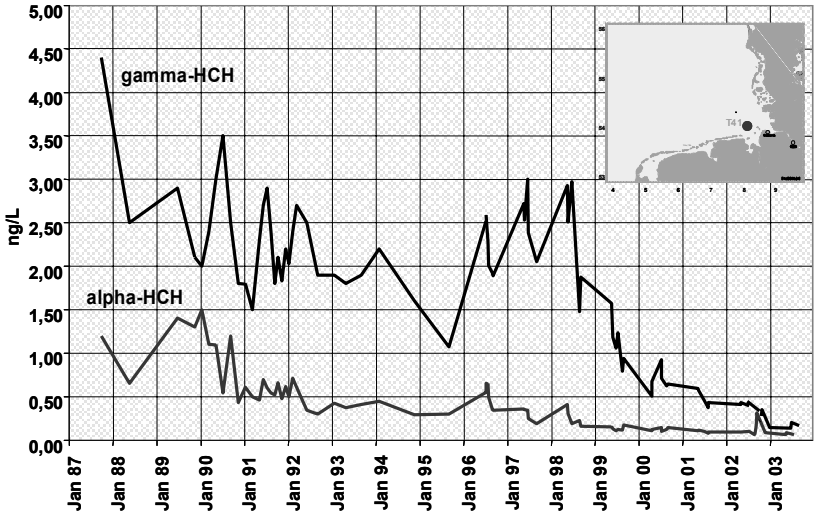

Fig. 1.2. Temporal trend of α-HCH and γ-HCH concentrations (ng l^{-1}) in surface water for the German Bight since 1986. Measurements were performed at Station T 41 shown on the map in the upper right corner. Source: BSH (2005).

The North Sea is a region particularly vulnerable to POPs as it is surrounded by highly industrialised countries releasing large amounts of POPs. Monitoring campaigns show that nearly all known POPs were found in the North Sea due to their persistence in sea water and long-range transport from distant sources (OSPAR 2000; Weigel et al. 2002). Some POPs in the North Sea have experienced reducing concentrations since the early 1990s (Fig. 1.2). However present-day levels still threaten the environment (OSPAR 2000).

With regard to the availability of comprehensive data on POPs, the North Sea is comparatively well assessed. The datasets have been accumulated through national and international monitoring programmes (e.g. OSPAR 2000) and research projects (e.g. Sündermann 1994). Thus, the data coverage at least for some compounds (e.g. lindane (γ-HCH), α-HCH and some PCB congeners) is sufficient for the modelling of POPs and evaluating the model results.

1.5 Objectives and outline of this study

While new pollutants are being produced and released into the environment a modelling tool is required to assess their environmental fate. As mentioned in Sect. 1.4 , the role of the oceans in general and shelf and coastal seas in particular as an exchange compartment and/or permanent sink for POPs is yet to be fully understood. The major objective of this study is to advance our understanding of the

fate of POPs in the aquatic environment. This objective was approached in three steps.

First, a fate and transport ocean model (FANTOM) was developed based on current knowledge about the cycling of contaminants in the environment. The fate of contaminants in sea water depends on a number of mechanical (transport with ocean currents), chemical (amalgamation with other chemicals, transfer to gaseous state, chemical decay, etc.), physical (transfer to another aggregative state, adsorption) and biological (pollutants accumulation and transport by biota) processes. These processes can only be fully taken into account with a three-dimensional, hydrodynamic ocean model.

Second, the model was applied to the North Sea and the calculations were performed based on measured levels of γ-HCH, α-HCH and PCB 153 in sea water. The measurements are discrete in time and space. Therefore the objective of such calculations was to obtain realistic spatial and temporal distributions of these three contaminants which have different physical-chemical properties and sources. This is the first study of its kind.

Third, the multi-year fate of γ-HCH, α-HCH and PCB 153 in the North Sea was investigated. The questions which were addressed in this study fall into the following categories:

(a) What are the key processes controlling the fate of these three contaminants in the North Sea? Do these processes have the same importance for the North Sea as a whole or do the local dynamical processes dominate in the subregions of the North Sea?

(b) What is the explanation of the measured levels of these three pollutants in the North Sea? What is the role of local versus remote sources as well as primary versus secondary emissions?

(c) What are the current and possible future exposures of the North Sea environment to contamination by POPs?

Chapter 2 describes the model architecture. A description of the model setup for the simulations of the fate of γ-HCH, α-HCH and PCB 153 in the North Sea is given in Chapter 3. An evaluation of the model and an exploration of the model's uncertainties are presented in Chapter 4. Then Chapters 5 and 6 describe the results of using the model to investigate the pathways of selected POPs and the contribution of individual processes to the cycling. Finally Chapter 7 describes the main findings from the various investigations and presents an outlook for current and future developments.

2 The Fate and Transport Ocean Model (FANTOM): Model Description

The Fate and Transport Ocean Model (FANTOM) is a three-dimensional numerical model designed for simulating the long-term fate of POP-like contaminants in the shelf and coastal aquatic environment. FANTOM is aimed at tracing substances released from point or diffuse sources.

The pollutants can enter the model domain via rivers, adjacent seas or atmospheric deposition. The key processes are described in Fig. 2.1. They fall into four broad categories.

(a) *Transport by ocean currents*. In sea water a pollutant is transported by ocean currents via horizontal and vertical advection and turbulent diffusion (Sect. 2.1).

(b) *Air–sea exchange*. Air–sea exchange (Sect. 2.2) is represented by three mechanisms: reversible gaseous exchange, dry particle deposition and wet deposition.

(c) *Phase distribution*. A pollutant is either dissolved or bound to suspended particulate matter (SPM) present in sea water (Sect. 2.3). The fraction bound to SPM is subject to gravitational sinking and deposition to the bottom sediments. Redistribution of particles takes place in the sediment due to the disturbance of sediment layers by biological activity (bioturbation). It can also be re-mobilised back to the water column when disturbed by erosion processes.

(d) *Degradation in sea water*. Both fractions of a pollutant (dissolved and particle bound) are subject to degradation in sea water (Sect. 2.4).

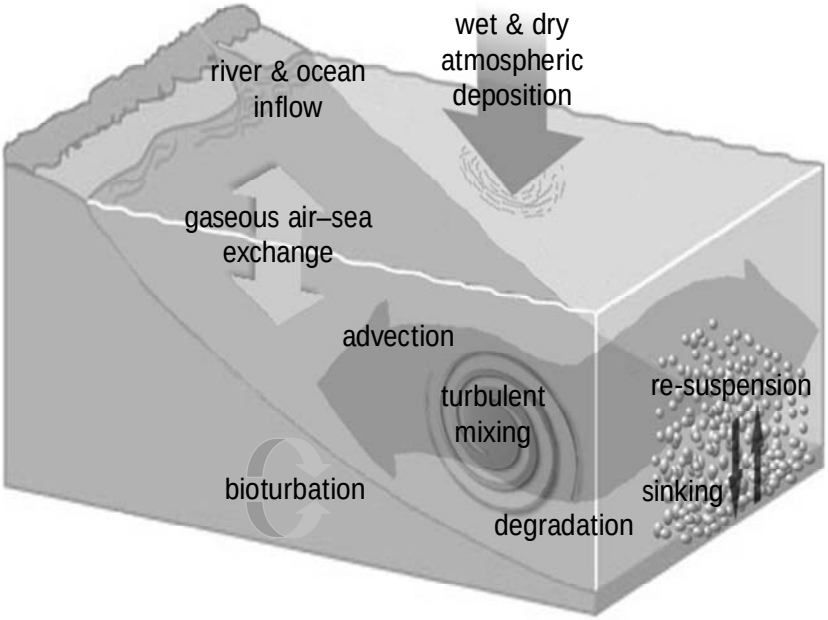

Fig. 2.1. Illustration of key processes affecting the fate of POPs which are included in FANTOM.

2.1 Transport with ocean currents

In the ocean, pollutants like POPs are transported both vertically and horizontally together with ocean waters. Evolution of the total (dissolved and particle bound) concentration of a pollutant at a fixed location results from a combination of sources, sinks, and mechanical transport by a flow field. The last of these has a key role in shaping a pollutant's distribution in sea water. It has two components: transport governed by the averaged current velocity field (advection) and transport due to the presence of the random fluctuations in the velocity field (turbulent diffusion). Averaged and turbulent movement of the ocean waters is highly sensitive to the density stratification when waters with higher density are located deeper than those with lower density. Turbulence in the ocean is determined by the current velocity gradients, surface and deep perturbations, and sea water stratification. It plays an important role in the intensity of the diffusion processes and thus a pollutant's spatial distribution (Baumert et al. 2005).

Due to advective (induced by currents) and turbulent horizontal transport the POPs can be distributed throughout the ocean. Speeds of the vertical transport in the ocean are 2-3 orders of magnitude lower than those of the horizontal transport.

However in some regions, fairly stable zones of upwelling or downwelling are observed.

Transport of pollutants due to advection and turbulence is calculated in FANTOM in a way similar to that used by Pohlmann (1987) where only the passive transport of conserved and dissolved pollutants in the North Sea was considered. Because POPs do not behave as conservative matter, pollutants in FANTOM may undergo additional processes in sea water (Fig. 2.1) which are represented by sources (Q_C) or sinks (R_C) in the model. Therefore the behaviour of a pollutant with concentration C is described by:

$$\frac{\partial C}{\partial t} = \frac{\partial}{\partial x}\left(K_x \frac{\partial C}{\partial x}\right) + \frac{\partial}{\partial y}\left(K_y \frac{\partial C}{\partial y}\right) + \frac{\partial}{\partial z}\left(K_v \frac{\partial C}{\partial z}\right) - \left(u\frac{\partial C}{\partial x} + v\frac{\partial C}{\partial y} + w\frac{\partial C}{\partial z}\right) + Q_C(t,x,y,z) - R_C(t,x,y,z) \tag{2.1}$$

Components of the horizontal flow field in the eastern and northern directions (u, v) at every model grid point are input parameters used for calculating the horizontal advection of the pollutant. These flow components are provided by an ocean circulation model, with the vertical component of the flow field w being calculated from (u, v) using the continuity equation. In addition the horizontal and vertical turbulent diffusion is calculated using the horizontal diffusion coefficients (K_x and K_y) and the vertical diffusion coefficient (K_v); these coefficients are also provided by the ocean circulation model (Sect. 3.2).

An Eulerian description of motion is used. This implies that changes in the fluid field are considered at a fixed point in the fluid. Eq. 2.1 has to be supplemented by the initial and boundary conditions (Sect. 2.2 and Sect. 3.4), as well as by the equations for the phase redistribution of POPs (Sect. 2.3).

2.2 Air–sea exchange

Atmospheric deposition to the oceans by wet and dry processes and volatilisation from the oceans are key processes affecting the dynamics and sinks of POPs. Furthermore, air–sea exchange is believed to be the major pathway for atmospheric input to oceans and seas for many persistent organic contaminants (Bidleman et al. 1995; Iwata et al. 1993; Lakaschus et al. 2002; Wania and Mackay 1999). Atmospheric deposition can occur as dry gaseous or dry particle deposition, or as wet deposition of gases and particles incorporated into rain droplets or snow. Hence, the net flux to the sea surface from the atmosphere, F_{surf} (ng m^{-2} s^{-1}), is represented in FANTOM by the net gaseous air–sea flux, $F_{a\text{-}w}$ (Sect. 2.2.1), the dry

particle deposition flux, F_{dry} (Sect. 2.2.2) and the wet deposition flux, F_{wet} (Sect. 2.2.3), so that:

$$F_{surf} = F_{wet} + F_{dry} + F_{a-w} \tag{2.2}$$

Previous studies have shown that gaseous air–sea exchange dominates over wet and dry particle depositions of organochlorine compounds. Exceptions occur in regions and seasons with intensive precipitation and areas with a high concentration of atmospheric aerosol particles. The relative importance of the different mechanisms of the air–sea exchange is still in debate.

2.2.1 Gaseous air–sea exchange

The gaseous air–sea transfer can be treated as a diffusion of the trace gases through spatially and temporally varying thin boundary layers in both media whose thicknesses are a function of near-surface turbulence and molecular diffusivity (Schwarzenbach et al. 1993). For most trace gases the limiting process for the transfer rate across the air–sea interface is the transfer across a thin boundary layer on the water side of the interface (e.g. Liss and Slater 1974); this is due to the diffusion of gases through water being much slower than through air. The air phase and the water below the surface boundary layer are assumed to be well mixed by turbulence, and so the gas concentrations in these regions are effectively constant. Wania and Mackay (1999) showed with some illustrative calculations that these assumptions should be reasonable for the air–sea exchange of POPs. Thus, for any particular location, the flux of POPs between the air and the sea is the product of two principal factors: the difference in partial pressure of POPs between the air and the bulk water, which can be considered as the thermodynamic driving force, and the gas exchange rate (transfer velocity), which is the kinetic parameter. The transfer velocity incorporates both the diffusivity of the gas in water (which varies with temperature and between different gases), and the effect of physical processes within the water boundary layer.

The kinetics of air–sea exchange in the open ocean is driven by near-surface turbulence with wind stress being the major controlling factor. In a wind driven ocean–atmosphere system, turbulence is generated due to shear, buoyancy, and large- and micro-scale wave breaking. The gas transfer dependency on wind speed over the ocean is often non-linear (Wanninkhof 1992). In low wind conditions, when buoyancy may dominate in generating the turbulence, this dependency is weak. Other factors such as gas exchange by bubbles created by breaking waves, organic films in the sea-surface microlayer, and enhancement by chemical transformations, may also affect the transfer velocity at sea. Additionally, variability is introduced by the presence of small-scale waves and rain. However, the impact of these factors on the air–sea exchange of organic contaminants is not yet fully understood. Many organochlorines are semi-volatile so they can occur in the atmosphere in both gaseous and condensed states under ambient temperatures. Therefore temperature may also play a central role in the air–sea transfer of POPs.

FANTOM uses a description of the gaseous air–sea gas exchange based on the stagnant two-film theory formulated by Whitman (1923) and restated by Liss and Slater (1974), with the adoption of the fugacity formulation as described by Mackay (2001). Accordingly, the net mass transfer across the air–sea interface is expressed as a product of a kinetic parameter (which represents the resistance to interfacial transfer) and a term representing the deviation from the chemical equilibrium between air and water as a driving force for interfacial transfer. The chemical equilibrium between the two compartments is controlled by the ambient parameters (e.g. temperature and wind speed), physical-chemical properties of the pollutant and its abundance in the environment.

The two mass transfer coefficients, u_1 and u_2 (m s^{-1}), for the stagnant (unstirred) atmospheric boundary layer and for the stagnant water layer close to the air-water interface are calculated as a function of wind speed, WS (m s^{-1}), at 10 m above the surface using relationships (according to Schwarzenbach et al. 1993):

$$u_1 = 6.5 \cdot 10^{-4} \cdot (6.1 + 0.63 \cdot WS)^{0.5} \cdot WS \tag{2.3}$$

$$u_2 = 1.75 \cdot 10^{-6} \cdot (6.1 + 0.63 \cdot WS)^{0.5} \cdot WS \tag{2.4}$$

Fugacity capacity describes the capacity of a medium to retain a POP at a certain fugacity in that medium. The fugacity capacities of air and water, Z_a and Z_w (mol m^{-3} Pa^{-1}), at air temperature T_a (K) and sea surface temperature T_w (K) are calculated as:

$$Z_\mathrm{a} = \frac{1}{R \cdot T_\mathrm{a}} \tag{2.5}$$

$$Z_\mathrm{w} = \frac{1}{H_\mathrm{c}(T_\mathrm{w})} \tag{2.6}$$

where R is the ideal gas constant ($R = 8.314$, Pa m^3 mol^{-1} K^{-1}) and H_c is the Henry's law constant (Pa m^3 mol^{-1}) at T_w.

H_c is used to describe the equilibrium partitioning of trace gases between air and water. Experimentally derived relationships for H_c are calculated from a temperature dependent equation (Kucklick et al. 1991; Paasivitra et al. 1999; Sahsuvar et al. 2003) using slope m (K) and intercept b:

$$\log H_c = b + \frac{m}{T_w} \tag{2.7}$$

The overall exchange rate constant, D_{wa} (mol Pa^{-1} s^{-1}), for volatilisation from sea water is calculated according to Mackay (2001) and Wania et al. (2000):

$$D_{wa} = \frac{A_w}{1/u_1 \cdot Z_a + 1/u_2 \cdot Z_w} \tag{2.8}$$

where A_w (m^2) is the surface area of the water. Since transfers from the atmosphere to the sea surface by dry particle and wet depositions are also calculated (Sect. 2.2.2 and Sect. 2.2.3), the gaseous exchange rate constant for the dry gaseous deposition is assumed to be the same as that for volatilisation from sea water.

The net mass transfer rate, $m_{a\text{-}w}$ (mol s^{-1}), is calculated for the pollutant gaseous concentrations in the air, C_a (mol m^{-3}), and dissolved in sea water, C_w (mol m^{-3}):

$$\frac{dm_{a-w}}{dt} = D_{wa} \cdot \left(\frac{C_a}{Z_a} - \frac{C_w}{Z_w} \right) = D_{wa} \cdot \left(C_a \cdot R \cdot T_a - C_w \cdot H_c(T_w) \right) \tag{2.9}$$

The air–sea flux, $F_{a\text{-}w}$ (ng m^{-2} s^{-1}), to the surface is then re-calculated from Eq. 2.9 using the pollutant's molar mass M (g mol^{-1}). The direction of the flux $F_{a\text{-}w}$ is determined by its sign (i.e. positive values of $F_{a\text{-}w}$ indicate gaseous deposition, and negative values indicate volatilisation from the sea surface).

2.2.2 Dry particle deposition

Organic contaminants sorbed to atmospheric aerosol particles can settle to the sea surface by dry particle deposition. This process is known to be an important source of several anthropogenic, particulate-bound POPs in critically important waters such as the north Atlantic Ocean, the coastal mid-Atlantic waters, and the North Sea. The North Sea is especially subject to deposition of anthropogenic air pollutants as it lies in close proximity to heavily polluted urban and industrial areas.

The dry deposition flux F_{dry} (ng m^{-2} s^{-1}) from the atmosphere to the sea surface, is expressed in FANTOM as a product of the pollutant particle-bound con-

centration in air, C_{ap} (ng m^{-3}), at some reference height and an empirical parameter called dry deposition velocity, v_{dep} (m s^{-1}), giving:

$$F_{dry} = C_{ap} \cdot v_{dep} \tag{2.10}$$

Dry deposition velocities depend on particle size, underlying surface properties and meteorological parameters (e.g. wind speed). Accordingly, the pollutant's deposition velocity over vegetated surfaces is a function of the vegetation activity, the canopy wetness, turbulent transport through the canopy to the soil, and uptake by the soil. The pollutant's deposition velocity over the oceans is controlled by turbulence. Over sea surfaces the following processes also play a role: bubble bursting causing the breakdown of the quasi-laminar boundary layer, scavenging of the sulphate aerosol by sea spray, and aerosol growth due to high local relative humidity.

The deposition velocity of a pollutant can be calculated using an analogue to Ohm's law in electrical circuits: $v_{dep} = (R_a + R_b + R_c)^{-1}$, where R_a is the aerodynamic resistance, which is the same for all gases, R_b is the quasi-laminar sublayer resistance, and R_c is the total surface resistance of the gas. The latter resistance encompasses several separate deposition pathways, depending on the surface type.

For this study a uniform value of $v_{dep} = 2 \times 10^{-5}$ (m s^{-1}) was used. This was based on an empirical relationship between v_{dep} and the mass median diameter (an average value used to describe aerosols particles) for oceanic conditions (McMahon and Denison 1979; Slinn 1983) and the assumption that a pollutant's distribution follows the air particles size distribution which peaks in the accumulation mode.

Atmospheric concentrations reported by the monitoring programmes often represent the total (gaseous and particle sorbed) pollutant concentration in air. The fraction of the total pollutant's concentration in air sorbed by aerosol particles, f_{ap}, is needed to estimate the dry particle deposition flux. It can be calculated based on an empirical relation which assumes that the equilibrium between the bound fractions of the gaseous and aerosol particles is determined by the substance vapour pressure and is independent of the particles' chemical properties (Junge 1977; Pankow 1987):

$$f_{ap} = \frac{s \cdot \theta}{P_{ol} + s \cdot \theta} \tag{2.11}$$

where P_{ol} (Pa) is a temperature dependent saturated vapour pressure for supercooled liquid (i.e. liquid water at temperatures less than 0°C). Its temperature dependency is calculated using the same relationship as is used for Henry's law con-

stant (see Eq. 2.7). The values of the specific aerosol surface, θ (m^2 m^{-3}), and adsorption constant, s (Pa m^{-1}), used in this study are treated as constants (Table A.1) which are representative of North Sea conditions (Pekar et al. 1998).

2.2.3 Wet deposition

Due to their semivolatility POPs are episodically scavenged from the atmosphere by precipitation in both the gas and particulate phases (Pankow 1987; Bidlemann 1988). During wet periods the removal of gaseous and particle sorbed compounds dominates other depositional processes. Because precipitation is an intermittent and a local phenomenon, it is crucial to consider its spatial and temporal variability.

The wet deposition flux, F_{wet} (ng m^{-2} s^{-1}), is calculated as a product of the pollutant concentration in precipitation, C_{pr} (ng l^{-1}), which includes both the dissolved and particulate phases, and precipitation rate, P (m s^{-1}), so:

$$F_{wet} = C_{pr} \cdot P \tag{2.12}$$

In the present model configuration no distinction is made between precipitation scavenging of vapours and particles. Spatial and temporal distributions of C_{pr} are based on measurements as described in Sect. 3.4.4. Fluxes of wet deposition contaminants have large fluctuations in the North Sea region due to differences in precipitation levels.

2.3 Phase distribution

Many POPs are hydrophobic which means that they have low solubility in water. They are also lipophilic implying that they have high solubility in lipids. These properties suggest that POPs may be present in sea water either freely dissolved or bound to the suspended particulate matter (SPM). Partitioning on SPM occurs because the particles typically contain spaces and their surfaces can resemble lipids.

Redistribution between the dissolved and particulate phases essentially affects the dynamics of the distribution of pollutant concentration in the marine environment. The dissolved pollutant fraction follows the path of the water masses, while the particles bound fraction quickly sedimentises (sinks to the bottom due to gravitation) and remains in areas where sedimentation is promoted. Transport of POPs from sediment to water is of great concern since it is suspected that historically polluted sediments may act as a source to the overlying water column (OSPAR 2000; BSH 2005), thereby prolonging the exposure of biota long after emissions have stopped.

In sea water, organic matter is strongly sorbing POPs. It is characterised by particulate organic carbon (POC). POC is an organic carbon fraction of SPM which is

used in FANTOM as a sorbing matrix for POPs. Such an approach is commonly used in modelling the accumulation of POPs in biota (Skoglund and Swackhamer 1999; Malanichev et al. 2004) and their export to the deep sea (Scheringer et al. 2004).

The pollutant fraction bound to POC, f_{POC}, is calculated (Skoglund and Swackhamer 1999; Scheringer et al. 2004) as:

$$f_{\mathrm{POC}} = \frac{K_{\mathrm{oc}} \cdot C_{\mathrm{POC}}}{K_{\mathrm{oc}} \cdot C_{\mathrm{POC}} + 1} \tag{2.13}$$

The organic carbon–water equilibrium partition coefficient K_{oc} (l kg^{-1}) is pollutant specific (Sect. 2.3.2) and C_{POC} (mg l^{-1}) is the concentration of POC in solution (Sect. 2.3.1).

Eq. 2.14 implies that the transfer of POPs and thus their transport behaviour are controlled by the abundance of POC. In that case increasing POC content will transfer the chemical from the dissolved to the particulate state. Higher POC concentrations result in lower concentrations of POPs in the particulate phase. Most of the POC present in sea water is in the form of particles (Sect. 2.3.1), which sink to the sea bed by gravitational settling with a sinking velocity v_{set} (m s^{-1}). Correspondingly, the fraction of chemicals bound to POC that is removed from the upper sea layers together with sinking particles, F_{set} (ng m^{-2} s^{-1}), is calculated as:

$$F_{\mathrm{set}} = v_{\mathrm{set}} \cdot f_{\mathrm{POC}} \cdot C \tag{2.14}$$

Many organic compounds are hydrophobic (i.e. they are not easily dissolved in water) and are characterised by high values of K_{ow} (>10^5). These compounds are mostly bound to POC and tend to disperse and accumulate in the sediment rather than in the water column.

2.3.1 Particulate organic carbon content

Sea water, especially the upper photic layer (a layer where solar radiation penetrates) and in the bottom layer with the resedimented particles, is rich in various suspended particulate matter. The total SPM in sea water consists of inorganic and organic portions, namely microflocs of mineral particles and organic matter. The fine sediment (mud) or particles smaller than 20 μm make up to 85% of SPM in the North Sea (Eisma and Kalf 1987). The composition of SPM in sea water is controlled by a number of factors such as the rate of primary productivity, the amount of lithogenous input to the sea, and the sinking rate. Biogeochemical processes leading to release and/or uptake of elements from sea water in the horizontal or vertical fluxes of SPM are also responsible for its composition.

The shelf seas are normally more productive than the open ocean. SPM concentrations in the North Sea, for instance, are in the order of 0.1–100 mg l^{-1} (Puls et al. 1994). Much of it is biogenic consisting of detritus and planktonic algae (Eisma and Kalf 1987). In winter the fraction of organic matter is about 20% of the total SPM, whereas in other seasons the appearance of SPM may be dominated by phytoplankton (Puls et al. 1994).

The concentration of POC, C_{POC} (mg l^{-1}), in FANTOM is a composite of the concentrations of biogenic organic carbon, C_{bio}, and sediment organic carbon, C_{sed}, so that:

$$C_{\mathrm{POC}} = C_{\mathrm{bio}} + C_{\mathrm{sed}} \tag{2.15}$$

The biogenic concentration, C_{bio}, is the POC consisting of phytoplankton, zooplankton, bacteria and slow sinking and fast sinking detritus suspended in the water column. These concentrations are calculated by an ecosystem model, described in detail by Pätsch et al. (2002).

Sediment organic carbon concentration, C_{sed}, is derived from plant and animal detritus, bacteria or plankton formed in situ, or from natural and anthropogenic sources in catchments. In the shallow regions under stormy conditions the bottom sediment can return to the sea surface. Measurements (van der Zee and Chou 2005) suggest that this sediment is an important contribution to the POC burden in the North Sea, especially in winter when sea currents are strong and storm events are frequent.

The sediment organic carbon is calculated in FANTOM as a portion of the total fine sediment distributed in the upper 2 cm of the sediment bed, a layer where nearly all the benthic biomass is found (Pohlmann and Puls 1994). The POC content, p_{POC}, of the bottom fine sediment, p_{mud} (in % of dry mass), is calculated based on the measurements reported by Wiesner et al. (1990):

$$p_{\mathrm{POC}} = \begin{cases} 5 - 1.4\log\left(p_{\mathrm{mud}}\right) & if \; P_{\mathrm{mud}} < 50\% \\ 2.6 & P_{\mathrm{mud}} > 50\% \end{cases} \tag{2.16}$$

The bottom sediment enters the near-bottom water layer of the model due to erosion. It is diffused to the upper water layers and may be returned to the bottom sediment via deposition by settling. In FANTOM the deposition of SPM and erosion of the bottom sediment are controlled by the bed shear velocity. This is a characteristic of the bed shear stress that depends on the wind and density driven currents, tidal currents and waves. The shear stress is calculated according to the formulation given by Soulsby (1997). Wave induced shear stress is dominant in shallow waters, such as the North Sea (Puls et al. 1994). Therefore, only bed shear velocity due to waves, v_*, is considered in the model. The threshold shear velocity for erosion, $v_*^{\mathrm{cr,e}}$, is 0.028 m s^{-1} and the one for deposition, $v_*^{\mathrm{cr,d}}$, is 0.01 m s^{-1}

(Pohlmann and Puls 1994). Thus, if $v_* > v_*^{cr,e}$, sediments from the disturbed sea bottom enter the water column and are distributed uniformly in the bottom water layer (Sündermann and Puls 1990). The amount of eroded SPM depends on the fraction of fine sediment at the bottom. Eroded SPM is then diffused through the water column. SPM in the water column is subject to gravitational sinking with the uniform settling velocity, v_{set}, of about 25 m day^{-1}. Further, if $v_* < v_*^{cr,d}$, a portion of SPM in the bottom water layer is deposited back to the bottom sediments.

In the sediment where oxygen is present, the deposited SPM is re-distributed vertically by benthic organisms (worms, bivalves and molluscs) which constantly disturb the sediment by burrowing and feeding. Such bioturbation generally increases the transfer of pollutants over the sediment-water interface. Vertical bioturbation is described in the model as a diffusive transport process similar to that used by Pohlmann and Puls (1994).

In the water column SPM settles due to gravitational sinking. In the deep sea this process is the ultimate sink for SPM, whereas in the shallow regions resuspension (erosion of previously deposited SPM) caused by currents and waves carries it back to the water column. Therefore, in sea water a certain fraction of particles is of resuspended origin. The gross sedimentation refers to the total load of particulate deposition to the sediments, and the net sedimentation is the gross sedimentation minus resuspension.

Pejrup et al. (1996) showed that when a water column is stratified the resuspended fraction of the gross sedimentation flux decreases exponentially from the bottom upwards. The implication of this for POC fluxes is that under stratified conditions essentially no POC was resuspended more than 6 to 10 m above the bottom in a shallow bay such as the one investigated (Aarhus Bight, Denmark). One other situation where the water column was mixed was also observed. This was encountered when the water column had vertically homogenous temperature and salinity. Thereby it became unstable, and so storm winds could mix the water and cause resuspended matter to be distributed throughout the water column.

Finally, knowing the mass of the bottom sediment in the water column at a specific time and its density allows the sediment organic carbon concentration, C_{sed}, to be calculated.

The approach described here provides realistic first order spatial and temporal distributions of POC. The description of the full SPM dynamics is given elsewhere (Pohlmann and Puls 1994; Puls et al. 1994; Sündermann and Puls 1990).

2.3.2 Fraction bound to particulate organic carbon

The calculation of the particle-bound fraction of POPs is based on the assumption that the equilibrium between the pollutant's concentrations in the dissolved and particulate phases is established instantaneously (Skoglund et al. 1996;

Skoglund and Swackhamer 1999). As equilibration time is neglected the following relationship is used:

$$\frac{C_{\mathrm{p}}}{C_{\mathrm{w}}} = K_{\mathrm{oc}} \cdot C_{\mathrm{POC}} \tag{2.17}$$

where C_{p} (ng l^{-1}) and C_{w} (ng l^{-1}) are the concentrations of POPs associated with POC and with the dissolved phase; and C_{POC} (mg l^{-1}) is the concentration of POC in solution (Sect. 2.3.1).

The organic carbon–water equilibrium partition coefficient, K_{oc} (l kg^{-1}), is commonly employed in modeling organic chemicals (Malanichev et al. 2004; Koziol and Pudykiewicz 2001) to calculate their partitioning in different aquatic particulate matrices. The K_{oc} value is compound specific. It is frequently estimated by an empirically derived relation based on the hydrophobicity expressed by the dimensionless octanol–water partition coefficient K_{ow}. So according to Karickhoff (1981) K_{oc} is given by:

$$K_{\mathrm{oc}} = 0.411 \cdot K_{\mathrm{ow}} \tag{2.18}$$

The octanol–water partition coefficient is the ratio of the concentration of a chemical in octanol and in water at equilibrium at a specified temperature. Octanol is an organic solvent that is used as a surrogate for natural organic matter. This approach to describing the phase partitioning in water is valid for the fast uptake into the organic matter.

Because natural organic matter has variable composition, one could expect its capacity to sorb a POP molecule to vary somewhat. Some studies have indicated that the composition of the organic matter (e.g. Carbon:Nitrogen ratio) seems to influence the degree of POP association to particles (Koelmans et al. 1997), as well as the uptake in organisms fed with contaminated organic matter of varying composition (Gunarsson et al. 1995).

Furthermore, equilibrium concentrations are not instantaneously established between water and organic matter. This implies that the particle size and content of more condensed organic matter influences the time to reach equilibrium. In the water column, a significant portion of the particles is living plankton (Sect. 2.3.1). It has been suggested that during high biological activity (i.e. during spring blooms) phytoplankton can grow at a faster rate than the POPs are sorbed on the plankton. Thus the uptake process may be far from the equilibrium and a kinetic description is more adequate (Skoglund et al. 1996; Axelman et al. 1997). However, on the time scale of years a kinetic approach is not needed (Swackhamer and Skoglund 1993).

2.4 Degradation in sea water

Some pollutants degrade in the environment. The period of degradation of a half mass of different POPs in the marine environment may vary from several weeks to several hundreds years. This degradation in the marine environment is due to several processes – the most significant of them are hydrolysis, photodegradation and biodegradation.

Combined abiotic (due to photolysis and hydrolisis) and biotic degradation in sea water is represented in the model by a first order rate decay coefficient, k_{deg} (s^{-1}), with the higher order kinetics being neglected. It is assumed that degradation is linearly dependent on the compound total concentration C:

$$\frac{dC}{dt} = -k_{\text{deg}} \cdot C \tag{2.19}$$

No measurements of degradation in sea water exist. Consequently the k_{deg} value for a pollutant (Table A.1) has been chosen on the basis of a thorough compilation of physical-chemical properties of selected POPs (EU TGD 1996; Klöpffer and Schmidt 2001). The k_{deg} for each pollutant is given by the fresh water values divided by a factor of 10 to account for reduced biotic degradation in sea water relative to fresh water. Following Lammel et al. (2001) and the EU Technical Guidance Document on Risk Assessment (EU TGD 1996) the k_{deg} value is assumed to double per 10 K temperature increase. Degradation in the sediment is neglected.

3 FANTOM: Model Setup

In this study FANTOM was applied for the North Sea. The model area is described in Sect. 3.1. Ocean circulation drives the transport of pollutants in the marine environment. The North Sea circulation pattern and circulation model setup are presented in Sect. 3.2. Then Sect. 3.3 introduces the distribution of POPs in terms of their physical-chemical properties and environmental behaviour. Finally Sect. 3.4 gives an overview of the boundary and initial conditions necessary to perform model simulations as well as providing a survey of the input data on the levels of POPs.

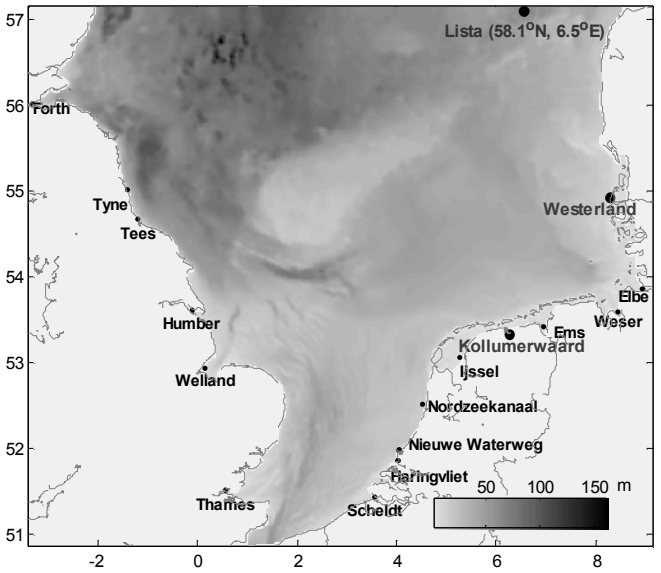

Fig. 3.1. FANTOM domain and bathymetry (depth in m) on a grid of 1.5'×2.5' (corresponding to 2.5–3 km). Geographical locations of three stations (Wseterland, Kollumerwaard and Lista) where measurements of γ-HCH, α-HCH and PCB 153 atmospheric concentrations were available are shown (Lista lies outside of the modelling domain). River mouths are indicated (the rivers Rhine and Meuse drain into the North Sea through Ijssel, Nordzeekanaal, Nieuwe Waterweg and Haringvliet).

3.1 Model Area

The model's domain covers the southern and central North Sea up to 57.1°N (Fig. 3.1); it is a shallow region with mean depth of 50 m and a maximum depth of 160 m. The area of the open water is 311,510 km^2 with a volume of 13,908 km^3. The horizontal resolution of the model is 1.5'×2.5' (corresponding to 2.5–3 km) and there are 21 vertical layers of varying thickness (i.e. 5 m in the upper 50 m and 10 m in lower layers).

In the North Sea the distribution and mixing of water masses is largely subject to tidal currents, meteorological conditions, and run-off from rivers into the Atlantic Ocean and the Baltic Sea. Westerly winds prevail over the North Sea. The predominant circulation driven by winds and tides is anti-clockwise along the North Sea coast (Fig. 3.2) causing short flushing times (i.e. retention time of water masses). That means that the existing climate happens to be favourable for the health of the North Sea ecosystem.

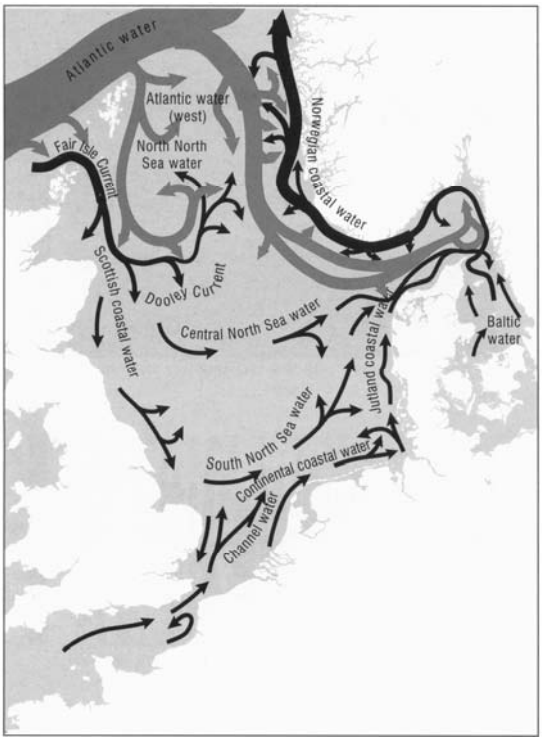

Fig. 3.2. Schematic diagram of general circulation in the North Sea. The width of arrows indicates the magnitude of volume transport; grey arrows indicate Atlantic water. Source: OSPAR, 2000.

Under the existing circulation pattern of the North Sea, the anthropogenic pollutants will be transported out of the system fairly fast. However, this circulation pattern can be reversed over part of the North Sea when transient prevailing easterly winds cause an extension of water mass flushing times (Sündermann et al. 2002). The flushing time of water, calculated by the inflows and outflows, is estimated to be about 1 year for the entire North Sea (OSPAR 2000). However the flushing time varies in different subregions: it ranges from 28 days in the northern part of the North Sea to 40 days in the central part (Lenhart and Pohlmann 1997). The prevailing currents cause polluted coastal waters to have high residence time and to be transferred along the coastline. This aspect is of key importance because, lying between land and sea, the coastal habitats are subject to a range of influences and are particularly sensitive to anthropogenic pressure.

3.2 Ocean circulation

The transport processes in FANTOM, which are driven by ocean currents, are calculated from the distribution of the flow field (Sect. 2.1) available from an ocean circulation model. In this study the HAMburg Shelf Ocean Model (HAMSOM) was coupled with FANTOM (Fig. 3.3). HAMSOM is a baroclinic, primitive equation circulation model based on a semi-implicit numerical scheme (Backhaus 1985; Pohlmann 1996).

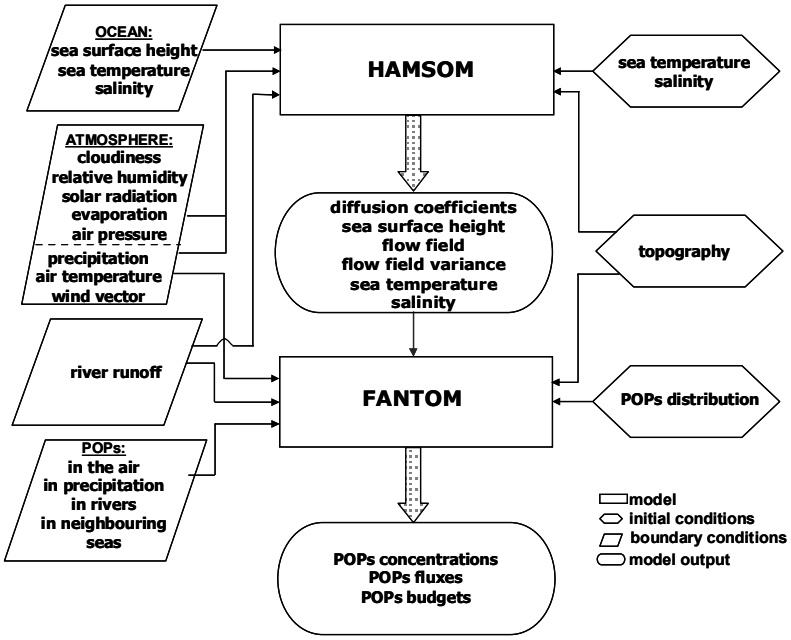

Fig. 3.3. The input-output diagram for the combined HAMSOM and FANTOM system.

HAMSOM covers the same domain and uses the same spatial resolution of 1.5'×2.5' as FANTOM (Fig. 3.1). Simulations were carried out with a time step of 10 minutes. Atmospheric forcing for HAMSOM is calculated using the ERA-40 data provided by ECMWF (ECMWF 2005). Boundary conditions for the open ocean (northern and southern boundaries) are obtained from a HAMSOM simulation covering the entire North Sea and a part of the north-eastern Atlantic with a coarser resolution (Pohlmann 1996).

The results of the circulation model (e.g. flow fields and their variances, vertical diffusion coefficients, sea temperature and salinity distribution, and sea surface height – see Fig. 3.3) are stored as daily means averaged over two periods of the predominant semidiurnal lunar tide M_2 (Bartels 1957). Such a coupling approach has been used previously (Pohlmann 1987; Luff and Pohlmann 1995).

3.3 Pollutant selection

The modelling approach used with FANTOM puts certain restrictions on the pollutants that can be studied with the model.

The first criterion is the environmental behaviour of the pollutant – it has to be retained in water. The physical-chemical properties in combination with environmental conditions in part control the fate of POPs in the environment. These properties include aqueous solubility, vapour pressure, partitioning coefficients between water-solid, air-solid or air-water, and half-lives in different media. Therefore, it is possible to assess the pollutant's environmental fate from its distribution properties.

Fig. 3.4 (after UNEP 2003) uses a space defined by the octanol–air and air–water partition coefficients log K_{OA} and log K_{AW} to characterise a chemical's distribution properties (octanol serves as a surrogate for organic matter in the environment). Increasing K_{OA} implies decreasing volatility, and increasing K_{AW} implies decreasing water solubility. Each organic chemical occupies a location in this chart. Most of the organic pollutants plotted on the chart (Fig. 3.4) fall into the part where categories "multi-hop", "single hop" and "no hop required" intersect. Furthermore, the boundaries between the categories are not sharp and a single pollutant can belong to more than one group.

Partitioning coefficients (e.g. K_{OA} and K_{AW}) are temperature dependant, meaning that categorisation of POPs and consequently their environmental fate may change depending on the ambient temperature.

The second criterion in selecting compounds is that data availability should be sufficient for the modelling experiments. For this study three compounds were chosen: the two hexachlorocyclohexanes, γ-HCH (lindane) and α-HCH, and PCB 153 which is a congener of polychlorinated biphenyls frequently found in the environment.

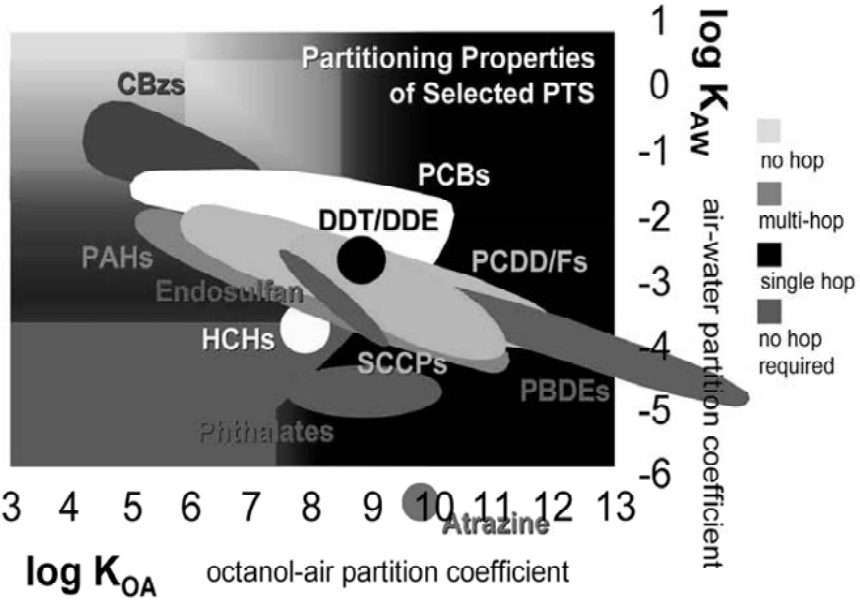

Fig. 3.4. Categorisation of the behaviour of organic substances as a function of their distribution characteristics defined by two physical-chemical properties: air–water and octanol–air partition coefficients (Adapted from UNEP Global Report, 2003). Four different behaviour categories are identified and assigned sections of the diagram. "*No hop*" – chemicals that are so volatile that they do not deposit to the Earth's surface and thus remain in the atmosphere. "*Multi-hop*" – chemicals that readily shift their distribution between the gas phase and condensed phase (soil, vegetation, water) in response to changes in environmental temperature and phase composition, and therefore can travel long distances in repeated cycles of evaporation and deposition. "*Single hop*" – chemicals that are so involatile or so water-insoluble that they can undergo long-range transport only by being attached to suspended solids in air and water. "*No hop required*" – chemicals that are sufficiently water soluble to undergo long-range transport by being dissolved in the water phase

3.3.1 Gamma–hexachlorocyclohexane (γ–HCH)

Hexachlorocyclohexane (HCH) is a manufactured chemical that exists in eight chemical forms called isomers. Technical HCH is pesticide consisting if a mixture of five stable isomers which have been shown to have serious short- and long-term health effects; the isomers are α: 60–70%, β: 10–12%, γ: 6–10%, δ: 3–4% and ε: 3–4% (Willet et al. 1998). The last two of these compounds are not routinely found in environmental samples. Lindane (almost pure γ-HCH) is a white solid that may evaporate into the air as a colourless vapour with a slightly musty odour. Lindane was chosen as it is a pollutant which is mostly observed in the dissolved phase in water. It is a semi-volatile compound with high vapour pressure, a rela-

tively high water-air partitioning coefficient and a low octanol-water partitioning coefficient (Table A.1).

Although HCH was first prepared in the 19th century, the insecticidal properties of lindane were discovered only in the early 1940s. Technical HCH was banned in the 1980 after its toxic effects became evident in the environment. Lindane contains more than 90% of γ-HCH, but the lindane used in many countries is almost pure γ-HCH (Willet et al. 1998). Lindane is still in relatively widespread use in developed nations as well as in the developing world as an insecticide in agriculture, a wood and building preservative, and a biocide to combat lice and scabies. It has been banned by the European Union countries for plant protection and California has banned lindane-based products used to treat lice and scabies. In Europe, lindane usage was reduced by two-third between 1970 and 1996 (Breivik et al. 1999). But despite restrictions and bans, α-HCH, β-HCH and γ-HCH are still widely found in the North Sea. A large proportion enters the water through flooding, run-off from treated areas and incorrect disposal of waste materials into farm drains and sewage systems. Atmospheric depositions can also contain γ-HCHs transported from remote regions (Semeena and Lammel 2005).

Human exposure to lindane happens mostly from eating contaminated foods or by breathing contaminated air in the workplace.

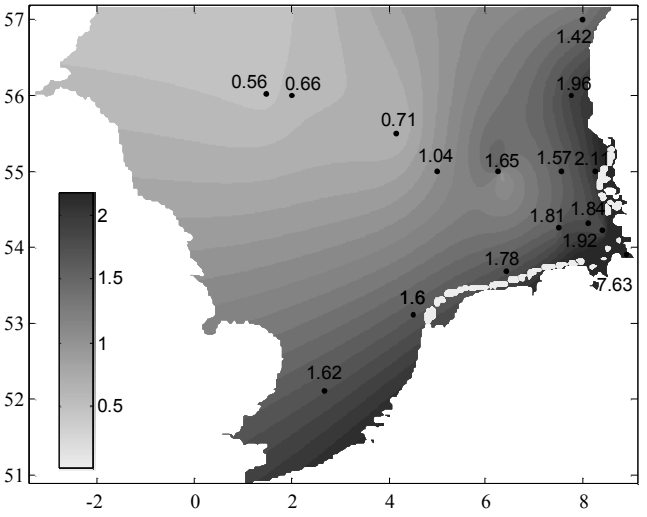

Fig. 3.5. Initial distribution of γ-HCH concentration (ng l^{-1}) in the North Sea in the summer 1995 restored from measurements. Points indicate locations where measurements were available.

Information about HCH isomers in general and γ-HCH in particular is relatively complete. γ-HCH is subject to regular monitoring in the sea through national (Bund-Länder monitoring programme) and international (OSPAR, HELCOM) monitoring programmes so its distribution is known with some confidence (Fig. 3.5).

3.3.2 Alpha–hexachlorocyclohexane (α–HCH)

Alpha-hexachlorocyclohexane (α-HCH) is another isomer of the technical HCH. It possesses properties similar to those of γ-HCH (Fig. 3.4), but it has a different environmental behaviour because α-HCH was banned two decades ago as a constituent of the technical HCH whereas lindane is still used in some countries as a separate product. The α-HCH has a high vapour pressure, high water-air partitioning coefficient and low octanol-air partitioning coefficient. It partitions more readily into water than into solid particles. Therefore α-HCH is often modelled as a pure gas-phase chemical (Hansen et al. 2004).

Release of α-HCH to the environment probably occurs mainly from the use of technical HCH as a pesticide. Small amounts of α-HCH may result from the isomerisation of lindane (γ-HCH) upon exposure to sunlight (Hühnerfuss et al. 1997). When released to water, α-HCH is not expected to volatilize or hydrolyze extensively. It will bioconcentrate slightly in fish and other aquatic organisms.

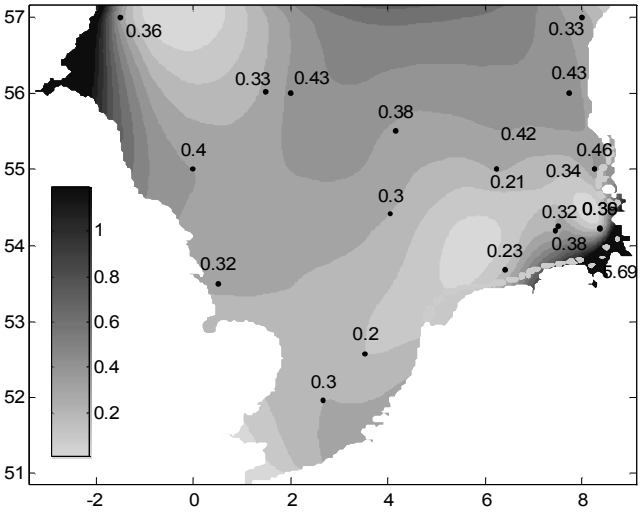

Fig. 3.6. Initial distribution of α-HCH concentration (ng l^{-1}) in the North Sea in the summer 1995 restored from measurements. Points indicate locations where measurements were available.

Monitoring data indicates that α-HCH is a contaminant in air, water, sediment, soil, fish and other aquatic organisms, food and humans. Human exposure results primarily from food. No data on the rate of hydrolysis of α-HCH is available. However, based on the relatively greater stability of α-HCH (in particular its (-) enantiomer) compared to lindane (which has a smaller number of axial chlorines), it may hydrolyze more slowly than lindane.

The distribution of α-HCH in the North Sea is shown in Fig. 3.6.

3.3.3 Polychlorinated biphenyl 153

Polychlorinated biphenyls (PCBs) are industrial chemicals which were synthesized and commercialized in 1929. PCBs were used as coolants and lubricants in transformers, capacitors, and other electrical equipment because they do not burn easily and are good insulators. The manufacture of PCBs was stopped in Europe in 1976 because of evidence that they build up in the environment and can cause harmful health effects. Restrictions on the use of PCBs stopped their production in all countries surrounding the North Sea by 1985 (SRU 2004).

Most of the input of PCBs into the environment occurred before 1980. The greatest share of their inputs into the North Sea comes from the atmosphere. Nowadays the sources of PCBs are largely thought to be waste and contaminated sites, especially non-regulated disposal of small capacitors that contain PCBs. High concentrations in the livers of cod have resulted in the issuing of warnings about the consumption of fish liver for many of the Norwegian fjords. Background concentrations for PCBs in blue mussels are exceeded by a factor of 2 to 20 (OSPAR 2000).

PCBs are a group of 209 individual chlorinated hydrocarbon compounds (known as congeners) with the same general chemical structure. Individual PCBs differ widely in terms of their vapour pressures, water solubilities and susceptibility to degradation; these differing properties influence their environmental fate (Coulston and Kolbye 1994). These differences in physical-chemical behaviours are determined by the number and pattern of chlorine substitutions in the individual congeners (Mackay et al. 2000). PCBs are almost insoluble in water because of their relatively high log K_{ow} values (Fig. 3.4). Generally, the solubility in water decreases as the number of chlorine substitutions increases. Similarly, the vapour pressure of individual PCBs decreases as chlorine substitutions increase. The environmental fate and behaviour of PCBs is largely governed by the degree of chlorination. However, all PCBs congeners are highly toxic, extremely persistent and bioaccumulating. This means that even though their manufacture and use have been stopped, their presence in the North Sea environment is still a threat.

PCB 153 is a congener of PCB and is often used as a PCB representative of all the others, and it constitutes around 10% of the total amount of PCBs. The measured PCB 153 distribution in the North Sea is shown on Fig. 3.7.

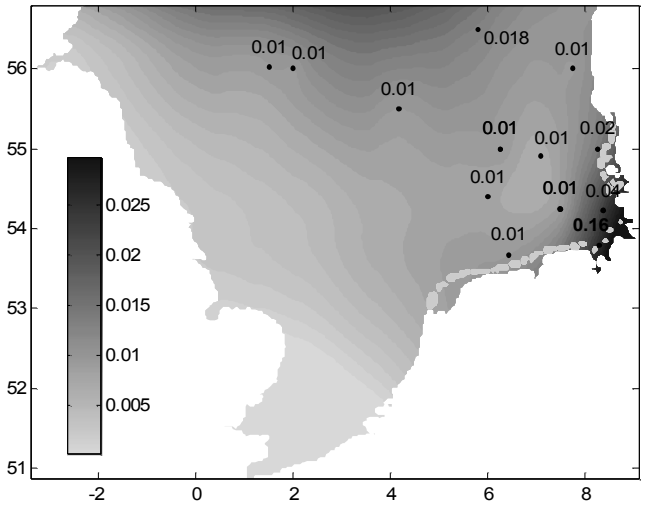

Fig. 3.7. Initial distribution of PCB 153 concentration (ng l^{-1}) in the North Sea in the summer 1995 restored from measurements. Points indicate locations where measurements were available.

3.4 Initial and boundary conditions

Physical-chemical properties of POP-like chemicals, environmental parameters and release data are required as input data for the model. Release data includes the initial distribution of the selected chemical and its values on the boundaries throughout the simulation period. For the modelling domain, the following boundaries are used: air–sea interface, boundaries with the neighbouring water bodies (i.e. Atlantic Ocean, Baltic Sea and English Channel), and the inflowing rivers that drain into the North Sea. Many of these parameters are of limited availability and have to be estimated by extrapolation and interpolation methods. Those values that are available for a given parameter often exhibit large variability and uncertainties.

Daily mean distributions of flow velocity components and their variances, sea surface height, diffusion coefficients, salinity and sea temperature were obtained from the corresponding HAMSOM simulations.

Compound specific physical-chemical properties and degradation rates in sea water are taken from Klöpffer and Schmidt (2001), Semeena and Lammel (2005) and Sahsuvar et al. (2003), and these are listed in Table A.1.

The influence of sources outside the model domain is taken into account by using measurements as boundary values.

3.4.1 Initialisation

The initial distribution of the selected POPs and their concentrations on the sea boundaries were interpolated based on non-filtered samples (Theobald et al. 1996) and therefore they represent the total concentration (dissolved and particle-bound). Initial conditions for the concentration are defined by the function C^0:

$$C(x,y,z,0) = C^0(x,y,z) \tag{3.1}$$

Initial distributions of γ-HCH, α-HCH and PCB 153 are shown on Fig. 3.5, Fig. 3.6 and Fig. 3.7.

3.4.2 Oceanic boundary conditions

The oceanic concentration of POPs at the North Atlantic, Baltic Sea and the English Channel boundaries are extrapolated from the measured values used for the initialisation. Boundary conditions for the water boundaries B are prescribed:

$$C\big|_{(x,y,z)\in B} = C^B(x,y,z,t) \tag{3.2}$$

where C^B is the concentration at the water boundary. The boundary condition at the coast is:

$$\frac{\partial C}{\partial n}\Big|_{(x,y,z)\in\Gamma} = 0 \tag{3.3}$$

At the bottom, with the bottom depth of H, the pollutant flux is:

$$F\big|_{z=H} = F_{\text{set}} \tag{3.4}$$

The settling flux, F_{set}, is calculated according to Eq. 2.14.

3.4.3 River loads

River input is a significant source for some POPs in the North Sea. The river loads of the POPs from the European continental rivers, including the Elbe, Weser, Ems, Rhine and Meuse, and Scheldt (Fig. 3.1), are calculated in FANTOM as a product of the daily fresh water discharge, Q_{riv} ($m^3\ s^{-1}$) (Lenhart and Pätsch 2004), and the

concentrations of the POPs at the last tidal gauge station of each river, C_{riv} (ng l^{-1}) (Fig. 3.9 in Appendix D). Data for C_{riv} from the German rivers, provided by the relevant Environmental Agencies (ARGE-Elbe 2005; NLÖ 2005), was used. The concentrations of POPs in the Dutch rivers were taken from the Dutch database DONAR. The loads of POPs reported to OSPAR (2000) were used for the Thames and the Humber. Values of C_{riv} are available with different temporal resolutions (e.g. monthly means) and have to be interpolated to fit the temporal resolution of the model.

3.4.4 Atmospheric boundary conditions

Boundary conditions at the air–sea interface are based on measured concentrations of POPs in the air and in precipitation available through the EMEP monitoring programme. The precipitation intensity is calculated using the ECMWF ERA-40 data. The measured values from several EMEP stations (Fig. 3.1) were interpolated to the whole domain. The pollutant's flux on the sea surface is determined as:

$$F\big|_{z=0} = F_{\text{surf}} \tag{3.5}$$

The flux F_{surf} is calculated according to Eq. 2.2. Atmospheric data is discussed in Sect. 3.4.5.

3.4.5 Data compilation and quality

Because many model input parameters are of limited availability they have to be estimated by extrapolation and interpolation methods. Those values that are available for a given parameter often exhibit large variability and uncertainty.

(a) *Atmospheric concentrations*. Monthly mean atmospheric concentrations used in this study for all three POPs were based on the monthly mean values from the EMEP network (EMEP 2005); separate values were available for concentrations in air and precipitation. The values used were those from Lista.

(b) *River loads*. Concentrations in the rivers were available with different temporal resolution: monthly means for the rivers Ems and Weser, and weekly or bi-weekly means for the other continental rivers.

The variation in atmospheric concentrations and river loads of γ-HCH, α-HCH and PCB 153 between June 1995 and January 2002 are given in Fig. 3.8 and Fig. 3.9 (see Appendix). Note that the atmospheric concentrations and river loads of α-HCH and PCB 153 and river loads of γ-HCH exhibit large differences and therefore are presented on a logarithmic scale in these figures.

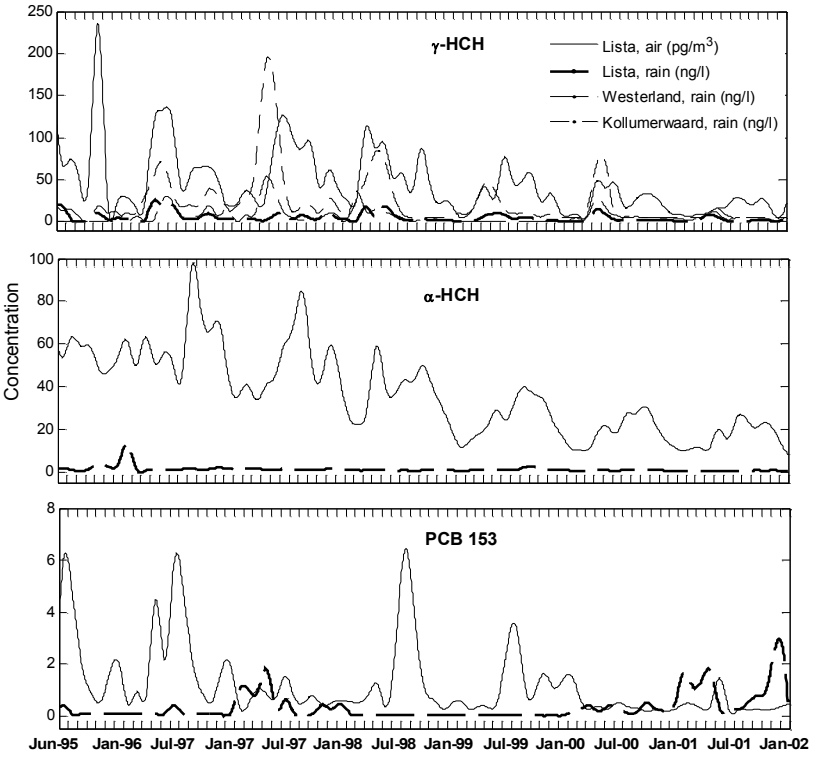

Fig. 3.8. γ-HCH, α-HCH and PCB 153 concentrations in the atmosphere at the EMEP stations. Geographical locations of the measurement sites are shown in Fig. 3.1.

Concentrations of γ-HCH in air (Fig. 3.8) and in the rivers (Fig. 3.9 in the Appendix) have decreased during the simulation period. Though only concentrations of γ-HCH in precipitation from Lista are used in this study, it is worth noting that there are significant differences in the measurements from Lista, Westerland and Kollumerwaard (Fig. 3.8).

Measured atmospheric concentrations of α-HCH and PCB 153 were available only at Lista between 1995 and 2001 (Fig. 3.8). Air concentrations of α-HCH measured at Lista decreased, whereas concentrations in precipitations remained more or less at the same level (EMEP 2005). For PCB 153 the concentrations in precipitation had slightly decreased by the end of 2001. In general, PCB 153 levels in the rivers and in the air do not show any trend within the studied period.

Atmospheric concentrations of the three selected pollutants used for this study were measured at coastal stations. Therefore there is no information on possible concentration gradients over the whole North Sea and in the subregions remote from the polluted coastal areas. For some pollutants, air concentrations over the coastal waters are expected to be higher than those over the open ocean waters be-

cause of the proximity to sources. However, there are indications that air sampled at Lista originates from the North Sea about 2/3 of the time (Haugen et al. 1998). Furthermore, measurements of atmospheric depositions of selected POPs in the Yellow Sea (Lammel et al. 2005) showed that gradients in air concentrations of "old" POPs over coastal waters are low. Since the measured air concentrations were available only from Lista they were used for the whole modelling domain.

Most of the data on the river loads of POPs is available through annual overviews which means that a large number of them cannot be used for nowcast simulations. Measured atmospheric concentrations of POPs have a very poor spatial coverage and monitoring stations are located only along the coasts. This can introduce additional uncertainties into the results from the model.

4 FANTOM: Model Evaluation

Model evaluation for the three POPs is presented in this chapter. Evaluation was preformed by comparing model results with measurements of the POPs in sea water over the period of simulation. Data used for evaluation is described in Sect. 4.1. Model evaluation for the POPs consisted of two stages.

(a) Calculated concentrations in sea water were compared with the measurements (Sect. 4.2, Sect. 4.3 and Sect. 4.4).

(b) Model sensitivity to input parameters was analysed (Sect. 4.5).

4.1 Data used for model evaluation

Although α-HCH, α-HCH and PCB 153 are well studied contaminants and are subject to national and international monitoring programmes, data availability remains an important constraint for constructing a measurement-based, spatially-resolved model. Unlike regular monitoring in the atmosphere, where monthly or even weekly measurements of these contaminants are available for the European region (e.g. EMEP), measurements of sea water concentrations are discrete in time and space due to operational constraints. This is illustrated by Table A.2 in the Appendix where the geographical location of each station, number of measurements of α-HCH, γ-HCH and PCB 153, and months when the sampling was made are listed. Measurements for PCB 153 were not available at locations N, O and P (Dutch EEZ) for the studied period. Furthermore, out of the three POPs considered in this study, measurements of PCB 153 are the scarcest.

Time series of measured α-HCH concentrations in sea water covering the simulation period were available from 18 locations (Fig. 4.1). Most of the data was provided by the German Oceanographic Data Centre (DOD 2005) covering only the German exclusive economic zone (EEZ) of the North Sea. Time series at locations N, O and P were from the Dutch EEZ of the North Sea provided by the Dutch database Waterbase (DONAR 2005).

At most of the locations, namely at A and G to P, measurements were made during warm seasons (May–September) when concentrations of pollutants were expected to reach a peak (Table A.2). At locations B, C, D and F measurements were conducted between November and February.

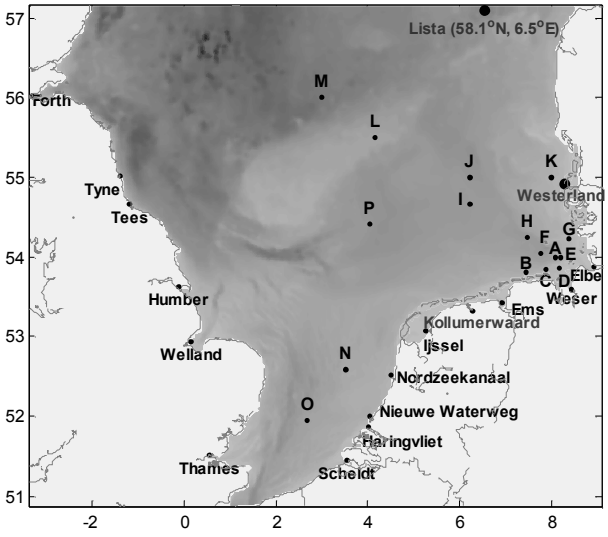

Fig. 4.1. FANTOM modelling domain and geographical locations of points where time series of observation were available for the model evaluation (labelled with letters). Data for points A to M was provided by the German Oceanographic Centre (DOD, 2005) covering only the German exclusive economic zone of the North Sea. Data for points P, N and O came from the Dutch database Waterbase (DONAR, 2005).

4.2 Comparison between modelled and measured concentrations of γ-HCH

The comparison between modelled and measured concentrations of α-HCH is summarised in Table 4.1. The results are only given for a location if there are sufficient measurements to give a meaningful comparison. The table shows that the highest concentrations, up to 3.95 ng l^{-1}, were found near the coast at locations such as A, G and K; the lowest ones, of less than 0.2 ng l^{-1}, were found in the open North Sea at locations L and P.

Daily averaged concentrations in the uppermost sea layer were compared with the individual measurements for some locations in different subregions of the North Sea (Fig. 4.2 and Fig. 4.3).

The model produces a clear seasonal pattern with higher concentrations in summer for most years at all locations. Similar patterns are also found in the atmospheric concentrations of α-HCH (Fig. 3.8) and in the continental river loads (Fig. 3.9 in the Appendix).

Table 4.1. Mean and range of measured and modelled γ-HCH concentrations and correlation coefficients between measured and modelled concentrations for stations used to evaluate the results from the model.

Symbol on the map	Measurements: mean and range [ng l^{-1}]	Model results: mean and range [ng l^{-1}]	Correlation coefficient
A	1.50 (0.37 – 3.00)	1.48 (0.58 – 3.03)	0.95
B	0.70 (0.10 – 3.00)	1.41 (0.81 – 2.24)	0.35
C	0.83 (0.10 – 3.00)	1.27 (0.68 – 1.88)	0.40
D	0.80 (0.10 – 2.00)	1.32 (0.69 – 1.32)	0.30
E	1.86 (0.10 – 3.00)	1.32 (0.67 – 2.47)	0.74
F	0.82 (0.10 – 2.00)	1.08 (0.62 – 1.52)	0.23
G	1.65 (0.43 – 3.95)	1.77 (0.86 – 3.00)	0.77
H	1.63 (0.42 – 2.55)	1.19 (0.68 – 1.76)	0.93
I	1.45 (0.30 – 3.49)	0.95 (0.38 – 1.31)	0.77
J	0.71 (0.23 – 1.32)	0.67 (0.35 – 1.23)	0.84
K	1.25 (0.42 – 2.75)	1.50 (0.74 – 2.33)	0.86
L	0.58 (0.17 – 0.95)	0.58 (0.22 – 0.91)	0.84
M	0.42 (0.28 – 0.70)	0.49 (0.38 – 0.59)	0.45
N	0.79 (0.20 – 1.80)	1.00 (0.63 – 1.51)	0.83
O	1.25 (0.50 – 0.70)	1.08 (0.96 – 1.15)	0.68
P	0.72 (0.10 – 1.20)	0.67 (0.32 – 1.07)	0.94
Q	1.16 (0.70 – 1.41)	0.96 (0.45 – 1.17)	0.93
R	0.80 (0.45 – 1.26)	1.06 (0.73 – 1.41)	0.92
Average	1.05 (0.28 – 2.29)	1.11 (0.64 – 1.67)	0.68

Concentration of α-HCH decreased at all locations throughout the simulation period. The biggest drop in α-HCH concentration, 6–7 times, was found in the German Bight, with the smallest, 3–4 times, in the central North Sea. Both measured and modelled concentrations in sea water at all locations increased during the first half of the simulation period, with the highest concentrations in 1997–1998. During the second half of the simulation, 1998–2001, there are negative trends in concentrations at all locations, both in the measurements and the results from FANTOM. Also atmospheric concentrations of α-HCH reflect such a pattern with the highest concentrations of α-HCH detected in precipitation during the spring and summer of 1997 and decreased concentrations during 1998–2001 (Fig. 3.8).

The time series of measured concentration of α-HCH in the southern North Sea surface water (SRU 2004) show a gradual decrease since 1982 due to the restriction in the use of α-HCH in the countries adjacent the North Sea. The model captures this decrease during the studied period. Furthermore, model results suggest that α-HCH concentrations declined over the entire modelling domain.

The jagged pattern in the time series of α-HCH concentrations in the German Bight (Fig. 4.2) is due to variability of the fresh water inflow. However, in the open North Sea (Fig. 4.3b, c) remote from the polluted estuaries, the time series are smoother and sea water concentrations seem to be balanced by the volatilisation-deposition process.

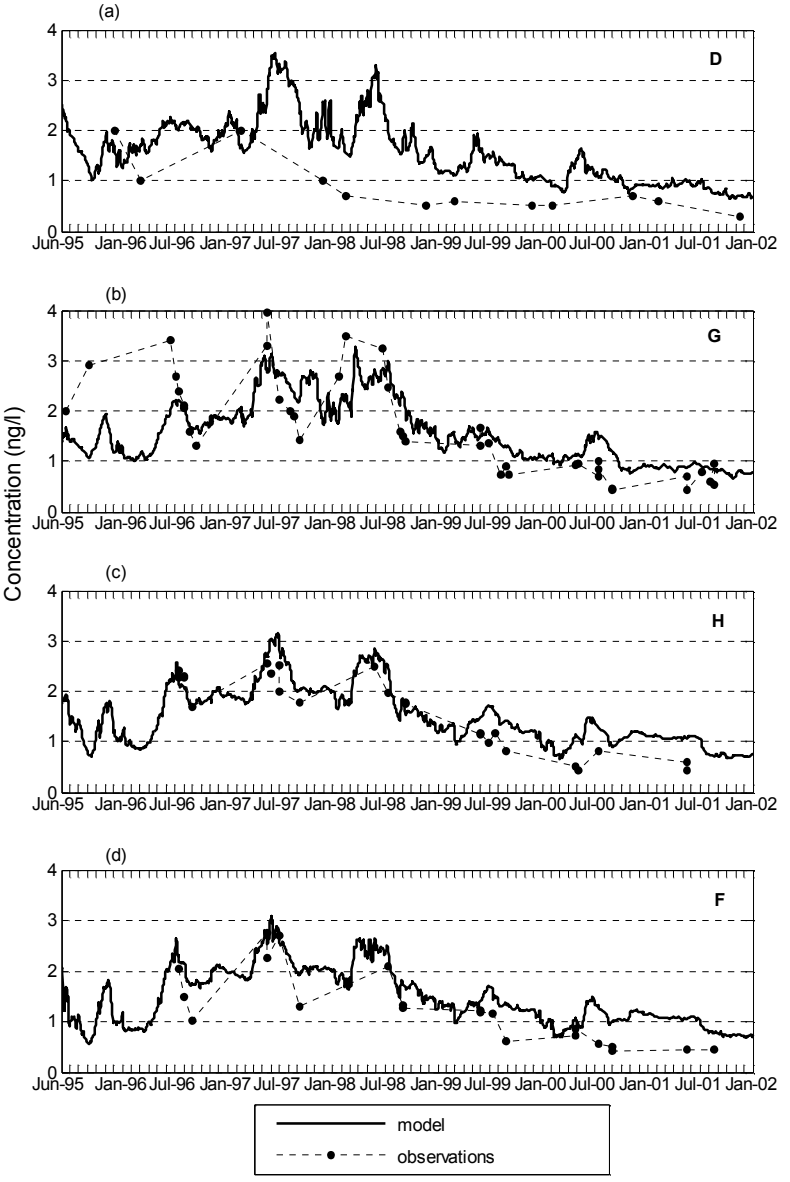

Fig. 4.2. Observed (dots) and modelled (solid line) α-HCH concentrations (ng l^{-1}) in the surface layer at locations D, G, H and F. Locations are specified in Table A.2 and shown on Fig. 4.1.

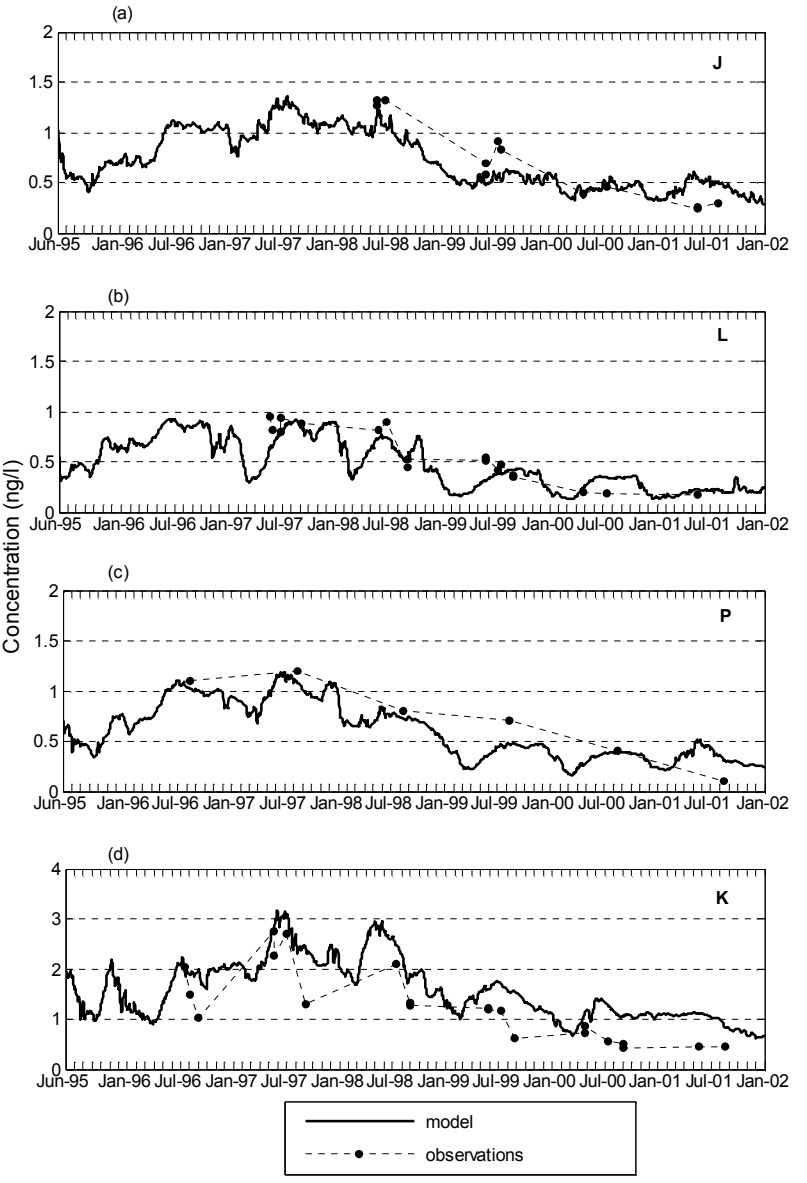

Fig. 4.3. Observed (dots) and modelled (solid line) α-HCH concentrations (ng l^{-1}) in the surface layer at locations J, L, P and K. Locations are specified in Table A.2 and shown on Fig. 4.1.

No measurements of α-HCH concentrations in the English Channel and on the northern sea boundary were available for this study. As concentrations in the whole North Sea have decreased it is likely that they have probably also decreased in the English Channel and on the northern sea boundary without being captured by the model. This offers an explanation for the overestimations in calculated concentrations during 2000–2001. The overestimation is most pronounced at location N, lying in the passage of the English Channel water.

In order to evaluate the model results, scatter plots of measured α-HCH concentrations against those from FANTOM were prepared for some locations (Fig. 4.4).

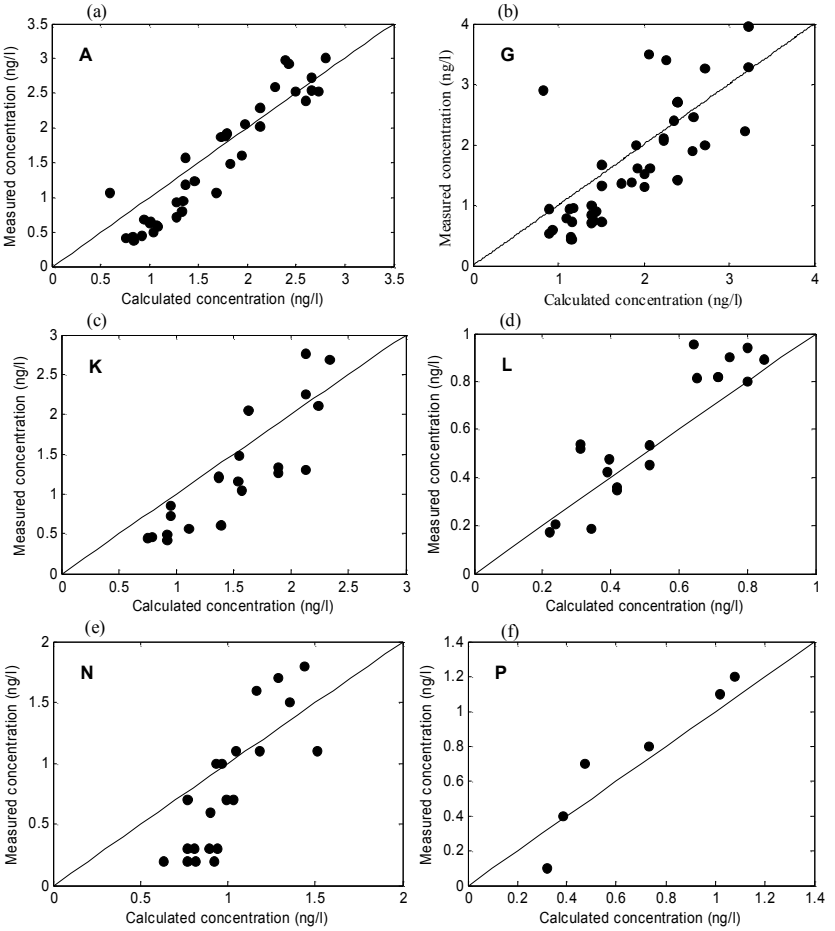

Fig. 4.4. Measured versus calculated α-HCH concentrations (ng l^{-1}) in the surface layer at locations A, G, K, L, N and P. Locations are specified in Table A.2 and shown on Fig. 4.1.

Correlation coefficients for all locations where time series were available are presented in Table 4.1. Good correlations were found for locations A, B and P with correlation coefficients of 0.94, 0.93 and 0.94. Lower correlation coefficients between 0.23 and 0.40 were found for the locations F, D, B and C where the time series consists of the measurements made between December and March. The number of measurements and their temporal resolution, in particular at the locations P, O and M, make further statistical analysis inappropriate.

Correlation coefficients calculated for locations B, C, D and F during the colder season are lower, even though they are situated only within a few model grid points from locations A, E, G and H, where measurements were conducted during warmer seasons and where correlations are much higher. Also calculated mean concentrations at locations B, C, D and F are higher than those measured. One explanation for this discrepancy could be that during winter the stronger winds that occur over the North Sea induce higher current speeds and thereby enhance stronger water mass flushing. Consequently there is an increase in the amount of less polluted waters from the open lateral boundaries being transported into the German Bight.

A scatter plot of measured against modelled concentrations of α-HCH for all locations was prepared (Fig. 4.5). In general there is a good agreement between the modelled and measured concentrations at nearly all locations where comparisons could be performed. Also this agreement is better for the lower and middle parts of the concentration spectrum (which is also the area of the plot into which most of the concentrations fall) than for the higher values (>2.8 ng l^{-1}).

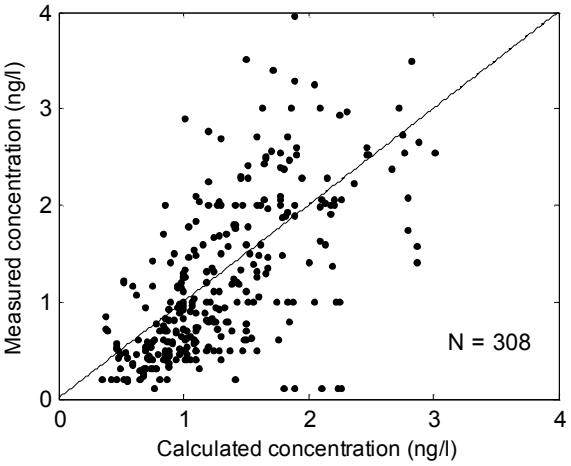

Fig. 4.5. Measured versus calculated α-HCH concentrations (ng l^{-1}) in the surface layer for all locations. Number of measurements is 308.

4.3 Comparison between modelled and measured concentrations of α-HCH

The comparison between modelled and measured concentrations of α-HCH is summarised in Table 4.2. The results are only given for a location if there are sufficient measurements to give a meaningful comparison. The highest concentrations, up to 0.7 ng l^{-1}, were produced by the model at locations near the coast (e.g. points A and K). The lowest concentrations, of less than 0.1 ng l^{-1}, were found in the open North Sea at locations L and P.

Daily averaged concentrations of α-HCH in the uppermost sea layer were compared with the individual measurements for a selection of locations (Fig. 4.6 and Fig. 4.7). The locations chosen are almost the identical to those used when making comparisons for γ-HCH.

The calculated concentrations have a clear seasonal pattern, similar to that found for α-HCH, for most years at all locations, with higher concentrations during warm seasons. Such a pattern also reflects the atmospheric concentrations (Fig. 3.8) and the continental river loads of α-HCH (Fig. 3.9 in the Appendix).

Table 4.2. Mean and range of measured and modelled α-HCH concentrations and correlation coefficients between measured and modelled concentrations for stations used to evaluate the results from the model.

Symbol on the map	Model results: mean and range [ng l^{-1}]	Measurements: mean and range [ng l^{-1}]	Correlation coefficient
A	0.28 (0.18 – 0.46)	0.23 (0.075 – 0.65)	0.75
B	0.31 (0.17 – 0.50)	0.26 (0.04 – 1)	0.51
C	0.34 (0.20 – 0.68)	0.43 (0.07 – 1)	0.27
D	0.34 (0.20 –0.70)	0.40 (0.04 – 2)	0.07
E	0.35 (0.19 – 0.76)	0.31 (0.04 – 1)	0.20
F	0.16 (0.27 –0.42)	0.40 (0.07 – 1)	0.05
G	0.46 (0.22 – 0.79)	0.46 (0.14 – 2)	0.38
H	0.27 (0.12 – 0.40)	0.22 (0.07 – 0.53)	0.81
I	0.25 (0.11 – 0.34)	0.20 (0.07 – 0.44)	0.68
J	0.22 (0.11 – 0.33)	0.19 (0.07 – 0.30)	0.85
K	0.30 (0.19 – 0.44)	0.26 (0.12 –0.63)	0.80
L	0.19 (0.08 – 0.33)	0.23 (0.09 – 0.38)	0.79
N	0.14 (0.04 – 0.25)	0.13 (0.10 – 0.30)	0.64
O	0.13 (0.10 – 0.18)	0.13 (0.10 – 0.30)	0.52
P	0.20 (0.12 – 0.32)	0.16 (0.10 – 0.30)	0.90
Q	0.20 (0.13 – 0.33)	0.15 (0.08 – 0.26)	0.91
R	0.23 (0.18 – 0.27)	0.16 (0.10 – 0.23)	0.24
Average	0.26 (0.14 – 0.43)	0.23 (0.08 – 0.70)	0.43

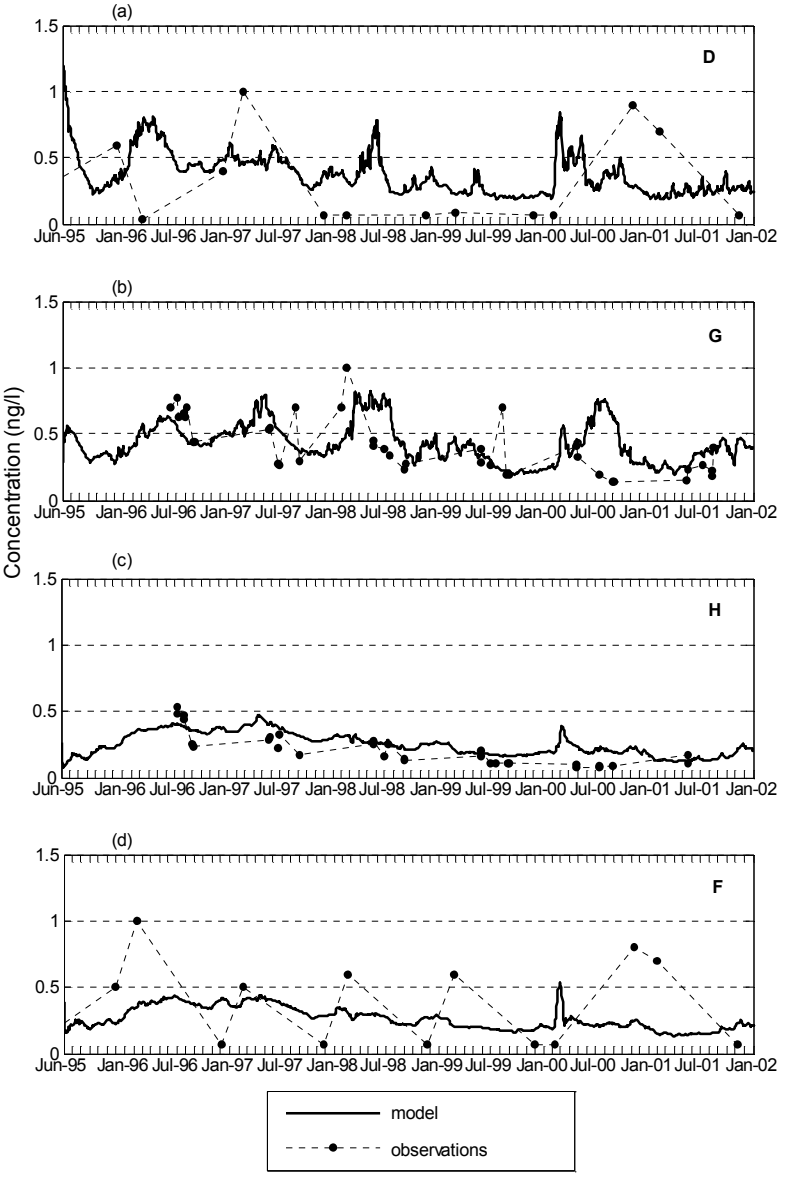

Fig. 4.6. Observed (dots) and modelled (solid line) α-HCH concentrations (ng l^{-1}) in the surface layer at locations D, G, H and F. Locations are specified in Table A.2 and shown on Fig. 4.1.

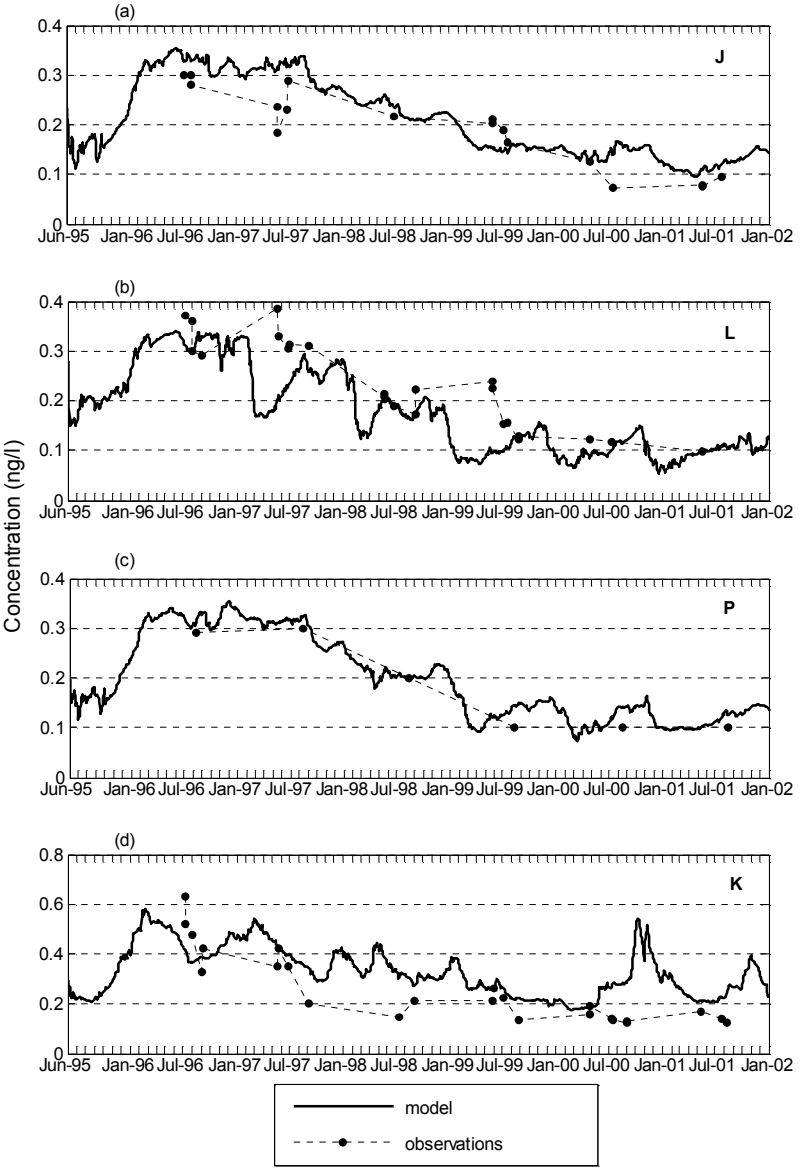

Fig. 4.7. Observed (dots) and modelled (solid line) α-HCH concentrations (ng l^{-1}) in the surface layer at locations J, L, P and K. Locations are specified in Table A.2 and shown on Fig. 4.1.

The calculated concentrations are in a good agreement with those from monitoring programmes carried out during the same period. Concentrations of α-HCH had decreased at all locations throughout the simulation period. However, unlike α-HCH concentrations, α-HCH concentrations dropped more or less homogeneously over the entire modelling domain indicating that the local sources of α-HCH are probably less significant in the entire North Sea than those for γ-HCH. Other studies also show that, following the ban on technical HCH, there is an ongoing decrease of α-HCH concentrations in the North Sea detected since 1982 (Theobald et al. 1996; Bethan et al. 2001; OSPAR 2000; SRU 2004).

Correlation coefficients between measured and modelled concentrations of α-HCH for all locations where time series were available are presented in Table 4.2. Good correlations, with correlation coefficient above 0.7, were found for locations A, H, J, K, Q, L and P. Low correlation coefficients below 0.3 were found for locations C, E, F and R. In order to evaluate the model results, measured α-HCH concentrations are plotted against calculated ones for all locations (Fig. 4.8). These results show that, as for the γ-HCH distribution (Fig. 4.5), the agreement between measured and modelled concentrations of α-HCH is better for the lower and middle parts of the concentration spectrum, than for the higher values (>0.5 ng l^{-1}).

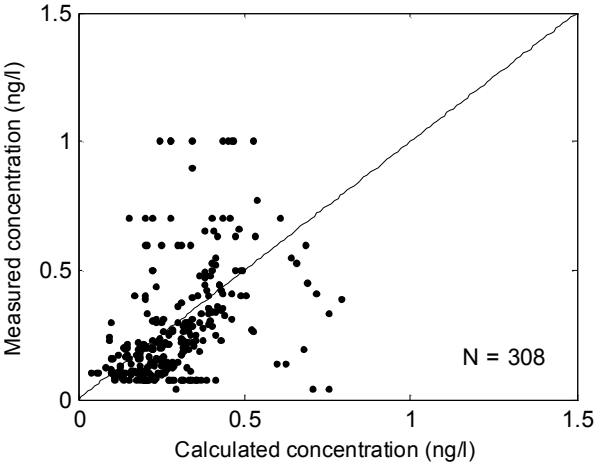

Fig. 4.8. Measured versus calculated α-HCH concentrations (ng l^{-1}) in the surface layer for all locations. Number of measurements is 308.

4.4 Comparison between modelled and measured concentrations of PCB 153

The comparison between modelled and measured concentrations of PCB 153 is summarised in Table 4.3. The results are only given for a location if there are sufficient measurements to give a meaningful comparison. Data from only the German EEZ was available for this study.

Daily averaged concentrations of PCB 153 in the uppermost sea layer were compared with the individual measurements and plotted for four locations (Fig. 4.9) located in different subregions of the North Sea.

In spite of significant reductions of PCB discharges since the 1970s, current measurements indicate the presence of these substances in sea water and other environmental media (Bruhn et al. 2003; Axelman et al. 1997; Hornbuckle et al. 1993).

Although emissions and concentrations have dropped since the 1970s, concentrations are now levelling off due to remobilisation of the sediments, via the water pathway, from the waste and contaminated sites. Some studies of PCB show a slight reduction between 1987 and 1992, with no further reduction evident thereafter. There is no pronounced trend in the time series. The model shows even a slight increase in the concentrations towards the end of the simulation period. This increase in sea water concentrations of PCB 153 at the end of the simulation period has also been detected in the rain concentrations measured at Lista (Fig. 3.8). A similar effect caused by a single wet deposition event influencing the whole statistical analysis for lead has been reported (Schlünzen et al. 1997). This implies that interannual variations are important.

Table 4.3. Mean and range of measured and modelled PCB 153 concentrations and correlation coefficients between measured and modelled concentrations for stations used to evaluate the results from the model**.**

Symbol on the map	Model results: mean and range [ng l^{-1}]	Measurements: mean and range [ng l^{-1}]	Correlation coefficient
A	0.046 (0.009 – 0.13)	0.091 (0.01 – 0.3)	0.17
B	0.036 (0.01 – 0.104)	0.226 (0.07 – 0.5)	0.02
C	0.070 (0.033 – 0.136)	0.218 (0.07 –0.5)	0.21
D	0.066 (0.015 – 0.126)	0.249 (0.07 – 0.5)	0.06
E	0.075 (0.013 – 0.144)	0.164 (0.07 – 0.2)	0.11
F	0.038 (0.009 – 0.104)	0.5 (0.5 – 0.501)	0.15
G	0.133 (0.017 – 0.26)	0.034 (0.01 – 0.154)	0.22
H	0.031 (0.014 – 0.07)	0.012 (0.01 – 0.033)	0.12
I	0.016 (0.008 – 0.036)	0.010 (0.01 – 0.01)	0.10
J	0.016 (0.005 – 0.040)	0.011 (0.01 – 0.024)	0.70
K	0.055 (0.018 – 0.177)	0.015 (0.01 – 0.055)	0.11
L	0.009 (0.003 – 0.019)	0.010 (0.01 – 0.011)	0.21
Q	0.012 (0.006 – 0.018)	0.011 (0.01 – 0.013)	0.32
Average	0.034(0.009 – 0.077)	0.084 (0.046 – 0.152)	0.12

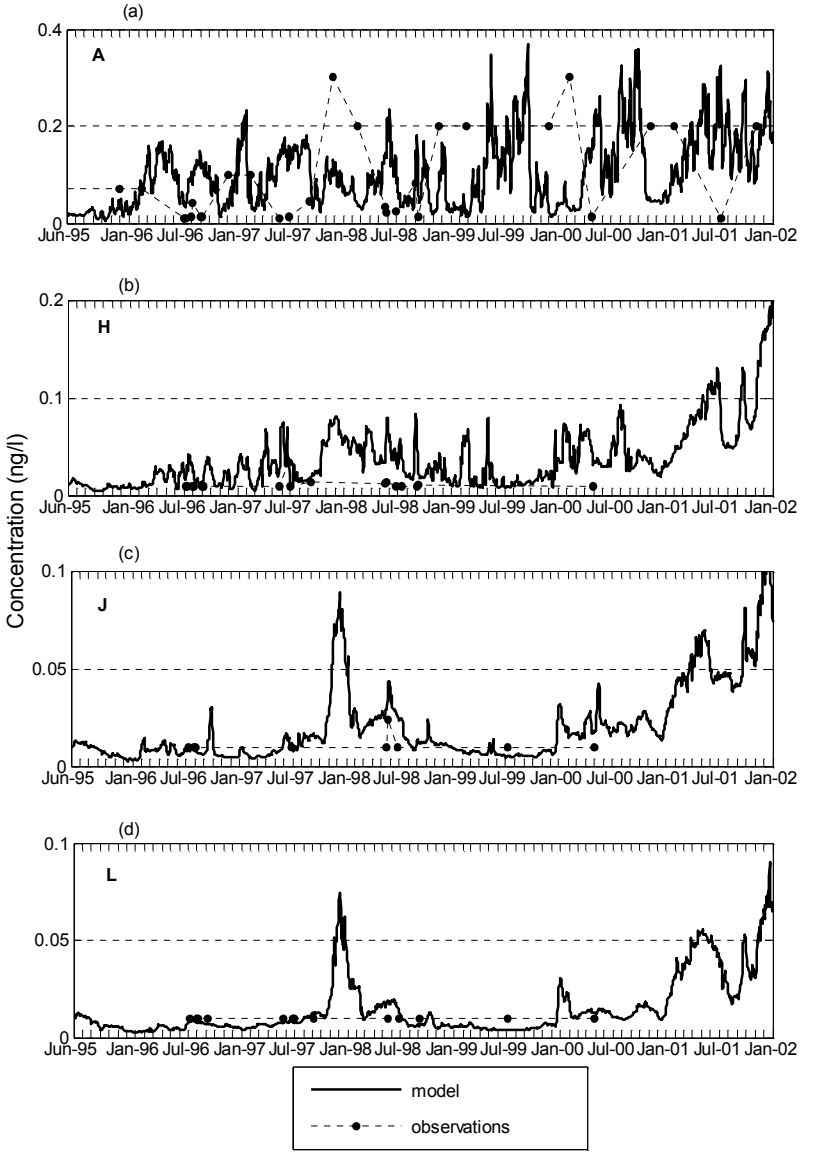

Fig. 4.9. Observed (dots) and modelled (solid line) PCB 153 total concentrations (ng l^{-1}) in the surface layer at locations A, H, J and L. Locations are specified in Table A.2 and shown on Fig. 4.1.

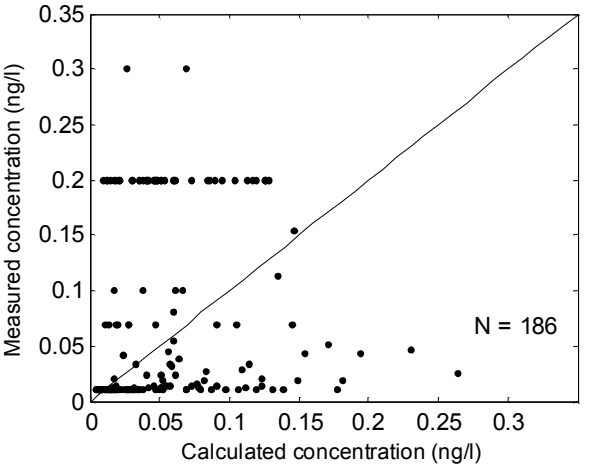

Fig. 4.10. Measured versus calculated PCB 153 concentrations (ng l^{-1}) in the surface layer for all locations. Number of measurements is 186.

Table 4.3 gives an overview of the correlation coefficients, mean and range of the measured and modelled PCB 153 concentrations in sea water. The daily averaged total concentrations of PCB 153 were in the range 0.003–0.26 ng l^{-1} with the highest values at locations A, C, E and K and the lowest at locations L, J, Q and I. There is a strong spatial gradient with very high concentrations of about 0.2 ng l^{-1} in the southern German Bight, near to urban areas, and very low concentrations elsewhere. The reason is that concentrations in the rivers, mainly in the River Elbe, were at least one order of magnitude higher than in other rivers throughout the whole simulation period. In addition the German Bight is an area where sediments contaminated with PCBs are deposited. Upwelling is common in this area and this may bring water to the surface with higher PCB levels as a result of contact with contaminated sediment. Concentrations in the rain are very low in comparison to the air and rivers.

PCB 153 is the most hydrophobic compound among those addressed in this study. According to theoretical expectations more hydrophobic compounds will be effectively exported with SPM downward out of the surface water than the more hydrophilic substances. For the higher chlorinated PCBs, this process can be so efficient that the downward loss cannot be compensated by air–sea exchange, creating a fugacity deficit in the surface water (Dachs et al. 2002).

Wania et al. (2000) concluded that, on average, volatilisation of PCBs exceeded gaseous deposition by a factor of ten for the Baltic Sea. The differences in the calculated fluxes found by various studies (Wania et al. 2000; Axelman et al. 2001; Bruhn et al. 2003) arise largely from the choice of Henry's law constant. The atmospheric particle bound deposition of PCBs in the Baltic reported in these studies was much greater while the gross gaseous deposition was much smaller.

Therefore, it seems that, as in the case of HCHs, the main uncertainty is due to the choice of physical-chemical properties.

Calculated PCB 153 concentrations are plotted against measured ones for all locations (Fig. 4.10). Correlation coefficients for all locations where time series were available are presented in Table 4.3. The best correlation for PCB 153 was found at location J with a correlation coefficient of 0.7. Low correlation coefficients between 0.1 and 0.3 were found at most other locations.

Due to low concentration of PCB 153 in sea water and the potential for shipboard as well as laboratory contamination, the analytical data is the most uncertain of all the contaminants. In addition concentrations often lie below the detection limit (BSH 2005.). This problem is illustrated by Fig. 4.9b, Fig. 4.9c and Fig. 4.9d in which measured concentrations remained constant (at the detection limit) throughout the simulation period, whereas the time series of modelled concentration mirrors the variability in the input data. To further illustrate this phenomenon the modelled and measured concentrations at the location E close to the River Elbe mouth were compared with the concentration supplement from the River Elbe (Fig. 4.11). Although the values of both measured and modelled concentrations lie in the same range, the concentration pattern is not reproduced. In fact the modelled concentration at this location is influenced by the River Elbe inflow which is also calculated using daily measurements data of the fresh water discharge and PCB 153 concentrations in the Elbe (see Sect. 3.4.3).

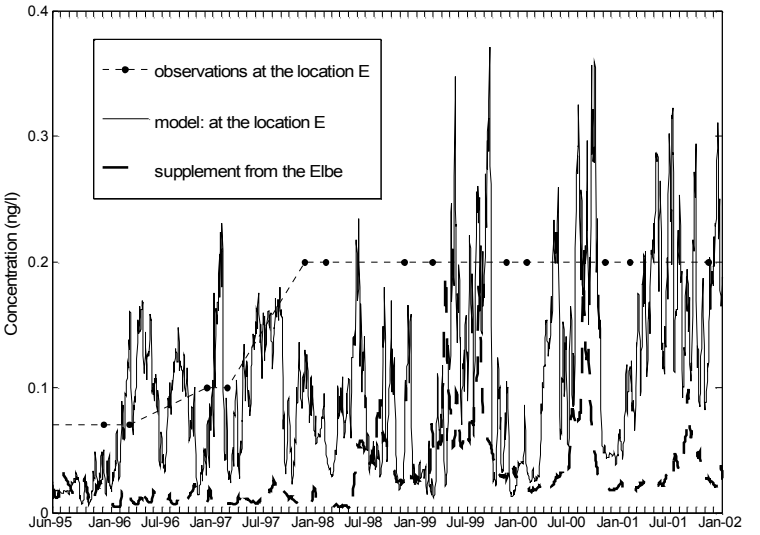

Fig. 4.11. Concentrations of PCB 153. Solid line – model simulation in the German Bight at location E. Dashed line – concentration supplement form the River Elbe. Dots – individual measurements at location E.

Unlike the two HCH isomers discussed earlier there is no clear annual signal detected in the time series of PCB 153 concentration. Other authors have also found the seasonal variability of gaseous PCB concentrations at marine stations in the southern Baltic Sea to be less than an order of magnitude (Bruhn et al. 2003; Agrell et al. 1999). Concentrations of PCB 153 in the North Sea appear to be stabilising at lower levels as a result of the declining use of PCB 153 since the 1970s (SRU 2004). This is reproduced by the model. No pronounced seasonal trend is detected in the modelled PCB 153 concentrations. In general, the modelled PCB 153 concentrations are in the same range as the measurements. However the agreement between measured and modelled concentration patterns is rather poor. This is probably due to both the model uncertainties and the uncertainties in the measurements.

4.5 Uncertainty and sensitivity analysis

Since data from field studies is scarce, quantitative comparison of model results with measurements is difficult. Therefore sensitivity and uncertainty analyses as well as model comparison studies are an important means of evaluating the model. The uncertainty in the modelling results can be attributed to the uncertainties in the following.

(a) Input data based on field studies (see Sect. 3.4).

(b) Substance properties (i.e. physical-chemical properties and degradation rates).

(c) Assumptions made in the model due to the lack of understanding about some aspects of the processes (e.g. see Chap. 2).

With regard to (a) the input data was discussed in Sect. 4.1. The available measurements are scarce. Therefore, it is difficult to obtain quantitative estimates of the uncertainties in the input data due to the sampling and analysis methods and data reporting.

As for the source of uncertainties mentioned under point (c), caused by the model formulation and simplification of processes, the sensitivity studies should be aimed at distinguishing the relative importance of the various processes. Such experiments are discussed in Chap. 6.

To evaluate the assumptions made under points (a) and (b), experiments aimed at explaining the differences between modelled and measured α-HCH concentrations were performed (Fig. 4.12). A similar set of experiments was carried out for α-HCH (Fig. 4.13).

4.5.1 Experiments with γ-HCH

In the first experiment it was assumed that the concentration of α-HCH in water flowing into the North Sea from the English Channel and from the Atlantic Ocean

at the northern boundary of the modelling domain is zero, i.e. $C^{B} = 0$ (Eq. 3.2). The resulting time series of the concentration was plotted for point A located in the German Bight (where the impact of inflow from lateral boundaries was expected to be less pronounced than elsewhere) and for point N lying in the passage of waters flowing from the English Channel.

In the second experiment the temperature dependency of Henry's law constant (H_c, Eq. 2.7) was calculated using the values obtained by Kucklick et al. (1991) instead of those by Sahsuvar et al. (2003) which are used in the other model runs (Table A.1).

Daily averaged concentrations in the uppermost sea layer resulting from the main simulation and both experiments were compared with the individual measurements at locations A and N (Fig. 4.12).

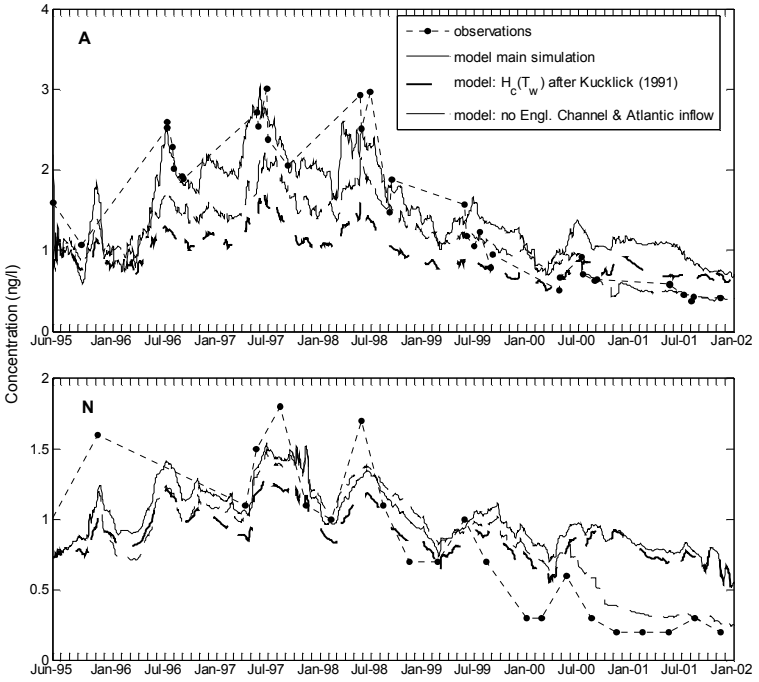

Fig. 4.12. Concentrations of α-HCH (ng/l) in the surface layer at locations A and N, under different model setups. Solid line – main model simulation. Dash-dot line – when α-HCH concentrations inflowing via the lateral boundaries were set to zero. Dashed – when air-sea exchange was calculated using Henry's law constants given by Kucklick et al. (1991). Dots – individual measurements. Locations are specified in Table A.2 and shown on Fig. 4.1.

As mentioned above, the decrease in α-HCH concentrations in the English Channel and on the northern boundary might not be correctly captured by the model leading to overestimated winter concentrations. This hypothesis is verified by the modelling experiment when α-HCH concentrations in the English Channel and on the northern boundary of the modelling domain were set to zero for the entire simulation period. Fig. 4.12 shows that concentration without inflow from the lateral boundaries was a significant component of the α-HCH burden until the second half of the 2000. This figure also suggests that the effect is more pronounced in winter than in summer, and this was confirmed by the correlation coefficients (Table 4.1). Furthermore, ongoing cycling of earlier leakages of α-HCH from inappropriate disposal may play a role.

The seasonal pattern produced by the model shows higher α-HCH concentrations during summer than during winter; this emphasises the importance of the temperature dependency of the air–sea exchange. For the Great Lakes and for the Arctic Ocean it has been found that during summer the air–sea gas transfer is net volatilisational, whereas during colder periods it is depositional (Ridal et al. 1996; Jantunen and Bidleman 1997).

Measurements suggest (Sahsuvar et al. 2003) that the temperature dependency of H_c has a profound effect on the gas exchange in the model. This hypothesis is also illustrated by Fig. 4.12 where α-HCH concentrations resulting from model calculations using two different temperature dependency coefficients of H_c are presented. This experiment shows that the most recent data (Sahsuvar et al. 2003) lead to higher (20–50%) sea water concentrations. Therefore, as parameterisation of the air–sea exchange seems to play a key role, its uncertainty should be reduced. Discrepancies in the experimentally determined values of H_c contribute to this uncertainty as may the physical processes not included in the model (see Sect. 2.2.1).

4.5.2 Experiments with α-HCH

Similar to those experiments with α-HCH , there was another set of experiments aimed at explaining the deviations in modelled and measured concentrations of α-HCH.

In the first experiment it was assumed that concentration of α-HCH in water flowing into the North Sea from the English Channel and from the Atlantic Ocean at the northern boundary of the modelling domain equals zero. The resulting concentration time series was plotted for location A and N (Fig. 4.13).

In the second experiment the temperature dependency of Henry's law constant was calculated using the values obtained by Sahsuvar et al. (2003) instead of those by Kucklick et al. (1991).

Daily averaged concentrations in the uppermost sea layer resulting from the main simulation and both experiments were compared with the individual measurements at A and N (Fig. 4.13).

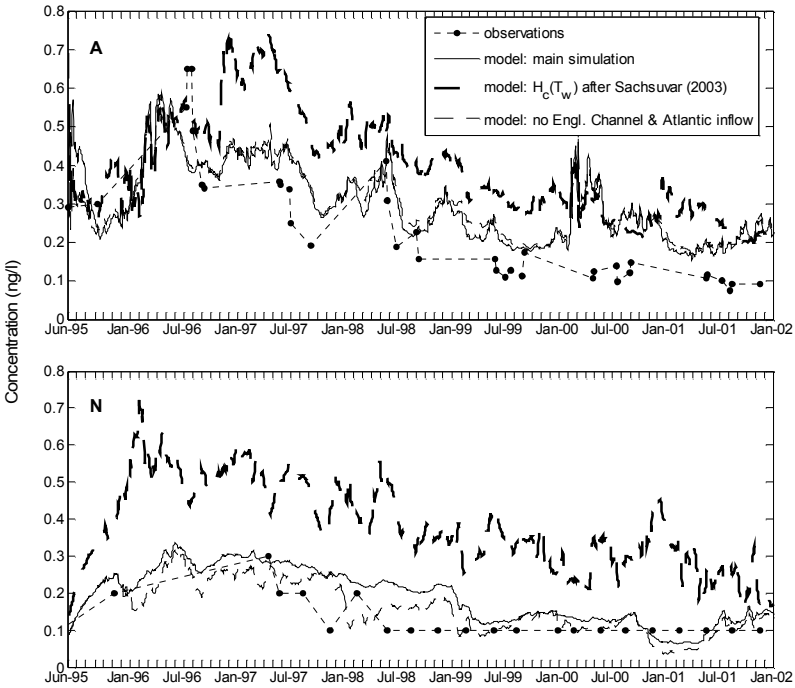

Fig. 4.13. Concentrations of α-HCH (ng/l) in the surface layer at locations A and N, under different model setups. Solid line – main model simulation. Dash-dot line – when α-HCH concentrations inflowing via the lateral boundaries were set to zero. Dashed line – when air-sea exchange was calculated using Henry's law constants given by Sahsuvar et al. (2003). Dots – individual measurements. Locations are specified in Table A.2 and shown on Fig. 4.1.

As with γ-HCH, the inflow from the lateral boundaries is more pronounced during winter than during summer. However, this inflow does not seem to play a significant role neither in the German Bight at location A nor at N close to the English Channel.

These model results (Fig. 4.13) suggest that, unlike γ-HCH concentrations, α-HCH in the German Bight is mostly due to the atmospheric transport from remote regions rather than transport by ocean currents. This phenomenon agrees with what is known about the expected fate of HCHs in the North Sea. Because of the ban of technical HCH in the 1980s the regional sources of α-HCH should be decreasing.

The model experiments show that the choice of the Henry's law constant for α-HCH has a profound effect on the model output, as was also shown for γ-HCH. For this experiment the model results using values reported by Kucklick et al. (1991) are in better agreement with the measured concentrations than those obtained by Sahsuvar et al. (2003). Again, as with γ-HCH experiments, more recent

data (Sahsuvar et al. 2003) leads to higher (up to 60%) sea water concentrations. Also this data leads to an underestimate of the volatility capacity of the sea compartment.

5 Occurrence and Pathways of Selected POPs in the North Sea

POPs that are discharged into the sea partly sorb to the organic fraction of suspended particulate matter present in sea water (i.e. phytoplankton cells, fecal pellets and other aggregates). Therefore they occur in dissolved form or as bound to particles. The distribution of POPs between dissolved and particulate phases depends on the physical and chemical characteristics of the contaminant and on the availability of adsorbing material in sea water. Dissolved and suspended substances have different transport behaviour: the dissolved portion follows the path of the water masses, while the bound portion quickly sedimentises.

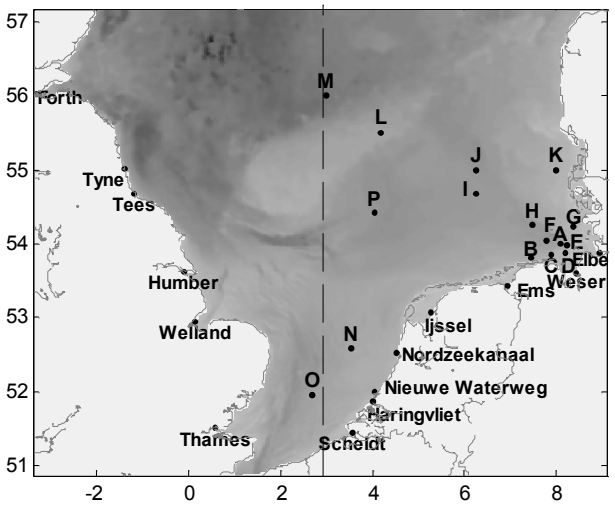

Fig. 5.1. FANTOM domain and 3°E line along which vertical sections are produced. Locations of points where temporal trends are available are labelled with letters. Rivers mouths are indicated.

The uptake of POPs by particulate matter in sea water is presented in Sect. 5.1. Sect. 5.2 shows horizontal and vertical spatial and temporal distributions of γ-HCH, α-HCH and PCB 153. Vertical distributions are presented along 3°E (Fig. 5.1) as it is the most representative vertical section of the modelling domain. It includes both regions remote from the coast and coastal subregions laying in the vicinity of estuaries and in the passage of water entering the North Sea from the English Channel. The ratio of the two HCHs isomers indicating their sources and the trends in their behaviour are analysed in Sect. 5.3.

5.1 Uptake of γ-HCH, α-HCH and PCB 153 by particulate matter in sea water

In deep oceans, the contaminant portion which sinks with particles to the see bottom is lost for further cycling in the environment. In shallow seas (e.g. the North Sea) sediments may be disturbed by sea currents and storms, and enter the water column again (resuspension). In most models the sorption to particulate organic carbon (POC) and subsequent sinking is treated as an ultimate sink for POPs, whereas in FANTOM resuspension of previously deposited POC is also taken into account. The major source of POC is the primary production, at least during the phytoplankton growth. Thus, total POC concentration, C_{POC}, in FANTOM consists of two components (as described in Sect. 2.3.1):

(a) POC from biological activity (e.g. phytoplankton, bacteria, detritus) using the C_{bio} calculated by an ecosystem model described in Pätsch and Kühn (2002).

(b) POC from bottom sediments using the C_{sed} calculated in FANTOM.

5.1.1 Distribution of particulate organic carbon in the North Sea

Vertically integrated spatial distributions of the two POC fractions, typical for winter and summer periods in the North Sea, are shown in Fig. 5.2 (see Appendix). The calculated winter biomass concentration (Fig. 5.2a) is low and lies in the range 0.015–0.15 mg l^{-1}. The concentration during the warm season (Fig. 5.2c) caused by the phytoplankton spring bloom is highest in the southern North Sea and in the shallow coastal zone with values of up to 0.8 mg l^{-1} (corresponding to 66 mmol C m^{-3}).

POC concentration due to resuspended sediment typical for winter (Fig. 5.2b) and summer (Fig. 5.2d) conditions in the North Sea do not differ significantly and have values of 0.05–0.2 mg l^{-1} for most of the domain. In general they correlate with the fine sediment accumulation on the sea bottom (Eisma and Kalf 1987). Winter concentrations (Fig. 5.2b) are slightly higher, in particular in the shallow southern North Sea. POC concentrations from biological activity and bottom sediments (Fig. 5.2) decrease from south to north with increasing depth.

The annual cycle of daily POC concentrations differs between the well-mixed German Bight and the stratified open North Sea (Fig. 5.3). Total POC in the German Bight is in the range 0.5–1.1 mg l^{-1}, and values in the open North Sea range between 0.1 and 0.5 mg l^{-1}.

In spring and summer POC is dominated by phytoplankton. In the German Bight the primary production values increase slowly during spring reaching a maximum of about 0.8 mg l^{-1} in May and remaining high during the whole summer. In the central part of the North Sea the distinct spring maximum of about 0.4 mg l^{-1} is followed by a sharp decline with values dropping to values as low as in winter (below 0.1 mg l^{-1}). A similar annual pattern of primary production was obtained by the modelling study of Moll (1998).

Resuspended sediment is an important contributor to the total POC content in both the German Bight and the open North Sea (Fig. 5.3). Resuspension of freshly deposited sediments occurs due to storm events which are more frequent in autumn and winter (Sündermann and Puls 1990). This seasonality is more pronounced in the shallow German Bight (Fig. 5.3 top) where disturbed sediment results in a maximum POC concentration of about 0.6 mg l^{-1} in November. Measurements (van der Zee and Chou 2005) also show that the contribution of resuspended POC to the total POC content is greater during winter.

The open North Sea is deeper, thus the surface POC concentration (Fig. 5.3 bottom) is less influenced by the resuspended portion which is also smaller.

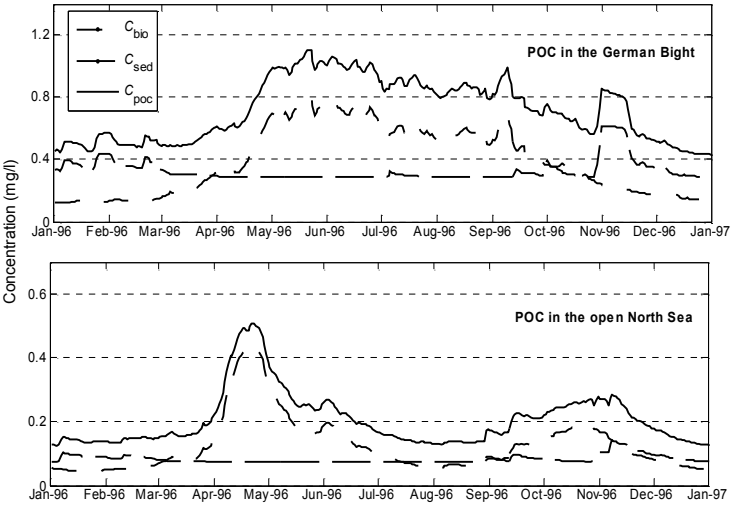

Fig. 5.3. Surface daily averaged concentrations of total particulate organic carbon C_{POC} (solid line) in 1996, consisting of primary production, C_{bio} (dots) (Pätsch and Kühn, 2005) and of resuspended fraction, C_{sed} (dashed line) calculated by FANTOM in the German Bight (location A) and in the open North Sea (location L shown on Fig. 5.1).

The modelling results suggest that total POC concentration in the German Bight in winter is dominated by resuspended POC (75–85%). During summer the situation is the opposite with up to 75% of POC resulting from primary production (Fig. 5.3 top). In the open North Sea the winter POC content is equally distributed between the two constituents, whereas in summer the primary production makes up to 85% of the total content (Fig. 5.3 bottom). These results are in a good agreement with other studies (Eisma and Kalf 1987; Sündermann 1994; Pohlmann and Puls 1994; Moll 1998; van der Zee and Chou 2005).

5.1.2 Fraction of γ-HCH, α-HCH and PCB 153 on particulate organic carbon in sea water

Most of the POPs have moderate or very low water solubility (UNEP 2003). Hydrophobic compounds – those not easily dissolved in water – are expected to be bound to POCs and thus tend to disperse in the sediment rather than in the water phase. Measuring the concentration of non-water-soluble pollutants (e.g. PCB 153 in sea water) is difficult because the concentrations often lie near to or below the detection limit for the substance.

Annual mean spatial distributions of γ-HCH, α-HCH and PCB 153 fractions bound to POC (f_{POC}) expressed as a percentage of the total sea water concentration (see Sect. 2.3.2) and averaged vertically for the whole modelling domain were calculated (Fig. 5.4a, Fig. 5.4b and Fig. 5.4c in the Appendix). The corresponding total POC concentration is shown in Fig. 5.4d. Note that the location of the vertical section is given in Fig. 5.1.

The amount of POP attached to organic matter is controlled by its lipophilicity which is often characterised by the octanol–water partition coefficient K_{ow} (see Sect. 2.3). Contaminants addressed in this study differ in their K_{ow} values with PCB 153 being the most lipophilic with a K_{ow} value of three orders of magnitude higher than those for γ-HCH and α-HCH (Table A.1). Consequently, the calculated f_{POC} for the two HCH isomers is about 0.15% for the whole North Sea (Fig. 5.4a and Fig. 5.4b in the Appendix) with the highest values of up to 1.2% in the river estuaries, where both POC content and γ-HCH and α-HCH concentrations are highest.

The f_{POC} values for PCB 153 (Fig. 5.4c) are relatively high, being more than 70% in the southern North Sea and in the coastal zones. Lower values of less than 45% were produced by the model for the open North Sea where the POC concentration is lower throughout the year (see Sect. 5.1.1 and Fig. 5.4d).

Generally the f_{POC} for all three contaminants (Fig. 5.4a, Fig. 5.4b and Fig. 5.4c in the Appendix) follows the total POC distribution (Fig. 5.4d) with higher values in the southern North Sea and in the coastal zone, and lower values in the deeper open North Sea. As was discussed in Sect. 2.3.2 The POPs fraction

sorbed to POC is expected to correlate with the POC distribution: higher POC concentration results in higher concentrations of POPs in the particulate phase. High biomass growth may lead to dilution of POP concentrations. Other studies for instance, showed that increased vertical fluxes in the water column and higher PCB concentrations in phytoplankton due to eutrophication have been observed (Gunnarsson et al. 1995; Jeremiason et al. 1999; Dachs et al. 1999).

Another indication of the correlation between the distributions of POC and POPs is demonstrated by the annual mean vertical distributions of γ-HCH, α-HCH and PCB 153 fractions bound to POC and the corresponding POC concentration (Fig. 5.5 in the Appendix). POC concentrations (Fig. 5.5d) increase with depth due to a higher content of resuspended sediment near the bottom and due to sinking of surface POC. Sinking organic carbon particles export contaminants to the lower water layers with their subsequent deposition at the bottom sediment.

The annual cycle of daily averaged PCB 153 concentration in the particulate phase and its total sea water concentration in 1996 at location A in the German Bight and location L in the open North Sea are shown on Fig. 5.6. Because both HCH isomers have very low particle-bound fractions they are not discussed here.

Uptake by biomass and subsequent sinking can deplete the dissolved concentrations of POPs in surface waters during periods of fast phytoplankton growth (Dachs et al. 1999; Schulz-Bull et al. 1998). The primary production in the North Sea generally shows a peak in spring followed by a decrease during the summer and a second peak in October–November caused by water column turnover (Moll, 1998).

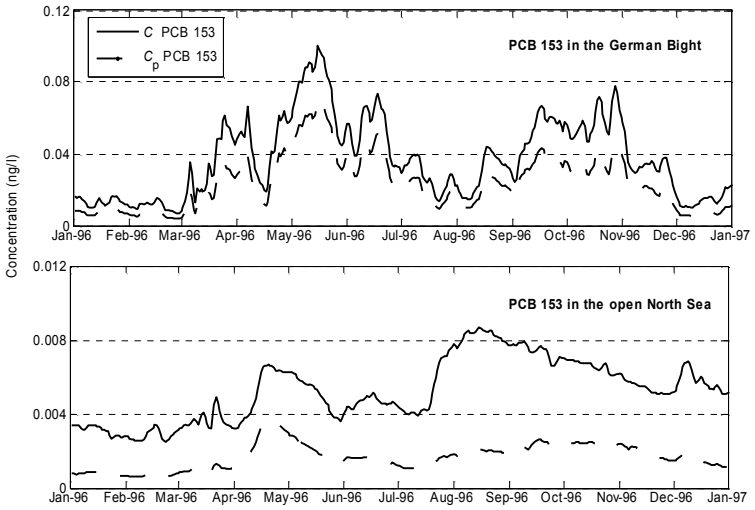

Fig. 5.6. Total C and bound to particles C_p concentrations of PCB 153 at the sea surface for German Bight (location A) and open North Sea (location L). Locations are shown on Fig. 5.1.

The dissolved concentration of PCB 153 in the North Sea is thus expected to be high during winter with a decrease in spring followed by relatively low concentrations during summer and an increase during late autumn. This annual cycle is captured by the model (Fig. 5.6). Such an annual cycle is supported by measurements conducted in the Kattegat Sea region (Sundqvist et al. 2004).

Other studies suggest that eutrophic conditions lead to a depletion of water column concentrations of PCB 153 due to POC uptake and settling export (Dachs et al. 1999). This hypothesis is supported by the model results showing that there is a link between the annual cycle of PCB 153 (Fig. 5.6) and POC concentrations (Fig. 5.3).

During the spring phytoplankton bloom in the German Bight (Fig. 5.3 top) nearly the entire PCB 153 is sorbed by particulates resulting in a drop in the PCB 153 concentration. Further, the increased POC concentrations in the German Bight due to sediment resuspension under stormy conditions cause an increase in PCB 153 concentrations (Fig. 5.6 top). In the open North Sea (Fig. 5.6 bottom) the particle bound fraction of PCB 153 is lower, (25–40%) than in the German Bight (up to 90%) (Fig. 5.4c in the Appendix), and the correlation between the POC and PCB patterns is weaker.

5.1.3 γ-HCH, α-HCH and PCB 153 content in the liver of the North Sea flatfish dab (Limanda Limanda)

Contaminants sorbed to phytoplankton enter the aquatic food webs moving through the various trophic levels in an ecosystem. If it bioaccumulates and biomagnifies (see Sect. 1.1), much of it will be in the bodies of organisms. Pollutants that dissolve in fats may be retained for a long time. It is traditional to measure the amount of pollutants in fatty tissues of organisms such as fish.

The North Sea flatfish dab (Limanda Limanda) is a widespread pelagic fish (Fig. 5.7) preferring sandy ground, often close inshore. The flesh is tasty, and is being commercially fished. Because it is widely available in the North Sea, dab is already playing an important role in international contamination monitoring programmes as it can be used as a biological marker of exposure to POPs.

Contents of γ-HCH, α-HCH and PCB 153 in dab livers measured in the German Bight were compared with the coastal water concentrations produced by FANTOM for these compounds. The comparison was made for the same time as the fish samples were taken (i.e. in September of each year according to the guidelines for the marine monitoring programmes).

The sampling period was chosen because in late summer till early spring the fish are far away from spawning time (dab in the southern North Sea show considerably more migration during the spawning period). Furthermore dab is in relative good condition and so the natural shift is relatively low at that time.

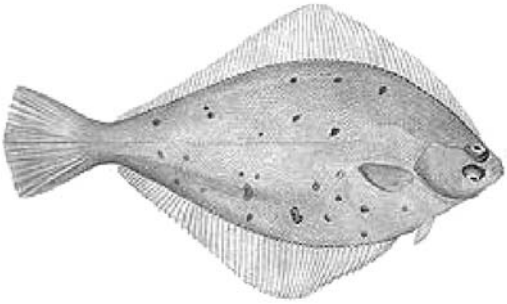

Fig. 5.7. The North Sea flatfish dab (Limanda Limanda). Source: Natural History Museum: http://www.nhm.ac.uk/, last visited 4 November 2005.

The dataset consists of data from individual fish samples where up to 25 fish from the same area caught in either one or two hauls. The median values calculated from these data are presented in Fig. 5.8. The median reflects the results for one area and one day. But as the concentration in dab livers will not change as rapidly as in water and due to the selected sampling time, the values will be adequate for a period of some weeks or even months (Haarich et al. 2005).

In the German Bight, for the investigation period from 1995 until 2001, only for α-HCH is a steadily decreasing trend observed (Fig. 5.8b). Lindane (Fig. 5.8a) shows low concentrations at the beginning, followed by an increase with a turning point in 1996. The highest concentrations both in dab and in sea water were in 1997. After 1998 lindane concentrations decreased continuously in both dab and sea water. High γ-HCH concentrations in the German Bight in 1995 can be explained by high runoff from the River Elbe in autumn 1995, where a correlation between the wet weight-based concentrations and suspended matter concentrations could be confirmed (v. Westernhagen et al. 2000). For PCB 153 (Fig. 5.8c) dab and sea water concentrations at the end of the investigation period were higher than at the beginning.

Modelled sea water concentrations for all three contaminants follow the pattern detected in dab (Fig. 5.8). Also, due to persistence and bioaccumulation, even very low contaminant concentrations in sea water can lead to much higher concentrations in fish, marine mammals and fish-eating birds. In spite of a total reduction in inputs of the investigated contaminants, their concentrations in dab have not decreased continuously in the German Bight and in other regions of the North Sea (Lang and Wosniok 2003). According to an OSPAR assessment (OSPAR 2000) the concentrations of organochlorines in fish from the North Sea are still 3 to 10 times higher than in catches from the Northern Atlantic.

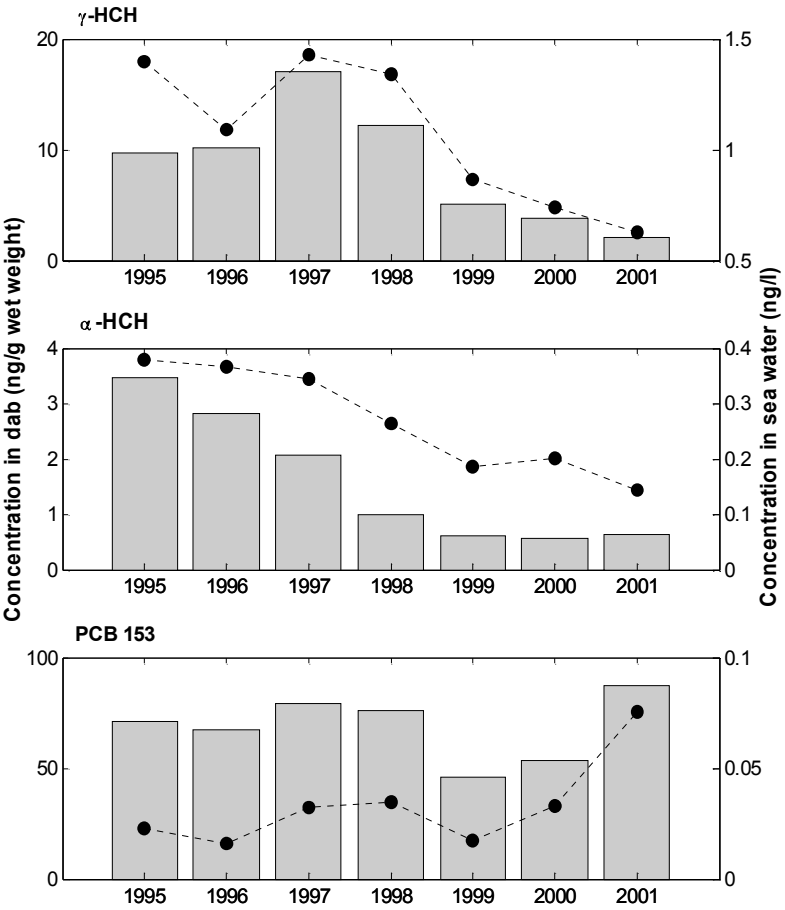

Fig. 5.8. Concentrations of γ-HCH, α-HCH and PCB 153 in flatfish dab liver (bars and values on the left-hand axis) represented as median values of individual measurements in the German Bight. Measurements were provided by the Institut für Fischereiökologie (Haarich pers. comm.). Vertically integrated annual mean modelled by FANTOM sea water concentrations in the same location of the German Bight (dashed lines and values on the right-hand axis).

5.2 Spatial and temporal distribution of γ-HCH, α-HCH and PCB 153 in sea water

An analysis of spatial and temporal distributions of the three pollutants is presented in the following sections. Vertical distributions of γ-HCH, α-HCH and

PCB 153 in sea water along the 3°E (Fig. 5.1) are plotted in Fig. 5.9, Fig. 5.10 and Fig. 5.11, whereas their horizontal annual mean concentrations averaged vertically are plotted in Fig. 5.12, Fig. 5.13 and Fig. 5.14 (see Appendix).

5.2.1 γ-HCH horizontal and vertical distributions

Measurements of γ-HCH in the North Sea's uppermost layer of 5 m thickness compiled during summer 1995 were interpolated onto the modelling domain of FANTOM (Fig. 3.5). The gradients with the highest concentrations were in the southern regions of the North Sea, in the estuaries of rivers and in the English Channel. The highest concentration of 8 ng l^{-1} was found close to the mouth of the River Elbe.

Annual mean γ-HCH concentrations averaged vertically for the whole modelling domain for 1996–2001 were calculated (Fig. 5.12 in the Appendix). These results show positive gradients of concentration towards the coasts; a similar pattern was found in the initial distribution (Fig. 3.5). During 1995–1997 the total concentration of γ-HCH in the continental coastal water was above 1 ng l^{-1} with a concentration of more than 25 ng l^{-1} in the Elbe estuary. As with the γ-HCH concentration at the selected locations (Fig. 4.2 and Fig. 4.3), concentrations in the whole modelling domain decreased. This effect is more pronounced in the southern regions of the North Sea where initial concentrations had been highest.

The vertical distribution of sea temperature and salinity in January and August 1997 and the corresponding γ-HCH distribution from south to north along the 3°E are presented in Fig. 5.9 (see Appendix).

In winter the southern North Sea is generally well mixed from the surface to the bottom (Fig. 5.9a). This is also reflected in the distribution of total γ-HCH concentration (Fig. 5.9b). During warm seasons a stable thermal stratification is formed by summer heating (Fig. 5.9c) enhancing vertical gradients of total γ-HCH concentration in the northern part of the domain (Fig. 5.9d). High values of about 0.6 ng l^{-1} are found near the sea surface, and low values of less than 0.2 ng l^{-1} below where the Atlantic water flows in. Relatively high γ-HCH concentrations of more than 2 ng l^{-1} are found in the continental river estuaries in both January and August. As was already illustrated by the time series at individual locations (Fig. 4.2, Fig. 4.3 and Fig. 4.12), γ-HCH concentrations in August were higher than in January. Concentrations beneath the thermocline, if present, do not show seasonal variations.

There were no measurements available to determine the vertical distribution of γ-HCH concentrations in the North Sea. Model results suggest that the vertical structure of total γ-HCH concentration (Fig. 5.9b and Fig. 5.9d) is shaped by water column stratification and its seasonal variability (Fig. 5.9a and Fig. 5.9c).

Observed spatial distribution of total γ-HCH concentration with decreasing gradients towards the north-western part of the North Sea, similar to those shown by this modelling study (Fig. 5.12, Fig. 5.9b and Fig. 5.9d), have been reported (Gaul 1988; Theobald et al. 1996; Hühnerfuss et al. 1997, Lakaschus et al. 2002) and by the OSPAR Commission (OSPAR 2000). Low concentrations in the north-

western North Sea (Fig. 5.9b and Fig. 5.9d) are due to the inflow of cleaner Atlantic water. Along the coastline from southern Britain to Denmark close to the estuaries there are high concentrations; this indicates the importance of the river inflow which alters the local circulation. In fact, measurements in coastal waters close to large estuaries suggest that river input is a significant source for γ-HCH in the North Sea (Hühnerfuss et al. 1997; Sündermann 1994). This offers an explanation for the slower decrease in γ-HCH concentrations in the open North Sea than in the southern German Bight. This also implies that in coastal areas the waterborne inputs of γ-HCH may be dominant, whereas atmospheric deposition is more important in the open sea and can exhibit the same order of the magnitude as river inputs (Hühnerfuss et al. 1997). A correlation between γ-HCH concentrations in water (Fig. 4.2 and Fig. 4.3) and its concentration in precipitation and in the air is found.

5.2.2 α-HCH horizontal and vertical distributions

Measurements of α-HCH concentrations in the North Sea's surface water compiled during summer 1995 (Fig. 3.6) increase towards the southern and southeastern parts of the North Sea, with the highest concentration of 5-6 ng l^{-1} close to the mouth of the River Elbe.

Annual mean α-HCH concentrations averaged vertically for the whole modelling domain in 1996–2001 were calculated (Fig. 5.13 in the Appendix). These results show positive gradients of concentration towards the coasts; a similar pattern was found in the initial distribution (Fig. 3.6). During 1995–1998 the concentration of α-HCH in the continental coastal water was about 0.3 ng l^{-1} with a concentration of more than 5 ng l^{-1} in the Elbe estuary. Concentrations in the central and north-western parts of the North Sea were about 0.2 ng l^{-1}. The concentrations of α-HCH decreased further during 1999–2001 remaining below 0.2 ng l^{-1} in nearly the entire North Sea, except for the river estuaries. This indicates that rivers still contribute significantly to the α-HCH burden, in particular in the coastal zones. As was already demonstrated by α-HCH concentrations at selected locations (Fig. 4.6 and Fig. 4.7), concentrations in the whole modelling domain decreased over the simulation period.

Although α-HCH and γ-HCH possess similar physical-chemical properties (see Sect. 3.3) their environmental behaviour is different due to various inputs throughout the last decades. Therefore the two isomers have noticeably different distributions in the North Sea. Firstly, all α-HCH sea water concentrations have been decreasing steadily throughout the simulation period, whereas γ-HCH concentrations experienced an increase in 1997–1998. Secondly, unlike the γ-HCH temporal distribution (for which the decrease was more pronounced in the southern regions of the North Sea where initial concentrations had been highest), the α-HCH concentration decreased more or less homogeneously with time. This results from the use of pure lindane (γ-HCH) in western Europe (SRU 2004). Thus, α-HCH can come only from degradation of γ-HCH or atmospheric transport.

The vertical distributions of α-HCH concentration in January and August 1997 from south to north along 3°E are shown in Fig. 5.10 (see Appendix). Winter concentrations of α-HCH are well mixed along the section, as are the water masses (Fig. 5.9a). The model produces vertical gradients in α-HCH concentration in the deeper northern part of the North Sea (Fig. 5.10b). Similar to the γ-HCH vertical distribution, the model results for α-HCH suggest that the vertical concentration pattern (Fig. 5.10) is shaped by water column stratification and its seasonal variability (Fig. 5.9a and Fig. 5.9c).

5.2.3 PCB 153 horizontal and vertical distributions

Annual mean PCB 153 concentrations averaged vertically for the whole modelling domain in 1996–2001 were calculated (Fig. 5.14 in the Appendix). Generally, concentrations decline away from the shore, though concentrations in the continental estuaries and in the Thames estuary off the East Anglian coast are higher than in the English Channel and in the open North Sea. Measurements of PCB 153 concentration in the North Sea's surface water compiled during summer 1995 and interpolated onto the modelling domain of FANTOM (Fig. 3.7) show positive gradients towards the east, with the highest concentrations in the eastern and south-eastern parts of the North Sea. The highest concentration of 0.16 ng l^{-1} was found close to the mouth of the River Elbe.

This pattern remains throughout the entire simulation period. Concentrations of PCB 153 in 1995–1999 (Fig. 5.14a, Fig. 5.14b, Fig. 5.14c and Fig. 5.14d in the Appendix) do not show any pronounced trend with the values between 0.025–0.05 ng l^{-1} in the southern North Sea and less than 0.01 ng l^{-1} in the open North Sea. In 2000 (Fig. 5.14e) and beyond the modelled concentrations show an increase with values more than 0.035 ng l^{-1} in nearly the entire North Sea in 2001 (Fig. 5.14f). As was shown before (Sect. 4.4), this increase was also detected in the measured sea water, riverine and atmospheric concentrations.

The vertical distribution of PCB 153 concentration in January and August 1997 from south to north along the 3°E is shown in Fig. 5.11 (see Appendix). The corresponding vertical profile structure for PCB 153 calculated by FANTOM looks different from the profiles for the two HCH isomers (Fig. 5.9 and Fig. 5.10). This is especially evident for the winter distribution of PCB 153 (Fig. 5.11a). In January a clearly defined stratification of PCB 153 concentration (Fig. 5.11a) in a well-mixed water mass (Fig. 5.9a) is produced by the model. As was illustrated in Section 5.1, PCB 153 is mostly bound to particulate matter in sea water, whereas α-HCH and γ-HCH are mainly dissolved. The model results suggest that the distribution of the particle bound fraction of PCB 153 follows the POC distribution (Fig. 5.4 and Fig. 5.5 in the Appendix). Because of sinking and resuspension of newly deposited sediments, higher concentrations of particulate matter are accumulated near the bottom. This phenomenon is reflected in the vertical distribution of PCB 153 (Fig. 5.11a).

The modelled vertical distribution of PCB 153 in August (Fig. 5.11b) does not show the same structure as in January suggesting that it was shaped by non-intermediate storm events typical for winter periods in the North Sea. Indeed, the summer PCB 153 concentration pattern (Fig. 5.11b) is similar to that for α-HCH and γ-HCH (Fig. 5.9d and Fig. 5.10b) which is influenced by the thermal stratification occurring in summer. The model outcomes are also supported by the measurements in the German Bight reported by Hühnerfuss et al. (1997).

Due to its high persistence and volatility, PCB 153 undergoes long-range transport in the atmosphere. One open question is whether the PCB 153 sea water concentrations are still largely controlled by primary discharges or by re-emission from the sediments which are a major repository of PCBs in aquatic environment. Recent studies favour the primary emissions.

Other contaminated water bodies, such as the Great Lakes of North America, have been reported to currently be net sources of PCBs to the atmosphere as a result of the release of PCBs which have accumulated in the sediments (Jeremiason et al. 1994). The mass balance studies performed by Wania et al. (2001) and Axelman and Broman (2001) indicate that the Baltic Sea is a net sink of PCBs.

The phenomenon illustrated by Fig. 5.11a shows the significance of the sediment contribution to the PCB 153 burden of sea water. This yields to re-emission control rather than to primary discharges. However, a deeper insight onto the atmospheric depositions of PCB 153 as well as its oceanic inflow and outflow is needed (see Sect. 6.1.3).

5.3 α-HCH to γ-HCH ratio in sea water

The most prevalent isomers in soil, water, and air samples are α-HCH and γ-HCH. The ratio of these isomers can be used to track global transport of HCHs. The ratio α/γ-HCH together with concentrations of each isomer are useful source indicators. Also this ratio is an indicator of the current use of technical HCH. It can also indicate that present concentrations are being influenced by past use of technical HCH. When technical HCH mixture is the source, α/β and α/γ ratios lie between 5 and 11 and 3 and 7, respectively (Jantunen and Bidleman 1996; Chernyak et al. 1996; Hargrave et al. 1988).

Furthermore, the α/γ-HCH ratio can be used to estimate the age of the air and water masses (Oehme 1991). Air or water masses are considered as being old (or POPs are transported over a long distance) when the α/γ-HCH ratio is greater than 3 (Laane 1992; Jantunen and Bidleman 1997) and as being young (or indicating fresh application of HCH) when the α/γ-HCH ratio is less than 1 (Hoff et al. 1992; Lakaschus et al. 2001). The ratio is strongly influenced by variable partitioning and persistence of the two isomers.

The spatial distribution of the α/γ-HCH ratio typical for winter and summer were calculated from the surface α-HCH and γ-HCH concentrations (Fig. 5.15). As was shown before (see Sect. 5.2.1 and Sect. 5.2.2), the vertical distributions of α-HCH and γ-HCH concentrations in sea water (Fig. 5.9 and Fig. 5.10 in the Ap-

pendix) were very similar in winter and summer, mainly shaped by the water mass stratification. Therefore, it is adequate to use surface sea water concentrations for further analysis.

A lindane source will show a α/γ-HCH ratio near or less than unity. The modelled value of the α/γ-HCH ratio was less than 1 in the entire North Sea; this could be explained by the ban of technical HCH more than two decades ago and by the geographic remoteness of the North Sea from the regions where technical HCH is applied (e.g. India, Philippines). High α/γ-HCH ratios are observed in the Sea of Japan and Okhotsk, as well as in the Chukchi and East and South China Seas (Olsson 2002).

The γ-HCH arriving in the North Sea comes not only from the surrounding regions but also via long-range transport. The α/γ-HCH ratios for the open parts of the North Sea are low (>0.5), so we can assume that the local emissions predominate and the water masses are young.

Winter values of the α/γ-HCH ratio are 0.3–0.5 higher than the summer ones (Fig. 5.15) which have typical values of 0.1–0.2 caused by higher inputs of γ-HCH from rivers and the atmosphere during summer. The higher levels found in winter are influenced by the low temperatures, and the presence of a thermocline, which minimises mixing and dilution.

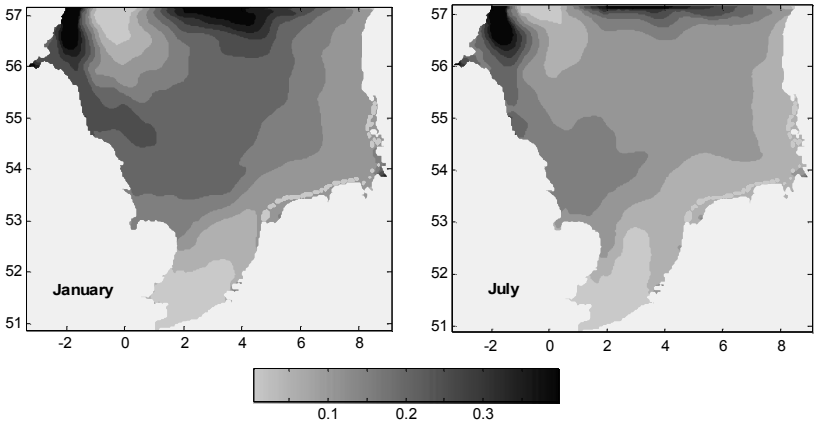

Fig. 5.15. Monthly mean α/γ-HCH ratio (calculated from the concentrations in the surface layer) in sea water in January and July 1997 calculated by FANTOM.

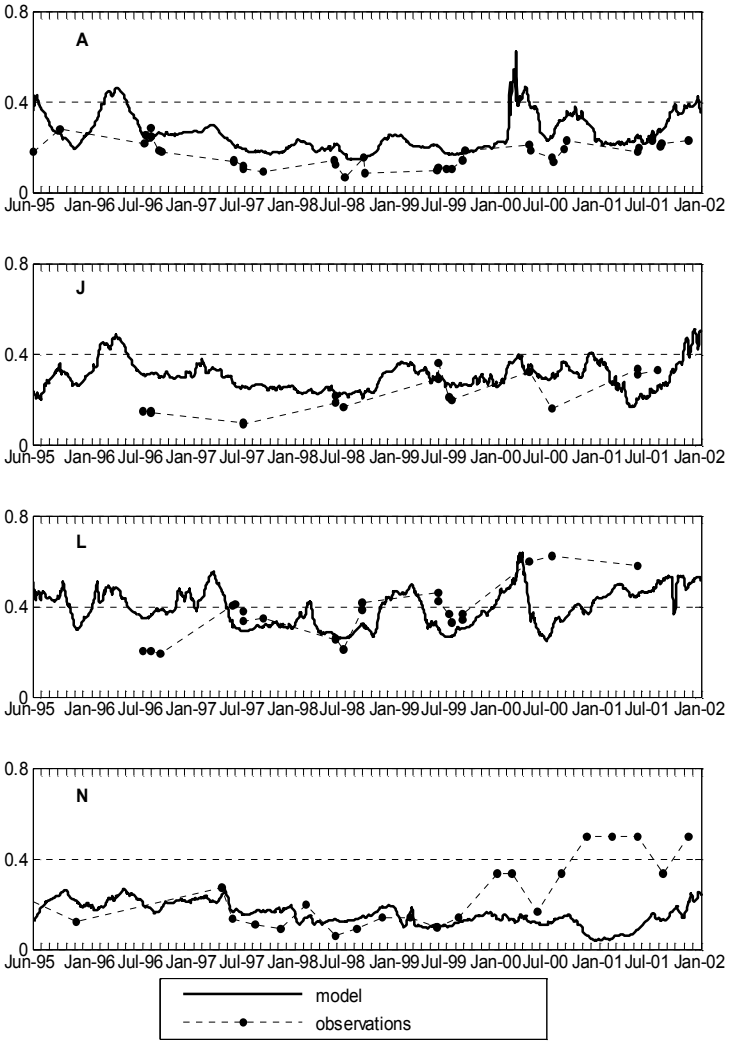

Fig. 5.16. α/γ-HCH concentration ratio in sea water at the locations A, J, L and N. Locations are shown on Fig. 5.1. Solid lines are model results derived from the main runs for α-HCH and γ-HCH. Dashed lines are derived from measurements.

The ratios between α-HCH and γ-HCH isomers can be used to explore time trends, because the relative concentrations are less affected by methodological differences. Temporal distributions of the α/γ-HCH ratio at different locations of the North Sea based on the daily averaged sea surface concentrations are calculated and compared with the corresponding ratios derived from measurements (Fig. 5.16). There was no pronounced trend in α/γ-HCH ratio from the model for the simulation period. Besides the annual signal, the values at the end of the simulation period are within a factor of 2 with regard to the starting values in all four locations (Fig. 5.16). In general, the α/γ-HCH ratios given by FANTOM are in good agreement with measurements. The underestimated values at point N near the English Channel are probably due to the overestimated lindane concentrations in this region as was discussed in Sect. 4.2. Other studies based on observations (Iwata et al. 1993; Lakaschus et al., 2002) showed that the α/γ-HCH ratio is observed to increase poleward, only to decrease on the Atlantic side as a result of the present usage of lindane in that region.

6 Contribution of Individual Processes to the Cycling of Selected POPs in the North Sea

A deeper insight on the pathways of contaminants in the environment can be obtained through their mass budgets in the respective compartments. Such budget calculations for the North Sea based on measurements have already been performed for cadmium, several organic contaminants (namely HCHs, PCBs and triazines), suspended matter and nutrients. These calculations resulted from the PRISMA[1] and ZISCH[2] experiments (Sündermann and Radach 1997).

The present study is the first attempt to estimate mass budgets of the three POPs based on model calculations. Mass budgets were calculated for individual years within the simulation period for the entire modelling domain and for the inner German Bight (Sect. 6.1). The residence times of the three POPs were calculated in order to understand the export and import relationships of the driving processes in the fate of POPs (Sect. 6.2). The contribution of the key processes to the burden of these POPs in the North Sea and in the inner German Bight are presented (Sect. 6.3) based on:

(a) Modelling scenarios when one key process was switched off for the entire simulation period.

(b) Dependencies of some processes on the environmental parameters, i.e. wind speed and sea surface temperature and air temperature.

6.1 Mass budgets of γ-HCH, α-HCH and PCB 153 in the North Sea

Mass budgets of α-HCH and γ-HCH and PCB 153 calculated by FANTOM are based on the inventories of a specific contaminant for a specified region during a specified period. For convenience annual data was used for the calculations. The inventories of the three contaminants include not only their concentrations in sea water but also their fluxes between air and sea water as well as between sea water and the upper sediment layers. In this way the budgets relate the burdens in the compartments to the fluxes between them.

---

[1] Prozesse im Schadstoffkreislauf Meer-Atmosphäre (PRISMA).

[2] Zirkulation und Schadstoffumsatz in der Nordsee (ZISCH).

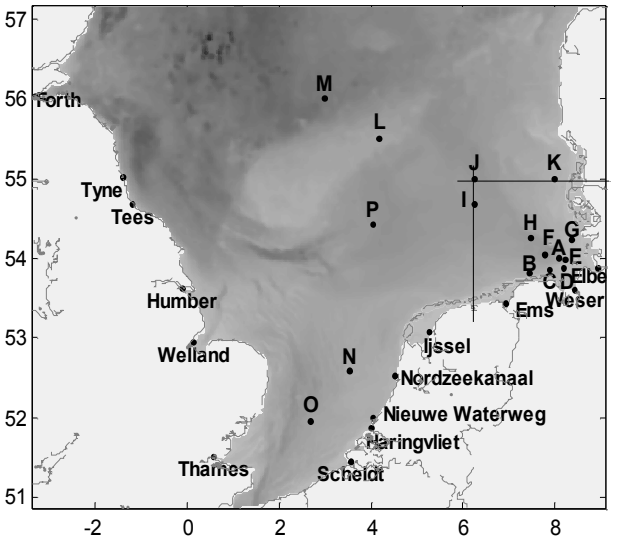

Fig. 6.1. Modelling domain of FANTOM and boundaries of the inner German Bight (lines) selected for the budgets calculations.

The mass budget calculations were performed for two regions (Fig. 6.1) referred to here as the North Sea (entire modelling domain) and the inner German Bight. In this context the inner German Bight is defined here as a region with its northern border at 55°N and the western border at 6°25'E, similar to the region defined in Sündermann and Radach (1997). The area of this region is 20,000 km^2 with a volume of 452 km^3 and a mean depth of 22 m.

Mass budgets of α-HCH and γ-HCH and PCB 153 integrated for the North Sea and the inner German Bight are constructed using:

(a) Flows of rivers and sea water through lateral boundaries into and out of the modelling domain.

(b) Wet, dry particle and gaseous atmospheric depositions and volatilisation.

(c) Loss due to degradation.

(d) Net transfer to the bottom sediments.

The mass balance equation of these processes, which are described in Chap. 2, can be written as:

$$M_t - M_0 = \int_0^t [Inflow]dt - \int_0^t [Outflow]dt + \int_0^t [Rivers]dt \tag{6.1}$$
$$+ \int_0^t [WetDep]dt + \int_0^t [PartDep]dt + \int_0^t [GasDep]dt - \int_0^t [Volatil]dt$$
$$- \int_0^t [Degrad]dt - \int_0^t [Sinking]dt + \int_0^t [Resuspen]dt$$

The modelled mass budgets for γ-HCH, α-HCH and PCB 153 in the North Sea are summarised in Table A.3, Table A.5 and Table A.7 and the inner German Bight are in Table A.4, Table A.6 and Table A.8 (see Appendix) and in Fig. 6.2 and Fig. 6.3 (see Appendix).

Because the processes presented on Fig. 6.2 and Fig. 6.3 differ in their scales (i.e. contribution of dry gaseous deposition into γ-HCH burden is almost four orders of magnitude larger than degradation), the results are presented on a logarithmic scale.

The question which is now addressed is whether the contribution of these processes to the contaminant burden is similar for the entire North Sea and for the inner German Bight. To answer this question an analysis of the annual budget calculations for each of the three substances was carried out.

6.1.1 Mass budget analysis for γ-HCH

For γ-HCH, the largest input for the North Sea for all six years occurs through gaseous atmospheric deposition and the lateral transport by ocean currents (Fig. 6.2a). The total atmospheric deposition (wet, dry gaseous and particle deposition) is much higher than the total flow through water pathways (i.e. inflow and outflow through the lateral boundaries and river inflow). Although the volatilisation flux has the same order of magnitude as the gas depositional flux, the net flux is positive for the North Sea as a whole. The model results also suggest that deposition of particles is negligibly low compared to other depositional processes. However, compared to the whole North Sea (Fig. 6.2a), the atmospheric input of lindane becomes less important on the scale of the inner German Bight (Fig. 6.3a).

The model results suggest that the river inflow is not the most dominant source with the values being more than one order of magnitude below those for the flux from the atmosphere (Table A.3). The inflow through the southern oceanic boundary was always greater than the outflow. This result supports the earlier conclusion that the English Channel contributed to the North Sea (entire modelling domain) burden of lindane throughout the simulation period (see Chap. 4). Large values of outflow through the northern oceanic boundary (Fig. 6.2a) indicate that the North Sea is influenced mainly by local discharges of γ-HCH.

In the inner German Bight the distribution of γ-HCH burdens between the processes differs from that for the entire North Sea (Fig. 6.3a and Table A.3). This is immediately apparent in the direction of the air–sea gaseous flux. The model results suggest that lindane was volatilised in the German Bight throughout the entire simulation period (Fig. 6.3a). Spatial distributions of lindane in the inner German Bight (Chaps. 4 and 5) showed increasing gradients towards the coast with the high concentrations being due to the proximity to the River Elbe and also due to the cyclonic circulation pattern in the North Sea. Indeed, the relative importance of the inflow from the rivers (i.e. Elbe, Weser and Ems) into the inner German Bight is higher than for the North Sea as a whole. The contribution from river inflow was up to 11% of the total input for the inner German Bight and less than 2% for the whole North Sea (Table A.3), varying between 0.65 t a^{-1} and 0.24 t a^{-1} for the entire North Sea and between 0.56 t a^{-1} and 0.20 t a^{-1} for the inner German Bight.

It is remarkable that although the fraction of γ-HCH bound to particulate matter was below 2% (see Chap. 5 and Fig. 5.4b in the Appendix) the contribution of sedimentation to the sea bottom calculated by FANTOM is identified as being among the most significant processes both for the North Sea and for the inner German Bight (Fig. 6.2a and Fig. 6.3a). This phenomenon is probably due to the relatively high content of organic carbon in the North Sea throughout a year compared to the global ocean. With the present model assumptions about the settling velocity and critical erosion velocity for particulate matter (see Chap. 2), the resuspension flux comprises around 10% of the sinking flux. On the time scale of years, it is a significant contribution: over 200 kg for the years 1996 to 1998 (Table A.3).

The total inflow of lindane through the oceanic boundaries of the inner German Bight varies between 5.4 and 3.3 t a^{-1} during the simulation period. Model calculations suggest that larger amounts of lindane are being transferred out of the inner German Bight than into it during the entire period. According to measurement-based mass budgets reported by Hühnerfuss et al. (1997) the outflow of γ-HCH is lower than the inflow. Their study suggests that the inner German Bight receives large amounts of γ-HCH due to river inflow and atmospheric deposition, with the wet deposition component being the largest one; this results in larger outflow than inflow into the region. Hühnerfuss concludes that the lower inflow from the inner German Bight is because (a) γ-HCH is being degraded more readily by photooxidation and marine microorganisms than α-HCH and (b) a partial isomerisation of γ-HCH to α-HCH induced by marine microorganisms occurs. The latter process is not resolved in FANTOM. This could explain the disagreement between results of this study and those from Hühnerfuss et al. (1997).

6.1.2 Mass budget analysis for α-HCH

The budget calculations for α-HCH in the entire modelling domain and in the inner German Bight are presented in Table A.5, Table A.6, Fig. 6.2b and Fig. 6.3b.

The major processes contributing to the α-HCH budgets in sea water, as is the case with γ-HCH, are atmospheric depositions and oceanic transport. Such similarities could be expected as the physical-chemical properties of α-HCH are similar to those of γ-HCH.

The calculated burdens suggest that the most significant pathways of α-HCH in sea water are atmospheric deposition and transfer through the northern boundary. The distinguishing feature of α-HCH budgets is the comparatively low values of wet deposition, in contrast to those found for γ-HCH. This is also seen from α-HCH concentrations in rain used as boundary conditions as discussed in Chap. 3. The net gaseous transfer of α-HCH was always positive (depositional) for the entire North Sea during the simulation period with the volatilisational flux being one order of magnitude lower than that for the gaseous deposit. The deposition of particles was negligibly small compared to other deposition mechanisms (Table A.5).

Although α-HCH is fairly water soluble, the flux into and from the bottom sediment layer is rather high, having a similar magnitude as the wet deposition flux. As in the case of lindane this is caused by high contents of POC in sea water. The resuspension flux for α-HCH compensates up to 20% of the loss due to settling to the bottom sediments.

The calculated annual burdens of α-HCH in the North Sea (Table A.5) suggest that inflow through the southern boundary from the English Channel was relatively insignificant, being three orders of magnitude less than the inflow through the northern boundary. In fact the modelled values of the net transfer of α-HCH through the southern boundary have the same magnitude as the degradation flux (Fig. 6.2b). According to the model calculations, the outflow from the northern boundary, ranging between 2.8 t a^{-1} and 3 t a^{-1}, is higher than the inflow which is in the range of 3.7 t a^{-1} and 4.1 t a^{-1}. Furthermore, the total outflow flux increased gradually during the six years of the model calculations. This, together with gradually decreasing α-HCH concentrations (Chaps. 4 and 5), suggests that the North Sea system as a whole can loose α-HCH due to washout through oceanic boundaries.

The major difference between the α-HCH burden in the inner German Bight given by the model (Fig. 6.3b) compared to that for the North Sea is the net volatilisational flux through the entire simulation period which exceeds even the transport through the lateral boundaries. Also sea surface temperatures in the inner German Bight are higher than in the North Sea in general. All this favours conditions for the reversed air–sea gaseous flux. The river inflow of α-HCH into the inner German Bight contributes up to 20% of the total inflow into the system. This phenomenon is supported by measured high river loads of α-HCH during the simulation period (Chap. 3).

The total transfer of α-HCH through the western and the northern boundaries of the inner German Bight is larger than the outflow comprising 0.5-1.39 t a^{-1} and 0.6-1.4 t a^{-1} for inflows and outflows respectively. These results are supported by the measurement-based study of Hühnerfuss et al. (1997) indicating that larger amounts of α-HCH are leaving the inner German Bight than actually transferred into this area through the ocean boundaries. Also results of this study presented in

Fig. 6.3b and Table A.6 suggest that the atmospheric inputs of α-HCH play a minor role in the inner German Bight as compared with the lateral inflow at the western boundary.

6.1.3 Mass budget analysis for PCB 153

Results of PCB 153 budget calculations are presented in Table A.7, Table A.8, Fig. 6.2c and Fig. 6.3c. PCB 153 is the least water soluble and the most lipophilic contaminant addressed in this study. As was shown earlier (see Sect. 5.1.2) about 30–50% of PCB 153 is in the particle bound fraction in the open North Sea and 90% and more in the inner German Bight. This provides an explanation for the large contribution of settling together with resuspension for the PCB 153 annual burdens both in the whole North Sea (Fig. 6.2c) and in the inner German Bight (Fig. 6.3c). In fact, the model calculation indicate that the sinking flux can be high enough to dominate all other key processes which showed its importance for the burdens of the two HCH isomers.

The importance of air–sea exchange is evaluated by comparing it to wet and dry particle depositional fluxes. The results suggest that wet deposition was a significant source of PCB 153 for the North Sea (Fig. 6.2c) during the studied period. The wet deposition flux even dominated the gaseous input of PCB 153 which ranged between 74 kg a^{-1} and 106 kg a^{-1}. The net gaseous flux was positive in 1996 and reversed in 1997 and 2001. During the other three years (1998–2000) the net air–sea flux integrated for the entire modelling domain was close to equilibrium.

The lateral inflow of PCB 153 was another significant process identified by the model (Table A.5). In particular, the flux through the northern boundary had the largest contribution with values from 30 kg a^{-1} to up to 260 kg a^{-1}. However, the inflow-outflow rates for the northern boundary were very close (Fig. 6.2c). The inflow through the English Channel was low in 1996, but was higher in 2000 and 2001. This phenomenon is supported by the annual mean PCB 153 concentrations (see Sect. 5.2.3) produced by the model, with relatively high values in 2001 compared to previous years.

The relative importance of the processes contributing to the PCB 153 budgets for the whole North Sea (Fig. 6.2c) did not show any trend throughout the simulation period; the same was found for its sea water concentration (see Sect. 5.2.3 and Chap. 4).

The net gaseous air–sea flux integrated for the inner German Bight was volatilisational during all six years of the simulation period (Fig. 6.3c). Also in this region the wet deposition dominates other depositional processes for PCB 153 as was already found for the entire North Sea (Fig. 6.2c).

The sinking and resuspension of PCB 153 in the inner German Bight are the next most important processes contributing to the overall burden. These fluxes were in the range 15.8 kg a^{-1} to 21.4 kg a^{-1} for the settling flux of PCB 153 and 6.34 kg a^{-1} up to 19.36 kg a^{-1} for the resuspended PCB 153. But in contrast to the whole North Sea, the ratio between sinking and resuspension of PCB 153 is close

to one for the inner German Bight. This follows the dynamics of POC in the German Bight discussed earlier (see Sect. 5.1.1). Particulate matter in the shallow German Bight is remobilised easier than in the open North Sea, and thus brings the previously settled PCB 153 back to the water column. Because PCB 153 is mostly prone to be carried with particles as compared to the two fairly water soluble HCHs, this phenomenon is also better demonstrated for PCB 153.

For the inner German Bight (Fig. 6.3c) the model produces high contributions of river inflow, which even exceeds the gaseous deposition of PCB 153 and the settling and resuspension processes in contrast to the entire North Sea. The river inflow ranging between 32.8 kg a^{-1} and 105.4 kg a^{-1} was also higher than the inflow from the western boundary. This is explained by very high concentrations of PCB 153 measured in the River Elbe (see Chap. 3). PCB 153 concentrations in sea water are very low, making measurements and further analysis difficult and prone to errors. The budget calculations depend a lot on the chosen input data as well as on physical-chemical properties of the compound. This can lead to uncertainties in the modelled values.

The transfer of PCB 153 through the lateral boundary is an important constituent of the mass budgets in the inner German Bight (Fig. 6.3c). The model results suggest that the inflow through the western boundary was greater than the outflow through the northern boundary. The total inflow into the inner German Bight lies between 30 kg a^{-1} and 117 kg a^{-1}. This phenomenon is supported by the large river inflow calculated for the inner German Bight during the simulation period (Table A.8). In accordance with the study by Hühnerfuss et al. (1997), the inner German Bight loses more PCB 153 through the northern boundary than is imported through the western boundary.

Model results discussed in this section can answer the question addressed in Chap. 5 about whether PCB 153 sea water concentrations are mostly controlled by primary discharges or by re-emission from the sediments. Other studies (Hornbuckle et al. 1993; Jeremiason et al. 1994) are in favour of the primary emissions. With large atmospheric inputs and oceanic inflow of PCB 153, similar conclusions can be drawn from this study.

6.2 Residence time of γ-HCH, α-HCH and PCB 153 in sea water

Residence times are commonly used as a measure of the retention of water or pollutants. The residence time is defined as the time it takes for a substance to leave the reservoir or how long a substance, starting from a specified location within a water body, will remain in the water body before exiting. It is conceived here as a measure of a pollutant's retention within defined boundaries. It is an important indicator for understanding the fate of contaminants in sea water.

The residence time of a pollutant in sea water can be calculated based on the mass conservation principle for a non-steady state (see Eq. 2.1 in Chap. 2). Ac-

cordingly, the rate of a pollutant mass accumulation in a given volume ($\partial C/\partial t$) is the rate of a pollutant flowing into this volume (F_{in}) minus the rate of a pollutant flowing out of this volume (F_{out}) plus the rate of introduction (Q_c) minus the removal rate (R_c). The equation for the residence time of a pollutant in sea water τ_{sw} is:

$$\tau_{sw} = \frac{M_{total}}{(F_{in} - F_{out}) + (Q_c - R_c)} \tag{6.2}$$

It follows from Eq. 6.2 that regions with a short residence time will export POPs more rapidly than regions with longer residence time.

Residence times of γ-HCH, α-HCH and PCB 153 were calculated based on their annual burdens. Overall residence times for the three compounds for the individual years during the six year simulation period in the entire North Sea and in the inner German Bight are summarised in Table 6.1 and Table 6.2.

The residence times presented in Table 6.1 and Table 6.2 have large variations from year to year. Residence times calculated in this way are strongly dependent on the physical-chemical properties of a pollutant, environmental conditions and input data (see also Chaps. 3 and 4). Therefore, variability and uncertainties in the input data will introduce variability and uncertainties in the residence times.

Table 6.1. Residence times of γ-HCH, α-HCH and PCB 153 in sea water (days) calculated by FANTOM for the North Sea based on yearly data.

τ_{sw} [days]	North Sea					
	1996	1997	1998	1999	2000	2001
γ-HCH	117.43	125.53	135.40	191.32	295.00	348.29
α-HCH	114.24	166.40	127.04	190.22	268.23	125.08
PCB 153	4391.6	3210	1438.2	1912.2	1372.4	642.7

Table 6.2. Residence times of γ-HCH, α-HCH and PCB 153 in sea water (days) calculated by FANTOM for the inner German Bight based on yearly data.

τ_{sw} [days]	Inner German Bight					
	1996	1997	1998	1999	2000	2001
γ-HCH	237.01	439.29	379.51	329.99	282.21	530.26
α-HCH	142.58	245.21	387.05	665.17	134.92	102.58
PCB 153	1479.8	1372.9	1089	1296	1505.6	1221.4

The largest variability is in the atmospheric data used in this study (i.e. air and precipitation concentrations of POPs). This could offer an explanation for the variation in residence times calculated for individual years. Moreover, the air–sea flux, particularly its temperature dependency, introduces uncertainties in the calculated magnitude and direction of the flux and the sea water concentrations of POPs (see Chap. 4).

The model results suggest that PCB 153 has the largest residence time of the three POPs addressed in this study, ranging between 1.8 and 4 years. Shorter residence times were found for the HCH isomers: 117–530 days for γ-HCH and 114–665 days for α-HCH.

The mean anti-clockwise pattern of currents commonly observed in the North Sea (Sect. 2.5.1) favours short residence times (stronger transport) of about 11 days for water mass along the south eastern coast and longer ones of about 40 days in the central North Sea (OSPAR 2000; Lehnart and Pohlmann 1997). According to the results obtained by Lenhart and Pohlmann (1997) the water masses of the German Bight are exchanged within 33 days in the mean. This value ranges from 10 to 56 days. The mean residence time of water masses for the whole basin determined by Lenhart and Pohlmann is about 167 days.

Weaker transports (or longer residence times) in some subregions of the North Sea suggest that concentrations of some POPs should be more sensitive to vertical exchange rates and less dependent on the horizontal circulation. This also implies that a relatively water soluble compound (e.g. HCH isomers which end up in these regions of the North Sea) may not be subject to transport with sea currents to any significant extent. On the other hand, POPs in the subregions with stronger transports (e.g. in the German Bight where the concentrations are also higher) will be transported northwards by the coastal current.

6.3 Relative importance of some key processes for the fate of POPs in sea water

6.3.1 The role of air–sea exchange, degradation, river and oceanic inflow

In order to demonstrate the importance of the key processes affecting the abundance of the studied POPs in the North Sea, some "everything but one process" model runs were performed. In each scenario the model was run without one process with the other processes working as usual. The following scenarios were used:

(a) "no atm. deposition" – wet, dry gas and particle depositions were switched off.

(b) "no volatilisation".

(c) "no degradation".

(d) "no rivers".

(e) "no EC and AO inflow" – the pollutant's concentrations on the lateral boundaries (English Channel and Atlantic Ocean) were set to zero.

Scenarios (a), (b), (c) and (d) are now discussed with the results presented in Fig. 6.4, Fig. 6.5 and Fig. 6.6 (see Appendix) for the two HCHs and PCB 153. Their concentrations were analysed and compared with concentrations obtained under the "all processes" run (when all processes were included) at two locations: one in the German Bight and one in the open North Sea. Results from the experiment identified under point (e) were discussed in Chap. 4 as part of the model evaluation.

6.3.2 "Everything but one process" scenario analysis for γ-HCH

The levels of γ-HCH in the German Bight seem to be controlled by the river inflow (Fig. 6.4a in the Appendix, see also Sect. 6.1.2). Moreover, the river inflow is responsible for the jagged pattern of the concentration. Concentrations obtained for the "no rivers" scenario lie below 3 ng l^{-1}, whereas they go up to 4 ng l^{-1} for the "all processes" run.

Spatial distributions (see Chap. 5) show that the highest levels of lindane are in the southern North Sea and around the German Bight. The Elbe and Weser estuaries in Germany have high concentrations of lindane up to 15 ng l^{-1} and the Humber Estuary in the UK has levels of 5.3 ng l^{-1}. It seems likely that higher levels around estuaries occur as a result of agricultural use of lindane.

Annual river input of lindane to the North Sea within the simulation period is estimated to be between 243 and 647 kg a^{-1} – although this does not include data from France and Sweden.

Although the lost due to volatilisation seems to be compensated by the atmospheric (wet plus dry) deposition (see Sect. 6.1.1), its contribution is responsible for doubling the concentration values. This effect is more pronounced during late summer. The results from the model experiment suggest that the atmospheric deposition is responsible for the annual cycle detected in the lindane concentrations (see Chap. 4). This phenomenon is better demonstrated by the results from the "no atm. deposition" scenario for the open North Sea (Fig. 6.4b in the Appendix).

In the open North Sea at location M (Fig. 6.4b) the importance of the river inflow is not pronounced suggesting that here the predicted levels of γ-HCH result mainly from the atmospheric deposition. Concentrations of lindane are three to four times lower than in the German Bight. The contribution of volatilisation is relatively low compared to that in the German Bight. The run without atmospheric deposition clearly shows that it is the main supplier of lindane into this area. This hypothesis is supported by the knowledge that the sea currents in this subregion of

the North Sea are also weaker which favours weaker exchange and thus longer residence times of water masses.

In both the German Bight and open North Sea the increase in concentrations due to the absence of degradation is not significant (Fig. 6.4a and Fig. 6.4b in the Appendix).

6.3.3 "Everything but one process" scenario analysis for α-HCH

For α-HCH concentrations in the German Bight, the river inflow (dominated by the River Elbe) can be responsible for more than 50% of the concentration increase (Fig. 6.5a). This phenomenon is more pronounced during spring when the fresh water inflow is the largest. As for lindane, the significant contribution of the river inflow explains the "unsmoothness" in the concentration patterns.

The scenario "no volatilisation" (Sect. 6.3.1) shows that volatilisation has a significant impact on levels of α-HCH (Fig. 6.5a and Fig. 6.5b). The concentrations without volatilisation are up to a factor of four higher than under conditions when all processes are included. The role of volatilisation is equally high at both analysed locations. There is a large impact on the open North Sea concentrations of α-HCH in the "no atm. deposition" experiment (Fig. 6.5b). This suggests that volatilisation of α-HCH is higher in the German Bight than in the open North Sea. The "no degradation" scenario shows that the contribution of degradation is very low deriving from high persistence of α-HCH.

The importance of re-emissions of some POPs from sea surfaces has been demonstrated for other water bodies, e.g. for the Great Lakes in USA as well as in the Arctic sea areas (Hornbuckle et al. 1993; Bidleman et al. 1995). Bidleman et al. (1995) showed that a decline in the atmospheric concentration of α-HCH in the Arctic had reversed the direction of net air–sea exchange. Thus some northern waters are now sources of α-HCH.

Air concentrations of α-HCH over the North Sea used in this study were low and gradually decreasing during the simulation period (Chap. 3). However, sea water concentrations in the North Sea experience a slower decrease. Therefore similar conclusions to those made by Bidleman et al. (1995) could be drawn from this study which suggests that some subregions of the North Sea, such as the German Bight, are also net sources of α-HCH for the atmosphere throughout the whole year (see also Sect. 6.2.2).

6.3.4 "Everything but one process" scenario analysis for PCB 153

Results of the "everything but one process" scenario for PCB 153 are presented in Fig. 6.6. The most distinctive feature following from these model experiments is that for PCB 153 the "no volatilisation" scenario has a large impact. This suggests that volatilisation is responsible for a factor of 6 increase in sea water concentrations of PCB 153 in the German Bight (Fig. 6.6a) and a factor of 20 increase in the

open sea (Fig. 6.6b). The latter phenomenon is less pronounced in the open North Sea (Fig. 6.6b) where sea water concentrations of PCB 153 were an order of magnitude lower than in the German Bight; this was also found under the "all processes" scenario.

The "everything but one process" scenario supports the conclusions made in Sect. 6.1.3 that not only the German Bight but also the North Sea as a whole can re-volatilise PCB 153 with the annual air–sea flux going from depositional to volatilisational for some years (see also Fig. 6.2c and Fig. 6.3c). Recent studies (Axelman et al. 2001; Wania et al. 2001) showed that the gaseous air–sea exchange is one of the most important processes governing the fate of PCBs. Measurement-based studies have shown that volatilisation is responsible for the major loss of PCBs in the Lake Superior (Hornbuckle et al. 1993; Hornbuckle et al. 1994; Jeremiason et al. 1994). However, as was shown by Bruhn et al. (2003) these estimates depend to great extent on the selected temperature dependency of Henry's law constant.

Measurements conducted in the Kattegat Sea showed that this region acts as a source of PCBs to the atmosphere but periods of net deposition also occur (Sundqvist et al. 2003). Other contaminated water bodies such as the Great Lakes have been reported to currently be net sources of PCBs to the atmosphere as a result of the release of PCBs which have accumulated in the sediments (Jeremiason et al. 1994). The mass balance studies performed by Wania et al. (2001) and Axelman et al. (2001) indicate that the Baltic Sea is a net sink of PCBs.

According to a previous modelling study (van Pul et al. 1997), the main removal process from the atmosphere for PCBs is deposition, making this process the major source of PCBs for the water bodies. The results of this study are in agreement with that finding.

In contrast to α-HCH, air concentrations of PCB 153 over the North Sea used in this study have not shown a fast decline. Although some localised trends may be apparent, overall no obvious changes in PCB 153 levels in sea water have been established.

6.3.5 The role of temperature and wind speed in the air–sea gaseous exchange

In the previous section it was shown that the gaseous air–sea flux plays a key role in controlling the fate of the three selected POPs in the North Sea. For the North Sea as a whole the net air–sea flux for γ-HCH and α-HCH was depositional, whereas for the inner German Bight it is volatilisational. PCB 153 concentrations showed potential for net volatilisation in the entire North Sea. In the inner German Bight the air–sea flux remained net volatilisational during the entire simulation period.

Besides the non-equilibrium state between air and sea concentrations, the air–sea gaseous flux is also driven by the wind speed and temperature (see Sect. 2.2.1). It is believed that the wind speed determines the rate of the air–sea flux,

whereas the temperature can have a significant role in determining the flux direction (Bidleman et al. 1995).

The fortnightly mean air–sea fluxes of γ-HCH, α-HCH and PCB 153 were plotted together with the corresponding air, sea surface temperatures (SST) and wind speeds for the German Bight and for the open North Sea for the entire simulation period (Fig. 6.7).

The sea surface temperature (SST) values calculated by HAMSOM (Sect. 3.2) lie between 1°C and 20°C in the German Bight (Fig. 6.7a) and between 4°C and 15°C in the open North Sea (Fig. 6.7c) during the simulation period. The measured air temperatures have higher temporal gradients, dropping to negative values in winter 1996. The peaks in the SST occur generally after the peaks in air temperatures, with the maxima of SST occurring in late August and minima in February. The wind speeds are generally higher in the winter season.

The values of the air–sea gaseous flux for γ-HCH range between $-0.3 \cdot 10^{-3}$ ng m^{-2} s^{-1} and $+0.8 \cdot 10^{-3}$ ng m^{-2} s^{-1} in the German Bight and $0.1 \cdot 10^{-3}$ ng m^{-2} s^{-1} and $1.2 \cdot 10^{-3}$ ng m^{-2} s^{-1} in the open North Sea. The air–sea flux of γ-HCH in the German Bight calculated for the six years revealed a clear seasonal pattern. In winter the air–sea flux of γ-HCH in the German Bight is volatilisational, but from April until June it turns to net depositional. Then from July to October it turns to volatilisational again, turning back to depositional from October to December. The maxima in depositional flux often corresponded to the maxima in the wind speeds which occurred in winter.

The air–sea exchange of γ-HCH both in the German Bight and in the open North Sea has gone to a near equilibrium state in 1999. Although the air–sea flux of γ-HCH in the open North Sea has a similar annual cycle as that in the German Bight, it was net depositional throughout the whole simulation. This pattern is in agreement with the results of budget calculations (Sect. 6.1.1).

The air–sea gaseous flux values for α-HCH ranges between $-0.5 \cdot 10^{-3}$ ng m^{-2} s^{-1} and $+1.2 \cdot 10^{-3}$ ng m^{-2} s^{-1} in the German Bight (Fig. 6.7b) up to $1.9 \cdot 10^{-3}$ ng m^{-2} s^{-1} in the open North Sea (Fig. 6.7c). The model results suggest that the air–sea gaseous flux in the German Bight has a seasonal cycle: it is mostly volatilisational in winter (i.e. between December and February) then the flux turns to depositional in March and remains so until August with episodic volatilisation events. In August until October the volatilisation prevails, later on reversing to deposition. The air–sea flux of α-HCH in the North Sea was always depositional with a near equilibrium state in 2001.

The air–sea gaseous flux of PCB 153 during the studied period was in the range $-6 \cdot 10^{-5}$ ng m^{-2} s^{-1} to $1.9 \cdot 10^{-5}$ ng m^{-2} s^{-1} in the German Bight and $-5 \cdot 10^{-5}$ ng m^{-2} s^{-1} to $2.1 \cdot 10^{-3}$ ng m^{-2} s^{-1} in the open North Sea (Fig. 6.7). These values are in agreement with the measurements-based atmospheric deposition fluxes calculated for the eastern Skagerak (Palm et al. 2004) which were 5.5 ng m^{-2} day^{-1} in summer and 0.57 ng m^{-2} day^{-1} in winter. The model indicates that volatilisation of PCB 153 occurred during spring although there was no clear seasonal cycle.

The major difference between the air–sea fluxes of the two HCHs and PCB 153 is that volatilisation of PCB 153 also occurs in the open North Sea, whereas the

HCHs volatilise in the German Bight. The temperature dependency of the air–sea flux was the process which is thought to be least certain under the present model setup. The temperature dependency of the Henry's law constant (HLC) was shown to be a very significant factor determining the magnitude and direction of the air–sea flux (see Chap. 4). The choice of different HLC values altered the HCH concentration by 50%. Such experiments were not performed for PCB 153 because of the lack of data about the HLC dependency on temperature.

7 Conclusions and Outlook

7.1 Conclusions

Persistent organic pollutants are harmful to human health and the environment. However their fate and pathways in the different environmental compartments are not yet fully understood. Models of POPs are recognised as helpful tools for assessing their cycling in natural systems. The application of models is encouraged under the Convention on LRTAP and the Stockholm Convention (see Chap. 1). The objective of this study was to advance our understanding of the fate of POPs in the aquatic environment as a basis for producing realistic estimates of their spatial and temporal distribution and pathways in the North Sea. With such information current and future exposure of the North Sea to contamination by POPs can be addressed.

In Chap. 2 the fate and transport ocean model FANTOM developed to assess the fate of POPs in the North Sea was described. FANTOM is based on current knowledge about the mechanisms governing POPs behaviour in sea water. The processes considered are transport with sea currents, atmospheric deposition and air–sea exchange, degradation in sea water, partitioning to particles suspended in sea water and subsequent sedimentation or resuspension from the bottom. In other models of POPs settling with particles in the oceanic compartment is treated as an ultimate sink. Recent measurements in the North Sea (van der Zee and Chou 2005) showed that resuspended sediments can have a significant contribution to the POC load in sea water. Consequently the resuspension of previously settled POC has been considered in FANTOM.

In Chap. 3 the model setup for investigating the sea water fate of γ-HCH, α-HCH and PCB 153 in the North Sea during 1995–2001 was presented. For the first time a measurement-based ocean model is applied on the regional scale. The three pollutants were chosen based on the differences in their physical-chemical properties (and consequently environmental behaviour) and data availability on the time scale of several years. To assure a realistic representation of POPs fate in sea water, a survey of physical-chemical properties and available observational data was performed.

- The physical-chemical properties in some cases can differ in more than one or even two orders of magnitude for the same compound. Recently reported physical-chemical properties were chosen for the model calculations.

- The compilation of measurements of POPs in the North Sea revealed that although it is relatively well assessed comparing to other seas, data for sea water is sparse in time and space. The data sets for γ-HCH and α-HCH were the best in terms of spatial and temporal coverage. Measured sea water concentrations of PCB 153 are low and were often very close or below the detection limit.

In Chap. 4 modelled γ-HCH, α-HCH and PCB 153 concentrations in the surface water were compared with measurements at different locations in the North Sea. No measurements of the vertical concentration profiles were available. As far as comparison was possible, it was found that FANTOM is able to reproduce the spatial distribution of γ-HCH, α-HCH and PCB 153 concentrations in sea water.

The model captured the gradual decrease in α-HCH sea water concentration. It also captured the increase in γ-HCH until 1998 and the subsequent decrease in concentration during 1998–2001. The decrease produced for the central part of the North Sea for both HCHs is slower than the one for the areas remote from the polluted estuaries. In most of the locations where comparison were made there is a good correlation between observations and the model results, with correlation coefficients up to 0.95. Weaker correlations were found for the colder periods when calculated concentrations were higher than observed. This could be due to insufficient temporal resolution of the observational time series and uncertainties in the temperature dependency of HLC (Henry's law constants) used for the air–sea flux calculations. The latter hypothesis was verified by the model experiments using two different temperature dependencies of HLC for γ-HCH and α-HCH. These model experiments revealed:

- Different HLC temperature dependencies are responsible for a 20–50% change in γ-HCH and up to a 60% change in α-HCH sea water concentrations.

A model experiment with boundary conditions set up at the lateral boundaries showed:

- Overestimations in the modelled concentrations of γ-HCH in 2000–2001 seem to be due to insufficient input data at the open sea boundaries.

- Inflows from the English Channel and the Atlantic Ocean at the northern boundary contribute to the loads of γ-HCH even in the German Bight. However this contribution seems to be decreasing now.

- A similar experiment for α-HCH showed that its transport through the oceanic boundaries is less significant for the levels of α-HCH in the North Sea than for γ-HCH.

The model captures the spatial and temporal gradients of the concentration for HCHs as well as the concentration range for PCB 153, although correlations between measured and modelled concentrations were no higher than 0.7 which is lower than for the two HCHs. Also the measurements of PCB 153 are more uncer-

tain due to its low concentrations in sea water. The model results suggest that the calculated PCB 153 pattern is determined by the input data variability. No clear temporal trend for PCB 153 is detected.

Concentrations in the atmosphere correlate with concentrations in sea water, indicating the significance of the atmospheric input of γ-HCH, α-HCH and PCB 153 in the North Sea. Although the air–sea exchange is one of the most important driving mechanisms, it also introduces major variability in the model results.

In Chap. 5 the occurrence of γ-HCH, α-HCH and PCB 153 and their pathways within the North Sea were studied. The model results showed:

- Absorption by suspended particles in sea water is expected to be most important for PCB 153 as it is the most lipophilic pollutant addressed in this study. FANTOM estimates that up to 90% of the total PCB 153 concentration can be in particulate form. For the two HCHs this fraction is below 2%. A correlation between the annual cycle of biomass and PCB 153 sea water concentrations is found.

- The temporal pattern of modelled concentrations of the three pollutants in sea water is reflected in fish concentrations of these POPs. Although PCB 153 sea water concentrations were up to two orders of magnitude lower than the concentrations of γ-HCH and α-HCH, the levels in fish for PCB 153 are up to two orders of magnitude higher than those of HCHs. The expected bioaccumulation potential of PCB 153 is confirmed. This implies that even very low concentrations of PCB 153 in sea water are still hazardous for the North Sea ecosystem.

- The vertical distributions of γ-HCH and α-HCH produced by FANTOM follow the water mass stratification, i.e. well mixed from the surface to the bottom in winter and stratified due to thermal stratification in summer. In the case of PCB 153, the vertical concentration is shaped by the dynamics of POC when there are sufficiently high concentrations of POC available and otherwise by water mass stratification.

- The calculated α-HCH/γ-HCH ratio shows no pronounced trend during the simulation period. The ratio values remained low (<0.5) in almost the entire modelling domain indicating the predominance of sources of lindane in the region.

In Chap. 6 the contribution of individual processes to the abundance of γ-HCH, α-HCH and PCB 153 was assessed. The annual mass budgets and residence times of these three pollutants were presented. The entire North Sea (i.e. the entire modelling domain) was compared to the inner German Bight.

- Atmospheric deposition and rivers are the two largest sources of γ-HCH, α-HCH and PCB 153 (for the North Sea). The relative importance of these sources is different for the inner German Bight and the North Sea as a whole. Atmospheric deposition contribution to the loads of the three selected con-

taminants was up to 85% in the North Sea (entire modelling domain) and below 45% in the inner German Bight. Air–sea flux and transport with sea currents are the major mechanisms which determine the cycling of the three POPs in the North Sea.

- According to the annual budgets, the net air–sea gaseous flux is depositional in the whole North Sea for γ-HCH and α-HCH. This is consistent with the finding from the POPCYCLING-Baltic project (Pacyna et al. 1999) that the air–sea flux of α-HCH was depositional in Skagerrak in 1980–2000. FANTOM produces volatilisational flux of γ-HCH and α-HCH in the inner German Bight. For PCB 153 it was both net depositional and volatilisational for individual years in the two regions. Measurements in the Baltic Sea showed that with regard to PCBs the temperature dependency of the HLC can significantly alter the magnitude and direction of the air–sea flux (Bruhn et al. 2003). This means that the choice of HLC introduces significant uncertainties to the calculated gaseous fluxes of PCB 153. A similar effect can be expected for HCHs based on test runs using another HLC temperature dependency.

- The contribution of water to POC partitioning of γ-HCH, α-HCH and PCB 153 in the budgets is also identified. This is probably due to the relatively high content of POC in the North Sea compared to the global ocean. Even for such a fairly water soluble compound as α-HCH, the sinking flux of POC associated fraction has the same order of magnitude as the river inflow. According to the model calculations, POC resuspension returns up to 80% of the previously deposited contaminants.

7.2 Outlook

Measurements of most POPs in sea water are still too limited (maybe with the exception of HCH isomers) to allow a comprehensive assessment of their spatial and temporal distributions. Therefore models have to be further developed and used to assess their sources and establish their environmental effects.

From this study it has become clear that transport models can address the fate of some POPs, at least on the regional scale. Despite the uncertainties in some input parameters and lack of observational data, FANTOM was capable of reproducing realistic multi-year temporal and spatial distributions of γ-HCH, α-HCH and PCB 153 in the North Sea and it can even indicate their concentrations in biota (fish tissue).

At present the model is still under development but it can still be used for several purposes.

- *Evaluating "new" substances*. The impact of historical (past time) emissions in the present conditions of the North Sea can be evaluated.

- *Evaluating import and export of POPs*. The import (influence of discharges of other countries to contamination in waters of a given country) and export (influence of discharges of each country to contamination of coastal waters of other countries) of a POP can be investigated. Moreover, if atmospheric depositions can be allocated to countries, the import and export evaluation can be performed with regard to atmospheric emission of these countries as well.

- *Elaborating case studies for possible scenarios*. For example scenarios of economic development and related usage of coastal and marine environments can be investigated.

- *Addressing the effects of climate change and variability in the 21st century*. Climate change and variability can have profound effects on the pathways of POPs globally and in the North Sea in particular, in response to both physical and biological factors. Ocean currents and the air–sea exchange of POPs are all subject to alteration as a result of climate change. Therefore the current exposure of the North Sea to contamination of POPs could alter dramatically as climate-related physical and biological phenomena change over the coming decades.

The modelling concept developed and applied in this study is also valid for simulating the fate of other contaminants in the North Sea which do not behave as passive tracers (e.g. radioactive substances or heavy metals). FANTOM can be also applied to other seas (e.g. the Baltic Sea or the Irish Sea).

The most significant gaps to be filled for future development and application of POPs fate models are as follows.

- *Improved input parameters*. More observational data and information about the physical-chemical properties of compounds is required. In particular information is needed about the HLC as it is the most important for model applications in the marine environment.

- *Refined description of the key processes*. The priority is to improve the air–sea flux parameterisation which is one of the major mechanisms driving the POPs fate in aquatic systems, but is far from being completely described (e.g. effect of rain, spray drops, surface films). For example, volatilisation could be limited by the presence of organic films. This would significantly change the budgets of PCB 153.

In conclusion, it remains a future task to investigate the fate of compounds with different environmental behaviours. This model could be the basis for further research on the contribution of different sources and sinks and the sensitivity of contaminants behaviour in the marine environment to the individual processes under present and future climate conditions.

Tables

Table A.1. Constant parameters used in FANTOM.

Parameter	Symbol	Units	Value, reference		
			γ-HCH	α-HCH	PCB 153
Molar mass	M	g mol^{-1}	290.85		360.88
Intercept of the temperature dependent Henry's law constant	b	–	10.14 ± 0.55 [1]	10.13 ± 0.29 [1]	14.05 [4]
			7.54 ± 0.54 [2]	9.31 ± 0.38 [2]	
Slope of the temperature dependent Henry's law constant	m	K	- 3208 ± 161 [1]	-3098 ± 84 [1]	-3662 [4]
			- 2382 ± 160 [2]	-2810 ± 110 [2]	
Octanol-water partitioning coefficient	K_{ow}	–	3.98×10^{3} [3]	5.89×10^{3} [3]	5.62×10^{6} [5]
Degradation rate in ocean water at 298 K	k_{deg}	s^{-1}	2.3×10^{-8} [3]	2.7×10^{-8} [3]	1.6×10^{-9} [5]
Dry particle deposition velocity	v_{dep}	m s^{-1}	2×10^{-5} [6], [7]		
Specific aerosol surface	θ	m^2 m^{-3}	1.5×10^{-4} [8]		
Adsorption constant	s	Pa m	0.17 [9]		
Settling velocity of SPM	v_{set}	m s^{-1}	3×10^{-4} [10]		
Threshold shear velocity for erosion of SPM	$v_*^{cr,e}$	m s^{-1}	0.028 [10]		
Threshold shear velocity for deposition of SPM	$v_*^{cr,d}$	m s^{-1}	0.01 [10]		

[1] Sahsuvar et al. 2003; [2] Kucklick et al. 1991; [3] Klöpffer and Schmidt 2001; [4] Paasivitra et al. 1999; [5] Beyer et. al. 2001; [6] McMahon and Denison 1979; [7] Slinn 1983; [8] Pekar et al. 1998; [9] Junge 1977; [10] Pohlmann and Puls 1994.

Table A.2. Stations used for evaluating the results from FANTOM, their geographical locations and number of measurements available for γ-HCH, α-HCH and PCB 153 within the simulation period (1995-2001)**.**

Symbol on the map	Lat.	Long.	Months of sampling	Number of measurements γ-HCH	Number of measurements α-HCH	Number of measurements PCB 153
A	54.00° N	8.00° E	5-9	36	36	31
B	53.72° N	7.45° E	11-2	14	14	14
C	53.85 ° N	8.06 ° E	11-2	14	14	14
D	53.86 ° N	8.13 ° E	11-2	14	14	14
E	53.98 ° N	8.22 ° E	11-3, 5, 7-9	26	14	14
F	54.05 ° N	7.86 ° E	11-2	14	14	14
G	54.22 ° N	8.38 ° E	1, 2, 5-9	41	40	21
H	54.25 ° N	7.50 ° E	5-9	25	30	17
I	54.67 ° N	6.33 ° E	5-9	20	17	10
J	55.00 ° N	6.25 ° E	5-8	12	17	9
K	55.00 ° N	8.25 ° E	5-9	21	25	22
L	55.50 ° N	4.17 ° E	5, 9, 12	18	23	0
M	56.00 ° N	3.00 ° E	7	4	0	0
N	52.58 ° N	3.53 ° E	2, 3, 5, 8, 11, 12	21	22	0
O	51.96 ° N	2.68 ° E	2, 5, 8, 11	7	7	0
P	54.42 ° N	4.04 ° E	8	6	6	0
Q	55.00 ° N	6.20 ° E	9, 10	8	8	6
R	55.00 ° N	8.00 ° E	5,6 8,9	7	7	0
Total number of measurements:				308	308	186

Table A.3. Cumulative contributions of different processes for the γ-HCH yearly mass budgets in kg a^{-1} calculated by FANTOM for the North Sea.

Processes contribution	γ-HCH in the North Sea					
[kg a^{-1}]	1996	1997	1998	1999	2000	2001
Wet deposition	5470.25	7074.4	4838	3480.65	3019.48	1673.42
Dry particle deposition	0.05218	0.04302	0.04389	0.02281	0.01788	0.01118
Dry gaseous deposition	8849.8	8562.3	8902.1	4854.7	3654.3	2339.1
Volatilisation	3415.3	3865	3498.9	2427.4	2059.3	1587.6
Degradation	2.49	3.41	2.69	1.93	1.7	1.26
Sinking	1964.9	2239.2	2064	1478.7	1308.8	983.19
Resuspension	213.92	241.66	207.91	138.2	116.67	98.123
River inflow	430.56	646.72	554.15	398.86	317.07	243.14
Lateral boundaries inflow	8273.5	7803.6	8410.6	8174	8399	7902.8
Lateral boundaries outflow	8415.43	8650.46	9716.3	9453.93	10044.11	8226.23
Total	3028.7	3291.7	2830.3	1931.3	1689.7	1388

Table A.4. Cumulative contributions of different processes for the γ-HCH yearly mass budgets in kg a^{-1} calculated by FANTOM for the inner German Bight.

Processes contribution	γ-HCH in the inner German Bight					
[kg a^{-1}]	1996	1997	1998	1999	2000	2001
Wet deposition	350	453	310	223	193	107
Dry particle deposition	0.0033	0.0027	0.0028	0.0015	0.0011	0.0007
Dry gaseous deposition	761.07	780.03	811.11	439.28	338.44	210.32
Volatilisation	605.25	885.33	861.8	514.19	449.65	326.11
Degradation	0.16	0.22	0.17	0.12	0.11	0.08
Sinking	63.8	72.7	67	48	42.5	31.91
Resuspension	6.94	7.84	6.75	4.49	3.79	3.19
River inflow	169.01	356.03	260.55	103.32	135.71	67.295
Lateral boundaries inflow	4339.6	5345.6	5427.8	3531.64	3044.9	2337.46
Lateral boundaries outflow	4474	5632.3	6096.4	3862.04	3274.35	2542.79
Total	313.221	422.390	415.019	237.515	213.592	178.727

Table A.5. Cumulative contributions of different processes for the α-HCH yearly mass budgets in kg a^{-1} calculated by FANTOM for the North Sea.

Processes contribution	α-HCH in the North Sea					
[kg a^{-1}]	1996	1997	1998	1999	2000	2001
Wet deposition	811.55	346.17	350.58	473.5	249.05	218.75
Dry particle deposition	0.0138	0.0101	0.0075	0.0048	0.0036	0.0034
Dry gaseous deposition	8978.3	7082.1	5893.8	3780.7	2949.9	2564.8
Volatilisation	4294.3	3745.9	3112.1	2242.1	1210.9	982.79
Degradation	2.7364	2.3641	1.8021	1.2815	1.2071	1.0405
Sinking	966.87	852.36	744.63	501.76	530.57	385.5
Resuspension	50.013	44.801	35.107	24.432	24.547	21.398
River inflow	258.5	265.7	558.78	257.41	308.22	201.26
Lateral boundaries inflow	2808.7	2850.6	3161.9	3009.3	3017.5	3017.3
Lateral boundaries outflow	3884.5	3765.9	3922.1	3746.1	4100.6	3352.6
Total	1173	1013.4	772.48	549.33	517.42	446.02

Table A.6. Cumulative contributions of different processes for the α-HCH yearly mass budgets in kg a^{-1} calculated by FANTOM for the inner German Bight.

Processes contribution	α-HCH in the inner German Bight					
[kg a^{-1}]	1996	1997	1998	1999	2000	2001
Wet deposition	51.96	22.16	22.45	30.32	15.95	14.01
Dry particle deposition	0.00089	0.00065	0.00048	0.00030	0.00023	0.00021
Dry gaseous deposition	774.76	641.18	530.24	338.27	277.62	235.02
Volatilisation	667.44	681.18	840.99	420.21	277.59	183.81
Degradation	0.18	0.15	0.12	0.08	0.08	0.07
Sinking	31.39	27.67	24.17	16.29	17.22	12.51
Resuspension	1.62	1.45	1.14	0.79	0.80	0.69
River inflow	151.61	183.49	468.76	102.2	155.02	85.814
Lateral boundaries inflow	1395.53	1314.41	1107.21	780.96	782.72	557.1
Lateral boundaries outflow	1460.32	1378.19	1246.69	870.17	888.61	619.82
Total	141.094	143.318	151.109	59.788	50.673	38.897

Table A.7. Cumulative contributions of different processes for the PCB 153 yearly mass budgets in kg a^{-1} calculated by FANTOM for the North Sea.

Processes contribution	PCB 153 in the North Sea					
[kg a^{-1}]	1996	1997	1998	1999	2000	2001
Wet deposition	266.58	301.1	350.76	326.7	358.16	457.81
Dry particle deposition	9.13E-06	5.62E-06	6.00E-06	5.34E-06	6.17E-06	5.25E-06
Dry gaseous deposition	106.25	74.15	95.06	82.47	99.29	72.71
Volatilisation	66.11	148.71	85.27	91.17	112.64	260.33
Degradation	2.08	2.83	2.29	2.2	2.52	2.91
Sinking	486.89	626.65	546.81	522.39	606.11	659.51
Resuspension	195.45	420.85	406.66	280.58	374.17	596.38
River inflow	37.45	28.85	11.23	95.32	91.78	86.72
Lateral boundaries inflow	71.9	73.3	85.8	82.4	79.8	79.5
Lateral boundaries outflow	83.7	80.5	85.3	82.3	88.6	73.1
Total	1333.95	1716.85	1498.12	1431.23	1660.6	1806.9

Table A.8. Cumulative contributions of different processes for the PCB 153 yearly mass budgets in kg a^{-1} calculated by FANTOM for the inner German Bight.

Processes contribution	PCB 153 in the inner German Bight					
[kg a^{-1}]	1996	1997	1998	1999	2000	2001
Wet deposition	4.233	9.521	5.460	5.837	7.212	16.668
Dry particle deposition	5.84E-07	3.60E-07	3.84E-07	3.42E-07	3.95E-07	3.36E-07
Dry gaseous deposition	8.9499	6.2955	7.4858	6.4532	7.9016	5.5588
Volatilisation	55.562	46.828	128.43	109.26	111.38	117.81
Degradation	0.133	0.181	0.147	0.141	0.161	0.186
Sinking	15.81	20.34	17.75	16.96	19.68	21.41
Resuspension	6.34	13.66	13.20	9.11	12.15	19.36
River inflow	32.889	23.82	105.37	87.968	84.899	78.653
Lateral boundaries inflow	30.362	80.801	117.177	57.081	111.729	216.44
Lateral boundaries outflow	45.357	112.47	164.464	112.126	175.816	260.61
Total	278.029	267.010	548.533	478.654	516.411	464.976

Figures

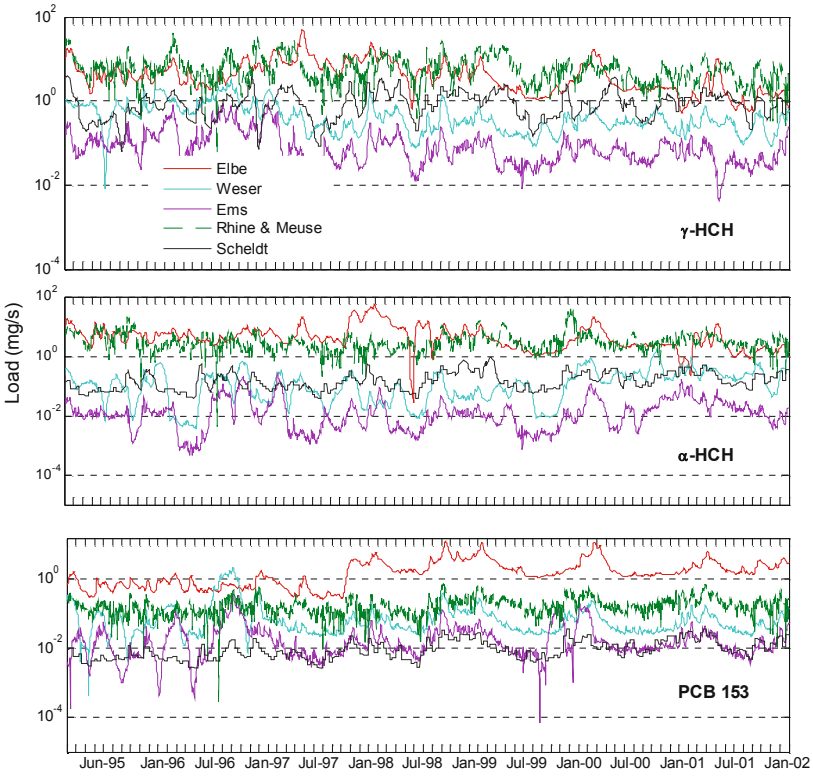

Fig. 3.9. γ-HCH, α-HCH and PCB 153 loads (Q_{riv} x C_{riv}) in the continental rivers. Geographical locations of the measurement sites in rivers are shown on in Fig. 3.1. Note that logarithmic scales are used.

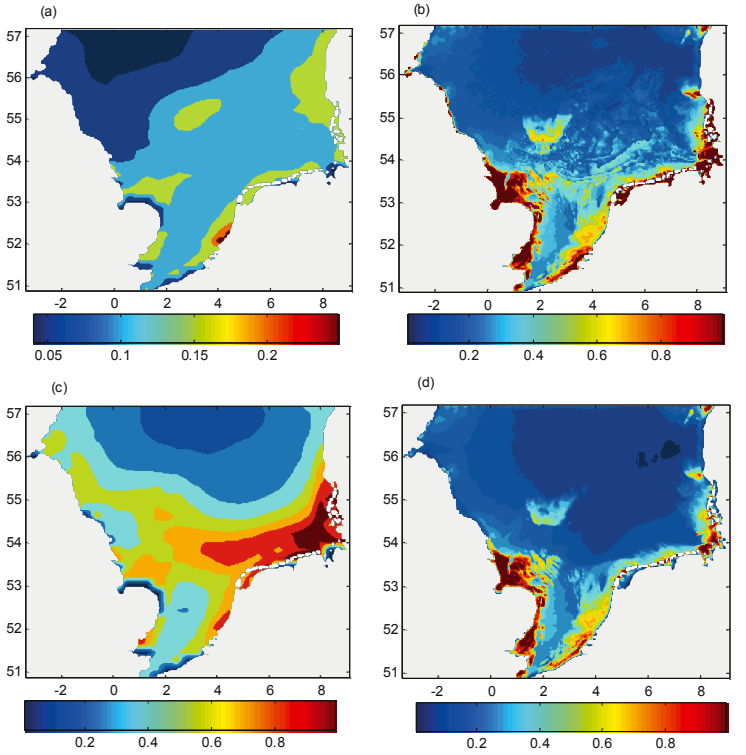

Fig. 5.2. (a) Vertically integrated concentrations (mg l^{-1}) of particulate organic carbon due to biological activity provided by Pätsch and Kühn (2005) and (b) POC concentrations originating from the bottom sediment calculated by FANTOM for winter 1996. (c), (d) As (a), (b) but for summer 1996.

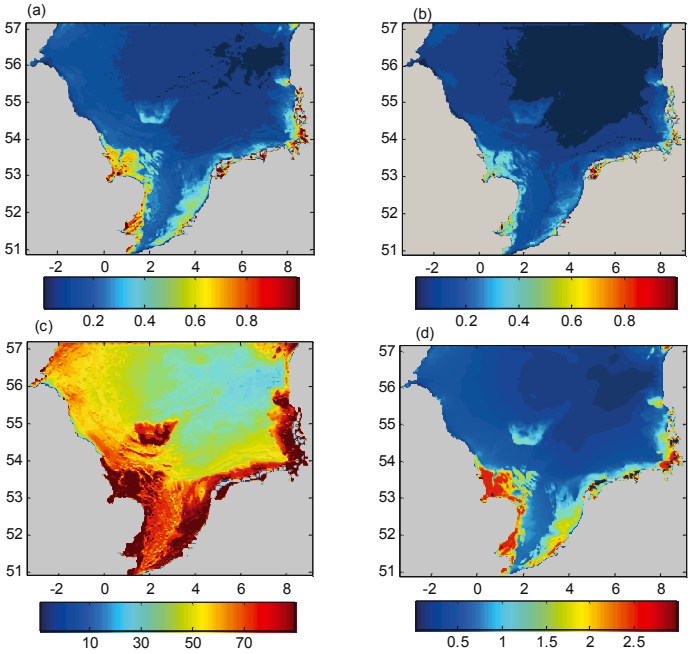

Fig. 5.4. Distributions of vertically integrated annual mean POPs fraction on POC (%) for (a) γ-HCH, (b) α-HCH and (c) PCB 153, and (d) vertically averaged total POC annual mean concentration (mg l^{-1}).

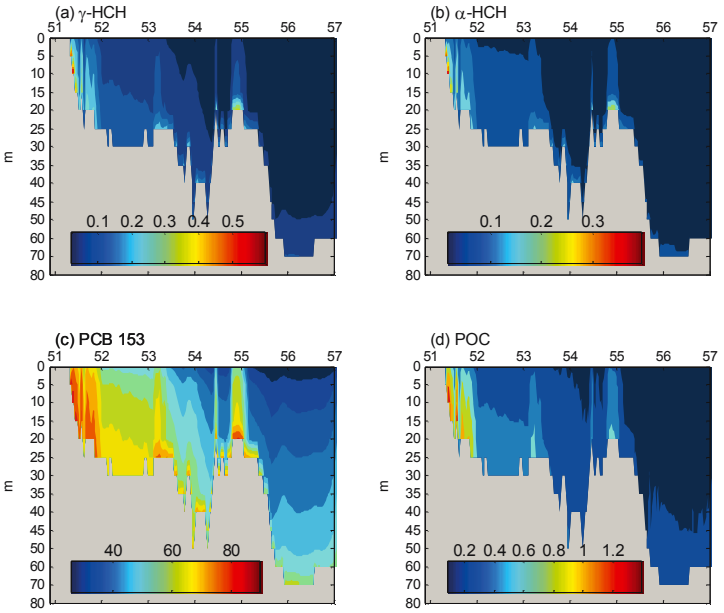

Fig. 5.5. Vertical sections from south to north along 3°E (see Fig. 5.1) of annual mean POPs fraction on POC (%) for (a) γ-HCH, (b) α-HCH and (c) PCB 153, and (d) annual mean total POC concentration (mg l^{-1}).

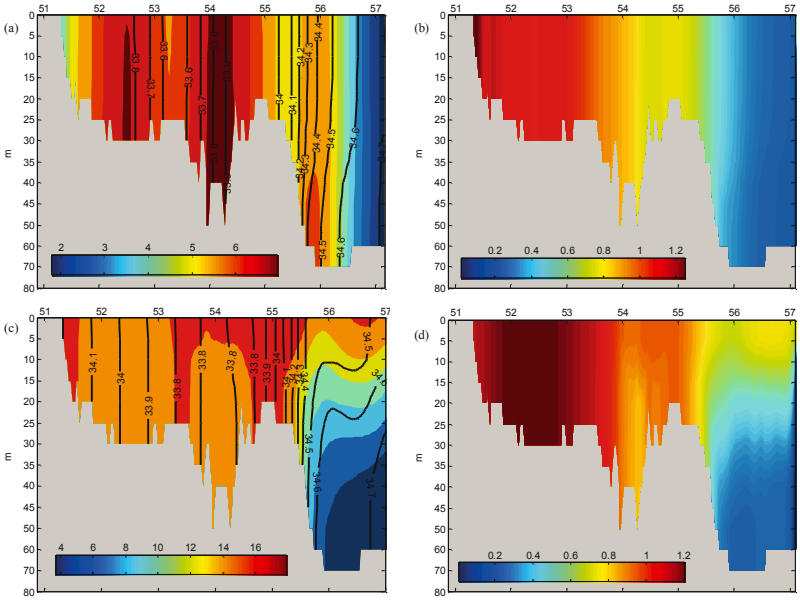

Fig. 5.9. Vertical sections from south to north along 3°E for (a) sea temperature (colours, °C) and salinity (lines) calculated by HAMSOM and (b) corresponding γ-HCH total concentrations (ng l^{-1}) calculated by FANTOM for January 1997. (c), (d) As (a), (b) but for August 1997.

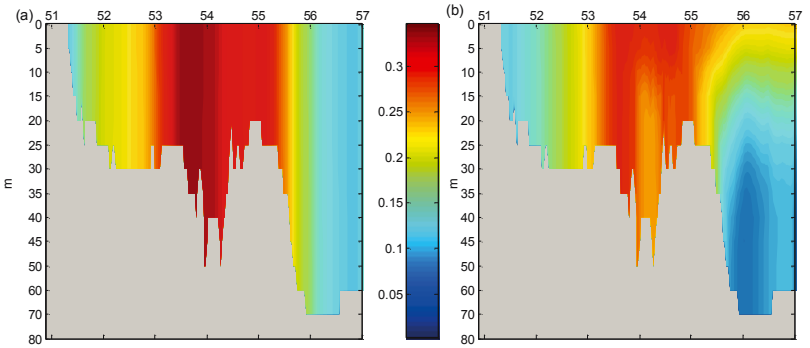

Fig. 5.10. Vertical sections from south to north along 3°E of α-HCH total concentrations (ng l^{-1}) for (a) January and (b) August 1997 calculated by FANTOM.

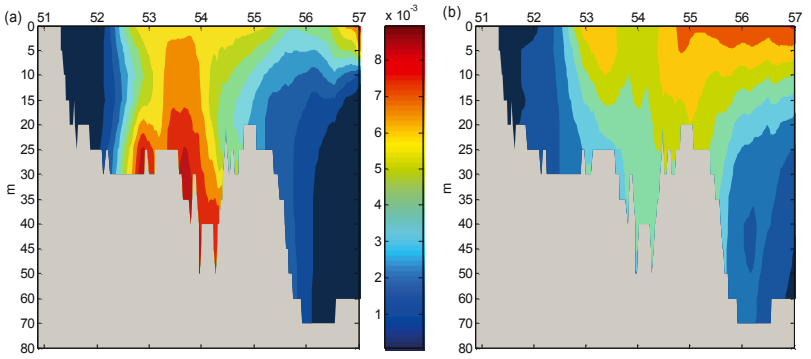

Fig. 5.11. Vertical sections from south to north along 3°E of PCB 153 total concentrations (ng l^{-1}) for (a) January and (b) August 1997 calculated by FANTOM.

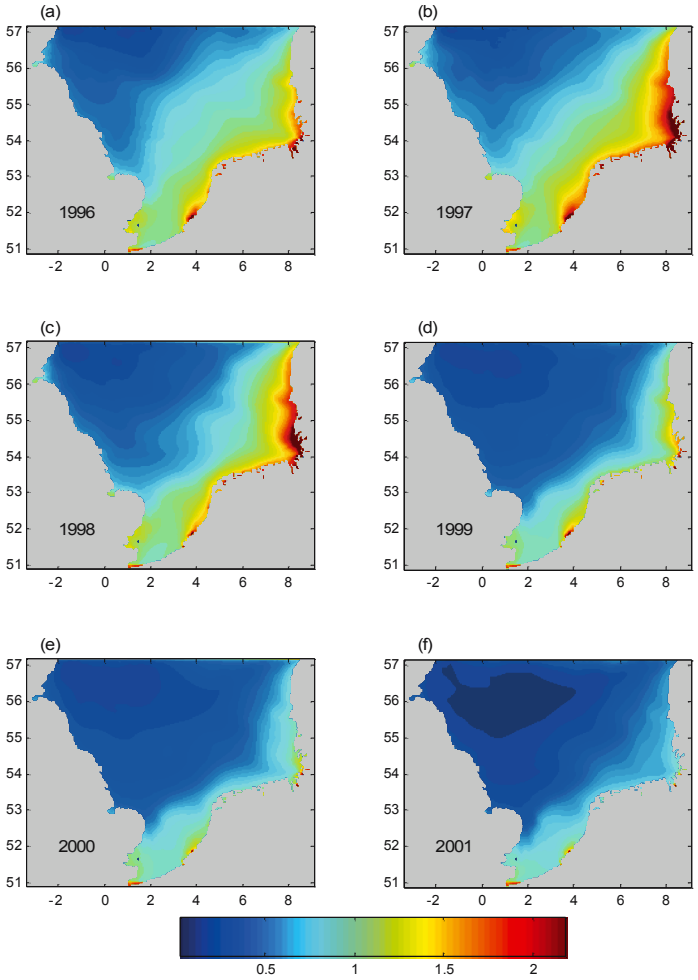

Fig. 5.12. Vertically integrated annual mean concentrations of γ-HCH (ng l^{-1}) in the North Sea calculated by FANTOM for 1996 through to 2001.

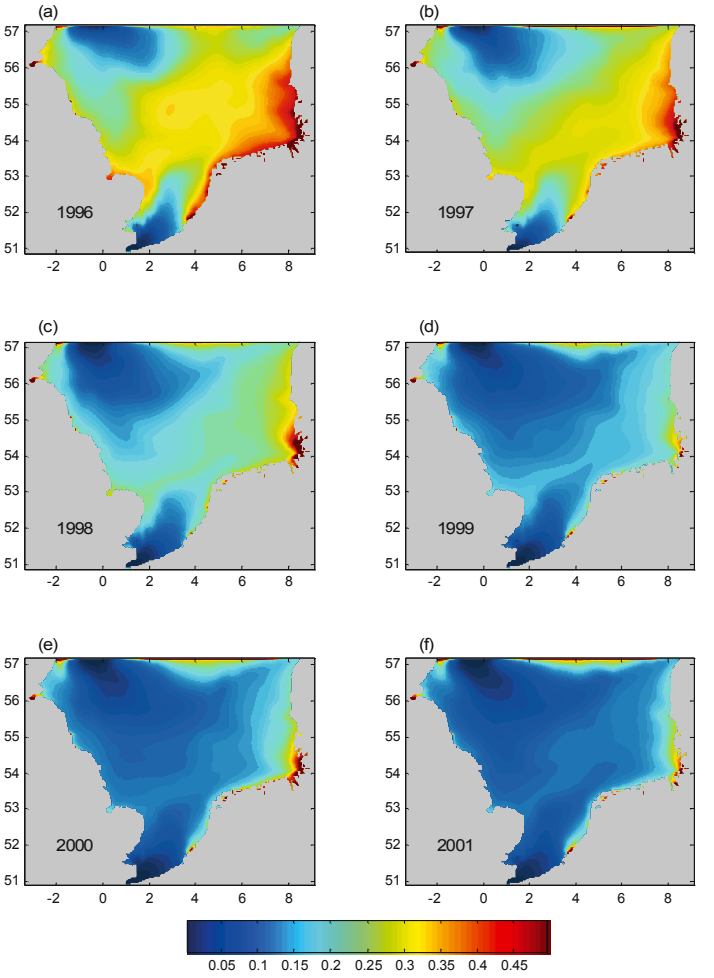

Fig. 5.13. Vertically integrated annual mean concentrations of α-HCH (ng l^{-1}) in the North Sea calculated by FANTOM for 1996 through to 2001.

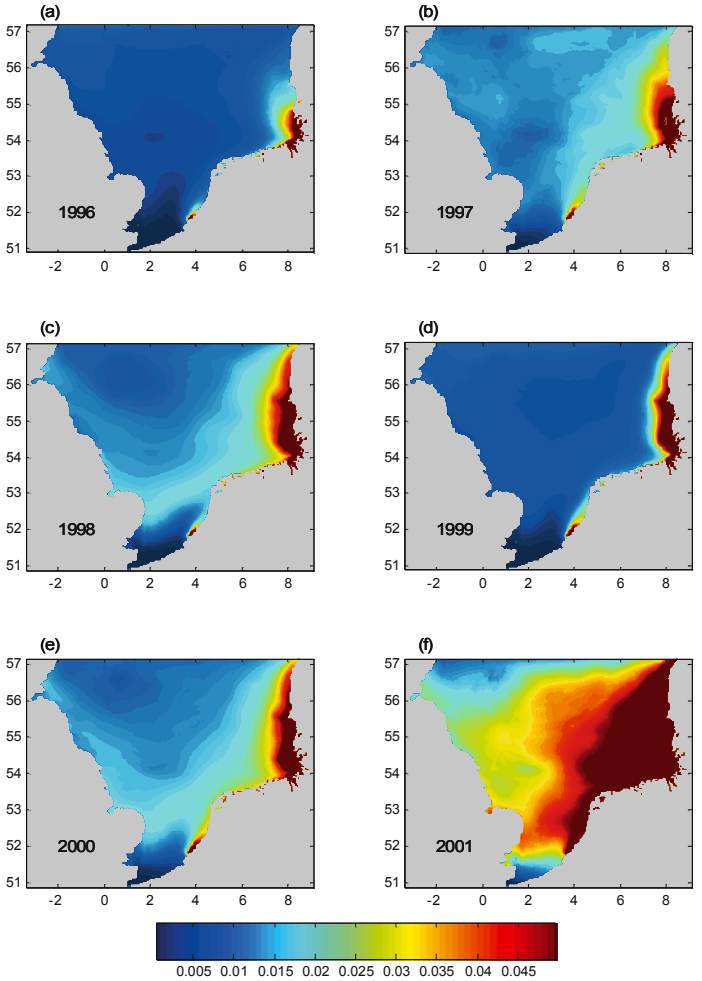

Fig. 5.14. Vertically averaged annual mean concentrations of PCB 153 (ng l^{-1}) in the North Sea calculated by FANTOM for 1996 through to 2001.

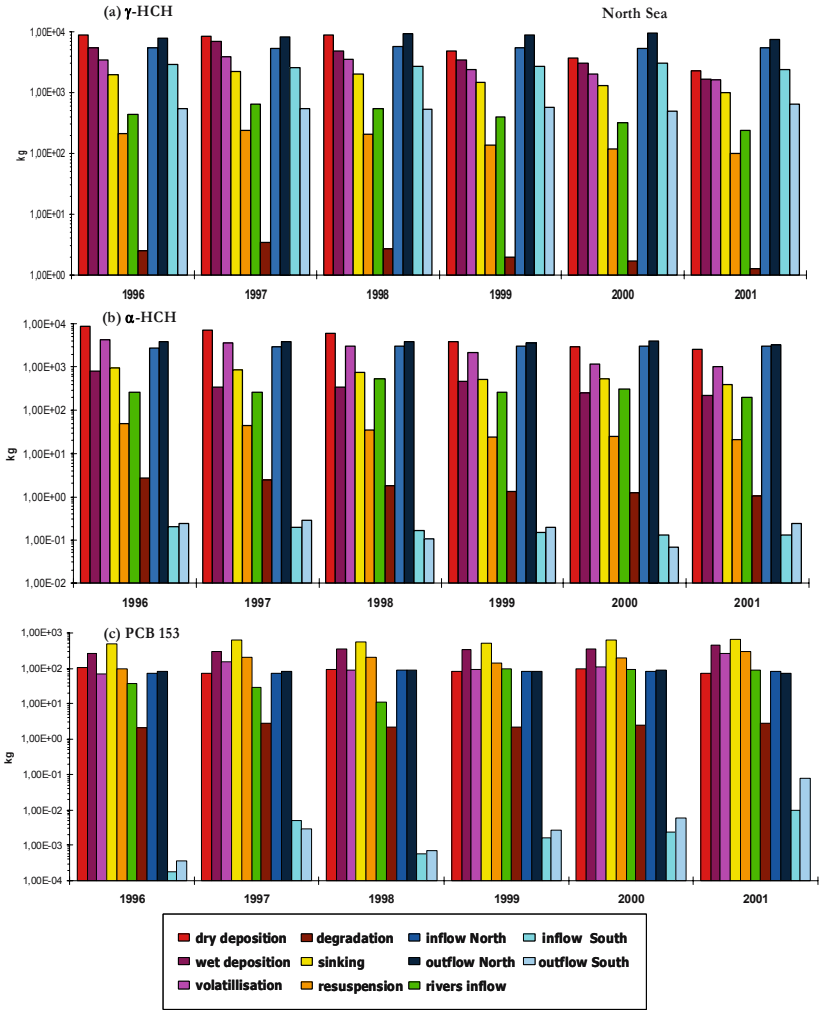

Fig. 6.2. Cumulative masses (kg) contributed by different processes acting in sea water as sources and sinks calculated by FANTOM for the North Sea (entire modeling domain) for each year for (a) γ-HCH, (b) α-HCH and (c) PCB 153. The sources are dry and wet atmospheric deposition, resuspension from the sea bottom, rivers inflow, and inflow from the Atlantic Ocean (through the northern boundary) and from the English Channel (southern boundary). The sinks are volatilisation, sinking to the sea bottom, degradation, and outflow through the northern and southern boundaries.

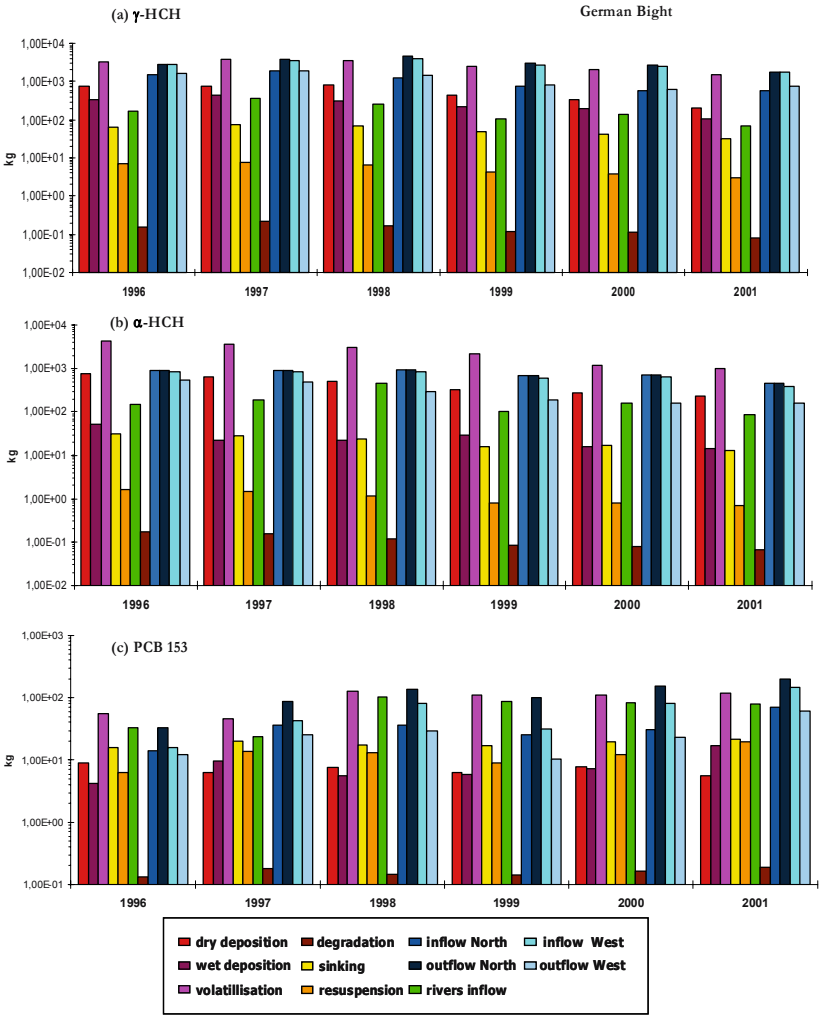

Fig. 6.3. Cumulative masses (kg) contributed by different processes acting in sea water as sources and sinks calculated by FANTOM for the inner German Bight for each year for (a) γ-HCH, (b) α-HCH and (c) PCB 153. The sources are: dry and wet atmospheric deposition, resuspension from the sea bottom, rivers inflow, and inflow through the western and the northern boundaries. The sinks are volatilisation, sinking to the sea bottom, degradation, and outflow through the northern and western boundaries.

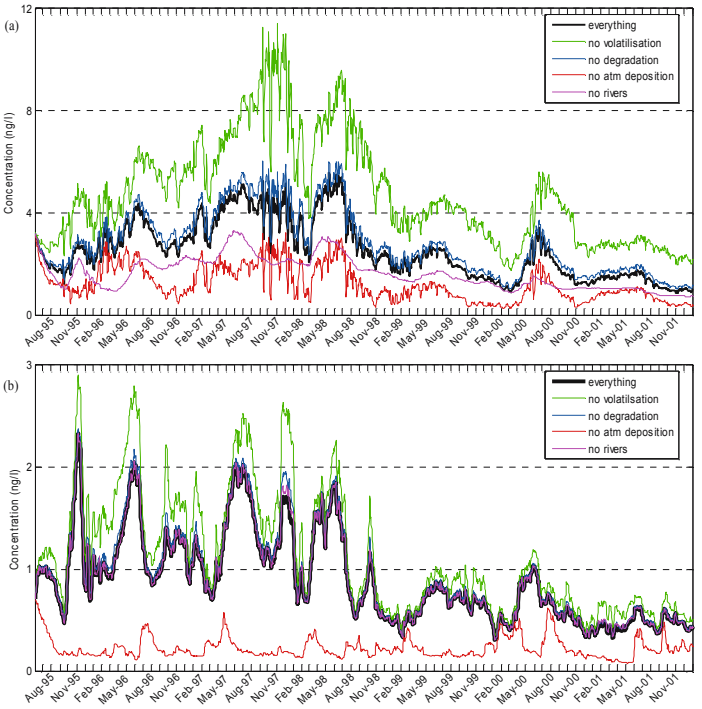

Fig. 6.4. γ-HCH concentrations in the surface layer for (a) inner German Bight and (b) open North Sea calculated by FANTOM under different model scenarios ("all but one process"). Black line – all processes included. Green line – model run without volatilisation. Red line – model run without deposition (both dry and wet) from the atmosphere. Magenta line – model run without river inflow. Blue line – model run without degradation in sea water.

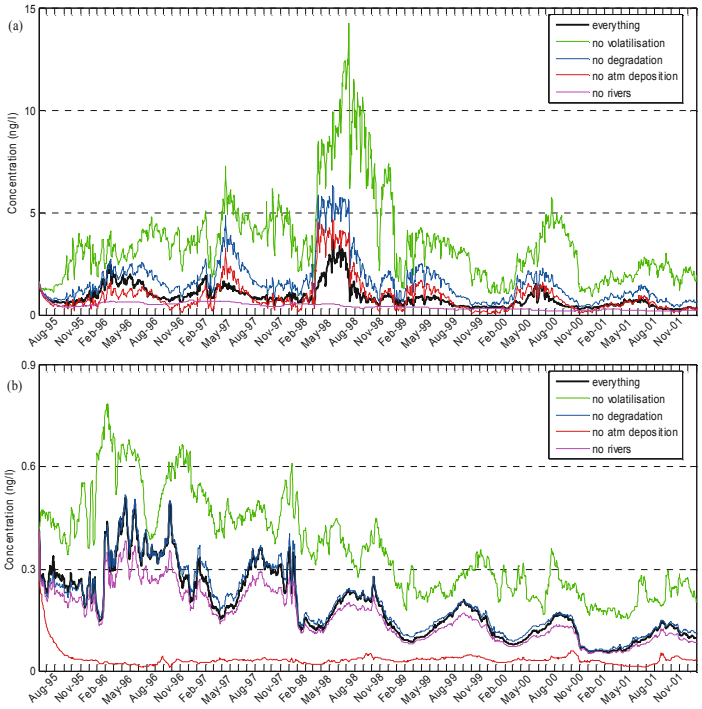

Fig. 6.5. α-HCH concentrations in the surface layer for (a) inner German Bight and (b) open North Sea calculated by FANTOM under different model scenarios ("all but one process"). Black line – all processes included. Green line – model run without volatilisation. Red line – model run without deposition (both dry and wet) from the atmosphere. Magenta line – model run without river inflow. Blue line – model run without degradation in sea water.

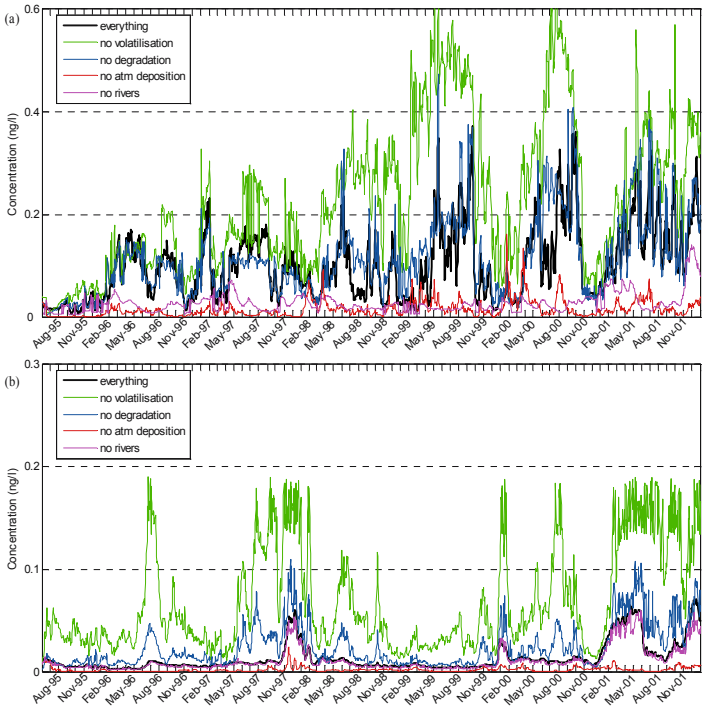

Fig. 6.6. PCB 153 concentrations in the surface layer for (a) inner German Bight and (b) open North Sea calculated by FANTOM under different model scenarios ("all but one process"). Black line – all processes included. Green line – model run without volatilisation. Red line – model run without deposition (both dry and wet) from the atmosphere. Magenta line – model run without river inflow. Blue line – model run without degradation in sea water.

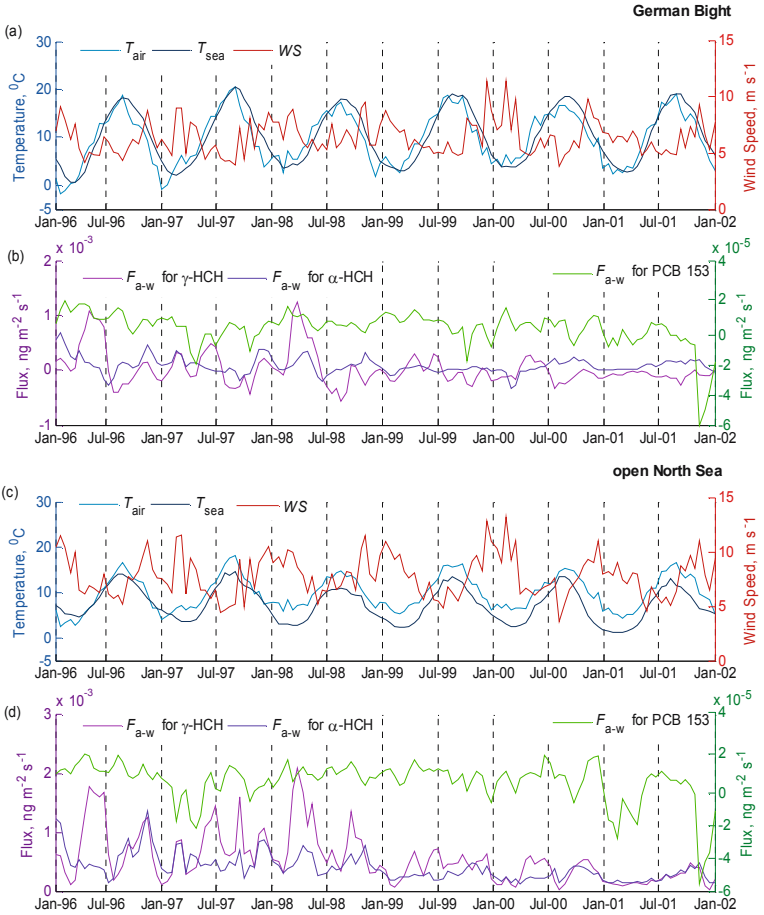

Fig. 6.7. (a) Fortnightly means of measured air temperature and sea surface temperature calculated by HAMSOM and (b) corresponding gaseous air-sea fluxes of γ-HCH, α-HCH and PCB 153 in ng m^{-2} s^{-1} calculated by FANTOM for the inner German Bight (location A). (c), (d) As (a), (b) but for the open North Sea (location M).

List of Symbols

A_w	[m^2]	Surface area of the water
b	-	Intercept of the linear regression equation
C	[kg m^{-3}]	Pollutant's total concentration in sea water
C_a	[mol m^{-3}]	Pollutant's gaseous concentrations in the air
C_{ap}	[ng m^{-3}]	Pollutant's particle-bound concentration in air
C_{bio}	[mg l^{-1}]	Concentration of biogenic organic carbon in sea water
C_p	[ng l^{-1}]	Pollutant's concentrations bound to POC in sea water
C_{POC}	[mg l^{-1}]	Concentration of POC in solution in sea water
C_{pr}	[ng l^{-1}]	Pollutant's concentration in precipitation
C_{riv}	[ng l^{-1}]	Pollutant's concentration in the river
C_{sed}	[mg l^{-1}]	Concentration of sediment organic carbon in sea water
C_w	[ng l^{-1}]	Pollutant's concentration dissolved in sea water
C^B	[kg m^{-3}]	Pollutant's concentration at the water boundary
C^0	[kg m^{-3}]	Pollutant's initial concentration in sea water
$Degrad$	[kg s^{-1}]	Pollutant's mass change in a unit of time due to degradation
D_{wa}	[mol Pa^{-1} s^{-1}]	Overall exchange rate constant for volatilisation from sea water
F	[ng m^{-2} s^{-1}]	Pollutant's flux at the bottom

$F_{a\text{-}w}$	[ng m^{-2} s^{-1}]	Net gaseous air–sea flux
f_{ap}	-	Fraction of the total pollutant's concentration in air sorbed by aerosol particles
F_{dry}	[ng m^{-2} s^{-1}]	Dry particle deposition flux
F_{in}	[kg s^{-1}]	Pollutant's rate flowing into a given volume
F_{out}	[kg s^{-1}]	Pollutant's rate flowing out of a given volume
f_{POC}	-	Fraction of the total pollutant's concentration in sea water bound to POC
F_{set}	[ng m^{-2} s^{-1}]	Pollutant's flux sinking to the bottom
F_{surf}	[ng m^{-2} s^{-1}]	Net flux to the sea surface from the atmosphere
F_{wet}	[ng m^{-2} s^{-1}]	Wet deposition flux
$GasDep$	[kg s^{-1}]	Pollutant's mass change in a unit of time due to gaseous deposition
H	[m]	Bottom depth
H_c	[Pa m^3 mol^{-1}]	Henry's law constant
$Inflow$	[kg s^{-1}]	Pollutant's mass change in a unit of time due to inflow through a lateral boundary
k_{deg}	[s^{-1}]	Pollutant's degradation rate in sea water
K_{AW}	-	Air–water partition coefficient
K_{OA}	-	Octanol-air partitioning coefficient
K_{oc}	[l kg^{-1}]	Organic carbon–water equilibrium partition coefficient
K_{ow}	-	Octanol-water partitioning coefficient
K_x	[m^2 s^{-1}]	Horizontal diffusion coefficient in the eastern direction
K_y	[m^2 s^{-1}]	Horizontal diffusion coefficient in the northern direction
K_v	[m^2 s^{-1}]	Vertical diffusion coefficient
m	[K]	Slope of the linear regression equation
M	[g mol^{-1}]	Pollutant's molar mass

$m_{a\text{-}w}$	[mol s^{-1}]	Pollutant's net mass transfer rate
M_0	[kg]	Pollutant's initial mass
M_t	[kg]	Pollutant's mass at time *t*
M_{total}	[kg]	Pollutant's total mass in sea water
Outflow	[kg s^{-1}]	Pollutant's mass change in a unit of time due to outflow through a lateral boundary
Q_C	[kg s^{-1}]	Pollutant's sources
Q_{riv}	[m^3 s^{-1}]	Daily fresh water discharge
P	[m s^{-1}]	Precipitation rate
PartDep	[kg s^{-1}]	Pollutant's mass change in a unit of time due to dry particle deposition
p_{mud}	[%]	Content of mud in the bottom sediment
P_{ol}	[Pa]	Saturated vapour pressure for supercooled liquid
p_{POC}	[%]	POC content of the bottom fine sediment
R	[Pa m^3 mol^{-1} K^{-1}]	Ideal gas constant
R_a	[s m^{-1}]	Aerodynamic resistance
R_b	[s m^{-1}]	Quasi-laminar sub-layer resistance
R_c	[s m^{-1}]	Total surface resistance of the gas
R_C	[kg s^{-1}]	Pollutant's sinks
Resuspen	[kg s^{-1}]	Pollutant's mass change in a unit of time due to resuspension from the sea bottom
Rivers	[kg s^{-1}]	Pollutant's mass change in a unit of time due to rivers inflow
s	[Pa m^{-1}]	Adsorption constant
Sinking	[kg s^{-1}]	Pollutant's mass change in a unit of time due to sinking to the sea bottom
T_a	[K]	Air temperature
T_w	[K]	Sea surface temperature
u	[m s^{-1}]	Horizontal flow field in the eastern di-

		rection
u_1	[m s^{-1}]	Mass transfer coefficient for the stagnant atmospheric boundary layer
u_2	[m s^{-1}]	Mass transfer coefficient for the stagnant water layer
v	[m s^{-1}]	Horizontal flow field in the northern direction
v_{dep}	[m s^{-1}]	Dry deposition velocity
v_{set}	[m s^{-1}]	Gravitational sinking velocity of SPM
v_*	[m s^{-1}]	Bed shear velocity due to waves
$v_*^{cr,d}$	[m s^{-1}]	Threshold shear velocity for deposition of SPM
$v_*^{cr,e}$	[m s^{-1}]	Threshold shear velocity for erosion of SPM
$Volatil$	[kg s^{-1}]	Pollutant's mass change in a unit of time due to volatilisation
w	[m s^{-1}]	Vertical bottomward flow field component
$WetDep$	[kg s^{-1}]	Pollutant's mass change in a unit of time due to wet deposition
WS	[m s^{-1}]	Wind speed at 10 m above the surface
Z_a	[mol m^{-3} Pa^{-1}]	Fugacity capacities of air and water
Z_w	[mol m^{-3} Pa^{-1}]	Fugacity capacities of air and water
θ	[m^2 m^{-3}]	Specific aerosol surface
τ_{sw}	[s]	Residence time of a pollutant in sea water

References

Agrell C, Okla L, Larsson P, Backe C, Wania F (1999) Evidence of Latitudinal Fractionation of Polychlorinated Biphenyl Congeners along the Baltic Sea Region. Environ Sci Technol 33: 1149-1156

ARGE-Elbe (2005) Annual Report. Arbeitsgemeinschaft für die Reinhaltung der Elbe. http://www.arge-elbe.de/

AMAP (1998) AMAP Assessment Report: Arctic Pollution Issues. Arctic Monitoring and Assessment Programme, Oslo

Axelman J, Broman D, Näf C (1997) Field measurements of PCB between water and planktonic organisms: influence of growth, particle size, and solute-solvent interactions. Environ Sci Technol 31: 665-669

Axelman J, Broman D (2001) Budget calculations for polychlorinated biphenyls (PCBs) in the Northern Hemisphere - a single-box approach. Tellus, vol 53B: 235-259

Baart A, Berdowski J, van Jaarsveld J, Wulffraat K (1995) Calculation of atmospheric deposition of contaminants on the North Sea. TNO-MEP-R 95/138, Delft

Backhaus JO (1985) A three-dimensional model for the simulation of shelf sea dynamics. Dtsch Hydrogr Z 38: 167-187

Bartels J (1957) Gezeitenkräfte, Handbuch der Physik. Band XLVIII, Geophysik II

Baumert H, Simpson J, Sündermann J. (eds) (2005) Marine Turbulence - Theories, Observations and Models. Cambridge University Press, Cambridge

Bethan B, Dannecker W, Gerwig H, Hühnerfuss H, Schulz M (2001) Seasonal dependence of the chiral composition of alpha-HCH in coastal deposition at the North Sea. Chemosphere 44(4): 591-597

Beyer A, Matthies M (2001) Long-Range Transport Potential of Semivolatile Organic Chemicals in Coupled Air-Water Systems. Environ Sci Pollut Res 8: 173-179

Bidleman TF (1988) Atmospheric process. Environ Sci Technol 22: 361-367

Bidleman TF, Jantunen LM, Falconer RL, Barrie LA, Fellin P (1995) Decline of hexachlorocyclohexane in the arctic atmosphere and reversal of air–sea gas exchange. Geophys Res Lett 22(3): 219-222

Breivik K, Pacyna JM, Münch J (1999) Use of alpha-, beta- and gamma-hexachlorocyclohexane in Europe, 1970-1996. Sci Total Environ 239: 151-163

Bruhn R, Lakaschus S, McLachlan MS (2003) Air/sea gas exchange of PCBs in the southern Baltic Sea. Atmos Environ 37(24): 3445-3454

BSH (2005) Nordseezustand 2003. Berichte des BSH vol 38

Chernyak SM, Rice CP, McDonnell LL (1996) Evidence of Currently-Used Pesticeds in Air, Ice, Fog, Seawater and Surface Microlayer in the Bering and Chukchi Seas. Marine Pollution Bulletin 32: 410-419

Coulston F, Kolbye A (eds) (1994) Regulatory Toxicology and Pharmacology vol. 20(2)

Dachs J, Eisenreich SJ, Baker JE, Ko FC, Jeremiason JD (1999) Coupling of Phytoplankton Uptake and Air-Water Exchange of Persistent Organic Pollutants. Environ Sci Technol 33: 3653-3660

Dachs J, Lohmann R, Ockenden WA, Mejanelle L, Eisenreich SJ, Jones KC (2002) Oceanic biogeochemical controls on global dynamics of persistent organic pollutants. Environ Sci Technol 36: 4229-4237

DOD (2005) German Oceanographic Data Centre, http://www.bsh.de/

DONAR (2005) Dutch Online Database Waterbase, http://www.waterbase.nl/

Eisma D, Kalf J (1987) Distribution, organic content and particle size of suspended matter in the North Sea. Netherlands Journal of Sea Research 21(4): 265-285

EMEP: EMEP Data Online, http://www.emep.int/

EU TGD (1996) EU Technical Guidance Document in support of Commission Directive 93/67/EEC on Risk Assessment for New Notified Substances, Commission Regulation (EC) No 1488/94 on Risk Assessment for existing substances and Directive 98/8/EC of the European Parliament and of the Council concerning the placing of biocidal products on the market. European Chemicals Bureau, ISPRA

Gaul H (1988) Der Eintrag von Organohalogenverbindungen über die Atmosphäre in die Nordsee. Dtsch Hydrogr Z 36: 191-212

Goldberg ED (1975) Synthetic organohalides in the sea. Proceedings of the Royal Society London, Series B 189: 277-289

Gunnarsson J, Broman D, Jonsson P, Olsson M, Rosenberg R (1995) Interactions between eutrophication and contaminants: towards a new research concept for the European aquatic environment. Ambio 24: 383-385

Haarich M, Theobald N, Bachor A, Weber Mv, Grünwald K, Petenati T, Schröter-Kermani C, Jansen W, Bladt A (2005) Organische Schadstoffe. Messprogramm Meeresumwelt (Heft 4): Zustandsbericht 1999–2002 für Nordsee und Ostsee. BSH, Hamburg und Rostock pp 195-218

Hansen KM, Christensen JH, Brandt J, Frohn LM, Geels C (2004) Modelling atmospheric transport of persistent organic pollutants in the Northern Hemisphere with a 3-D dynamical model: DEHM-POP. Atmos Chem Phys 4: 1339-1369

Hargrave BT, Vass WP, Erickson PE (1998) Atmospheric transport of organochlorines to the Arctic Ocean. Tellus 40B: 480-493

Haugen JE, Wania F, Ritter N, Schlabach M (1998) Hexachlorocyclohexanes in air in Southern Norway. Temporal variation, source allocation, and temperature dependence, Environ Sci Technol 32: 217-224

Hoff RM, Muir DCG, Grift NP (1992) Annual Cycle of Polychlorinated Biphenyls and Organohalogen Pesticides in Air in Southern Ontario. Air Concentration data. Environ Sci Technol 26: 266-275

Hornbuckle KC, Achman DR, Eisenreich SJ (1993) Over-water and over-land polychlorinated biphenyls in Green Bay, Lake Michigan. Environ Sci Technol 27: 87-98

Hornbuckle KC, Jeremiason JD, Sweet SW, Eisenreich SJ (1994) Seasonal variation in air-water exchange of polychlorinated biphenyls in Lake Superior. Environ Sci Technol 28: 1491-1501

Hühnerfuss H, Bester K, Landgraff O, Pohlmann T, Selke K (1997) Annual balances of hexachlorocyclohexanes, polychlorinated biphenyls, and triazines in the German Bight. Mar Pollut Bull 34: 419-426

Iwata H, Tanabe S, Sakai N, Tatsukawa R (1993) Distribution of persistent organochlorines in the oceanic air and surface seawater and the role of ocean on their global transport and fate. Environ Sci Technol 27: 1080–1098

Jacobs CMJ, van Pul WAJ (1996) Long-range atmospheric transport of persistent organic pollutants, I: Description of surface - atmosphere exchange modules and Implementation in EUROS. Report No722401013, National Institute of Public Health and the Environment, Bilthoven

Jantunen LM, Bidleman TF (1996) Air-water gas exchange of hexachlorocyclohexanes (HCHs) and the enantiomers of α-HCH in Arctic regions. Journal of Geophysical Research 101: 28837-28846

Jaward FM, Barbera JL, Booijb K, Jones KC (2004) Spatial distribution of atmospheric PAHs and PCNs along a north–south Atlantic transect. Environ Pollut 132: 173-181

Jeremiason JD, Hornbuckle KC, Eisenreich SJ (1994) PCBs in Lake Superior, 1978–1992: Decreases in water concentrations reflect loss by volatilization. Environ Sci Technol 28: 903–914

Jeremiason JD, Eisenreich SJ, Paterson MJ, Beaty KG, Hecky R, Elser JJ (1999) Biogeochemical Cycling of PCBs in Lakes of Variable Trophic Status: A Paired-Lake Experiment. Limnology and Oceanography 44(3): 889-902

Jones KC, de Voogt P (1999) Persistent Organic Pollutants (POPs): state of the science. Environ Pollut 100: 209-221

Junge CE (1977) Basic considerations about trace constituent in the atmosphere is related to the fate of global pollutant. In: Fate of Pollutants in the Air and Water Environment. Part I, I.H. Suffet (ed), John Wiley & Sons, New York pp 7-26

Jurado E, Lohmann R, Meijer S, Jones KC, Dachs J (2004) Latitudinal and seasonal capacity of the surface oceans as a reservoir of PCBs. Environ Pollut 128: 149-162

Karickhoff SW (1981) Semi-empirical estimation of sorption of hydrophobic pollutants on natural sediments and soils. Chemosphere 10: 833-846

Klöpffer W, Schmidt E (2001) A multimedia load model for the Baltic Sea. Environ Sci Pollut Res 8: 180-188

Koelmans AA, Gillissen F, Makatita W, van den Berg M (1997) Organic carbon normalisation of PCB, PAH and pesticide concentrations in suspended solids. Water Res 31: 461-470

Koziol A, Pudykiewicz J (2001) Global-scale environmental transport of persistent organic pollutants. Chemosphere 45: 1181-1200

Kucklick JR, Hinckley DA, Bidleman TF (1991) Determination of Henry's law constants for hexachlorocyclohexanes in distilled water and artificial seawater as a function of temperature. Mar Chem 34: 197-209

Laane RWPM (ed) (1992) Background concentrations of natural compounds in rivers, sea water, atmosphere and mussels. Report DGGW – 92.033

Lakaschus S, Weber K, Wania F, Bruhn R, Schrems O (2002) The air–sea equilibrium and time trend of hexachlorocyclohexanes in the Atlantic ocean between the Arctic and Antarctica. Environ Sci Technol 36: 138-145

Lammel G, Feichter J, Leip A, (2001) Long-range transport and multimedia partitioning of semivolatile organic compounds: A case study on two modern agrochemicals. Report No. 324 MPI for Meteorology, Hamburg

Lammel G, Ghim YS, Grados A, Hühnerfuss H, Lohmann R, Gao HW (2005) Organochlorine compounds in air at the Yellow Sea: measurements in Qingdao, China, and Gosan, Jeju Island, Korea. Organohalogen Compounds 67: 1052-1053

Lang, T, Wosniok W (2003) EFFSTAT Synthese und Analyse von marinen Daten über biologische Effekte und deren Ursachen mit Hilfe neuer statistischer Verfahren (in German) Abschlussbericht zum BMBF-Projekt 03F0264A, www.bfa-fish.de/news/news-d/index.html

de Leeuw FAAM (1996) Proceedings of the EMEP Workshop on European Monitoring Modelling and Assessment of Heavy Metals and Persitent Organic Pollutants. RIVM report 722401013, Beckbergen pp 3-5

Lenhart HJ, Pätsch J (2004) Daily loads of nutrients, total alkalinity, dissolved inorganic carbon and dissolved organic carbon of the European continental rivers for the years

1977-2002. Berichte aus dem Zentrum für Meeres- und Klimaforschung, ZMK, Hamburg
Lenhart HJ, Pohlmann T (1997) The ICES-boxes approach in relation to results of a North Sea circulation model. Tellus 49A: 139-160
Liss PS, Slater PG (1974) Flux of gases across the air–sea interface. Nature 247: 181-184
Luff R, Pohlmann T (1995) Calculation of water exchange times in the ICES-boxes with a eulerian dispersion model using a half-life time approach. Dtsch Hydrogr Z 47(4): 287-299
Ma J, Daggupaty S, Harner T, Li YF (2003) Impacts of lindane usage in the Canadian prairies on the Great Lakes ecosystem, 1. Coupled atmospheric transport model and modelled concentrations in air and soil. Environ Sci Technol 37: 3774-3781
Mackay D, Di Guardo A, Paterson S, Kicsi G, Cowen CE (1996) Evaluating the environmental fate of a variety of types of chemicals using the EQC model. Environ Toxicol Chem 15: 1627-1637
Mackay D, Shiu WY, Ma KC (2000) Physical-Chemical Properties and Environmental Fate Handbook. CD-ROM, Chapman & Hall / CRnetBASE, London
Mackay D (2001) Multimedia Environmental Models: The Fugacity Approach, second ed. Lewis Publishers, Boca Raton
McMahon TA, Denison PJ (1979): Empirical atmospheric deposition parameters – a survey. Atmos Environ 13: 571-585
Malanichev A, Mantseva E, Shatalov V, Strukov B, Vulykh N (2004) Numerical evaluation of the PCB transport over the Northern hemisphere. Environ Pollut 128: 279-289
Moll A (1998) Regional distribution of primary production in the North Sea simulated by a three-dimensional model. J Mar Systems 16: 151-170
NLÖ (2005) Niedersächsisches Landesamt für Ökologie, http://www.nloe.de/
Oehme M (1991) Dispersion and transport paths of toxic persis-tent organochlorines to the Arctic - levels and consequences. Sci Total Environ 106: 43–53
Olsson K (2002) Arctic surface ocean HCH data for model validation and scenario testing. Report to the Norwegian Ministry of Environment, Transport programme. Phase II, APN- 414. 01.2271, 29, Begrenset
OSPAR (2002) OSPAR Commission for the Protection of the Marine Environment of the North-East Atlantic Quality Status Report 2000. Region II – Greater North Sea, OSPAR Commission London
Paasivirta J, Sinkkonen S, Mikkelson M, Raantio T, Wania F (1999) Estimation of vapor pressures, solubilities and Henry's law constants of selected persistent organic pollutants as functions of temperature. Chemosphere 39: 811-832
Pacyna JM, Voldner E, Keeler GJ, Evans G (eds) (1993) First Workshop on Emissions and Modelling of Atmospheric Transport of Persistent Organic Pollutants and Heavy Metals. EMEP/CCC-Report 7/93, Norwegian Institute for Air Research, Lillestrøm
Pacyna JM (1999) Final Report for Project POPCYCLING-Baltic. EU DGXII, Environment and Climate Program ENV4-CT96-0214, CD-rom, NILU
Palm A, Cousins I, Gustafsson Ö, Axelman J, Grunder K, Broman D, Brorström-Lunden E (2004) Evaluation of sequentially-coupled POP fluxes estimated from simultaneous measurements in multiple compartments of an air-water-sediment system. Environ Pollut 128: 85-97
Pankow JF (1987) Review and comparative analysis of the theories on partitioning between the gas and aerosol particulate phases in the atmosphere. Atmos Environ 21: 2275-2283
Pätsch J, Kühn W, Radach G, Casiano S, Gonzalez JM, Davila M, Neuer S, Freudenthal T, Llinas O (2002) Interannual variability of carbon fluxes at the North Atlantic station ESTOC. Deep-Sea Research II 49: 253-288

Pejrup M, Valeur J, Jensen A (1996) Vertical fluxes of particulate matter in Aarhus Bight, Denmark. Cont Shelf Res 16: 1047-1064

Pekar M, Pavlova N, Erdman L, Ilyin I, Strukov B, Gusev A, Dutchak S (1998) Long-range transport of selected persistent organic pollutants. Part I: development of transport models for lindane, polychlorinated biphenys, benzo(a)pyrene. EMEP/MSC-E Report 2/98, EMEP/MSC-E, Moscow

Pohlmann T (1987) Validation of a three dimensional dispersion model for ^{137}Cs in the North European Shelf Sea. ICES CM, C: 34

Pohlmann T, Puls W (1994) Currents and transport in water. In: Sündermann J (ed) Circulation and Contaminant Fluxes in the North Sea. Springer, Berlin Heidelberg New York, pp 345-402

Pohlmann T (1996) Predicting the thermocline in a circulation model of the North Sea. Part I: Model description, calibration, and verification. Cont Shelf Res 7: 131-146

Prest I, Jefferies DJ, Moore NW (1970) Polychlorinated biphenyls in wild birds in Britain and their avian toxicity. Environ Pollut 1: 3–26

Puls W, Doerffer R, Sündermann J (1994) Numerical simulation and satellite observations of suspended matter in the North Sea. IEEE J Ocean Engin 19: 3-9

Ridal JJ, Kerman B, Durham L, Fox ME (1996) Seasonality of air-water fluxes of hexachlorocyclohexanes in lake Ontario. Environ Sci Technol 30: 852-858

Sahsuvar L, Helm P, Jantunen L, Bidleman TF (2003) Henry's law constants for α-, β-, and γ-hexachlorocyclohexanes (HCHs) as a function of temperature and revised estimates of gas exchange in Arctic regions. Atmos Environ 37: 983-992

Scheringer M (1997) Characterization of the environmental distribution behavior of organic chemicals by means of persistence and spatial range. Environ Sci Technol 31(10): 2891-2897

Scheringer M, Stroebe M, Wania F, Wegmann F, Hungerbühler K (2004) The effect of export to the deep sea on the lon-range transport potential of persistent organic pollutants. Environ Sci Pollut Res, 11: 41–48

Schlünzen KH, Stahlschmidt T, Rebers A, Niemeier U, Kriews M, Dannecker W (1997) Atmospheric input of lead into the German Bight - A high resolution measurement and model case study for April 23rd to 30th, 1991. Mar Ecol Prog Ser 156: 299-309

Schulz-Bull DE, Petrick G, Bruhn R, Duinker JC (1998) Chlorobiphenyls (PCB) and PAHs in water masses of the northern North Atlantic. Mar Chem 61: 101–114

Schwarzenbach RE, Gschwend PM, Imboden DM (1993) Environmental Organic Chemistry. Wiley, New York

Semeena VS, Lammel G (2003) Effects of various scenarios of entry of DDT and γ-HCH on the global environmental fate as predicted by a multicompartment chemistry-transport model. Fresenius Environ Bull 12: 925-939

Semeena VS, Lammel G (2005) The significance of the grasshopper effect on the atmospheric distribution of persistent organic substances. Geophys Res Lett doi:10.1029/2004GL022229

Skoglund RS, Stange K, Swackhamer DL (1996) A kinetics model for predicting the accumulation of PCBs in phytoplankton. Environ Sci Technol 30: 2113-2120

Skoglund RS, Swackhamer DL (1999) Evidence for the use of organic carbon as the sorbing matrix in the modelling of PCB accumulation in phytoplankton. Environ Sci Technol 33: 1516-1519

Slinn WGN (1983) A potpourri of deposition and resuspension questions. In: Pruppacher HR, Semonin RG, Slinn WGN (eds) Precipitation Scavenging, Dry Deposition and Resuspension. Elsevier, New York, pp 1361-1416

Soulsby R (1997) Dynamics of Marine Sands. Tomas Telford, London

SRU, The German Advisory Council on the Environment (2004) Marine Environment Protection for the North and Baltic Seas. Special Report, NOMOS, Baden-Baden

Strand A, Hov O (1996) A model strategy for the simulation of chlorinated hydrocarbon distribution in the global environment. Water Air Soil Pollut 86: 283-316

Sundqvist KL, Wingfors H, Brorström-Lundén E, Wiberg K (2004) Air–sea gas exchange of HCHs and PCBs and enantiomers of α-HCH in the Kattegat Sea region. Environ Pollut 128: 73-83

Sündermann J, Puls W (1990) Modelling of suspended sediment dispersion and related transport of lead in the North Sea. Mitt. Geol.-Paläont. Institut Univ. Hamburg 69: 143-155

Sündermann J, (ed) (1994) Circulation and Contaminant Fluxes in the North Sea. Springer, Berlin Heidelberg New York

Sündermann J, Radach G (1997) Fluxes and budgets of contaminants in the German Bight. Marine Pollution Bulletin 34: 395-397

Sündermann J, Beddig S, Radach G, Schlünzen H (1993) The North Sea – Problems and Research Needs. Centre for Marine and Climate Research, University of Hamburg

Swackhamer DL, Skoglund RS (1993) Bioaccumulation of PCBs by algae: kinetics versus equilibrium. Environ Toxicol Chem 12: 831–838

Theobald N, Gaul H, Ziebarth U (1996) Verteilung von organischen Schadstoffen in der Nordsee und angrenzenden Seegebieten. Dtsch Hydrogr Z Suppl 6: 81-93

UNEP (2003) Regionally based assessment of persistent toxic substances. Global Report, UNEP Chemicals, Geneva

Van Jaarsveld JA, van Pul WAJ, de Leeuw FAAM (1997) Modelling transport and deposition of persistent organic pollutants in the European region. Atmos Environ 31: 1011-1024

Van de Meent D, de Bruijn J (1995) A modeling procedure to evaluate the coherence of independently derived environmental quality objectives for air, water and soil. Environ Toxicol Chem 14: 177-186

Van der Zee C, Chou L (2005) Seasonal cycling of phosphorus in the southern bight of the North Sea. Biogeosciences 2: 27-42

Van Pul WAJ, de Leeuw FAAM, van Jaarsveld JA, Sliggers CJ (1997) The atmospheric transport potential of substances. Report 259101005, RIVM, Bilthoven

Wania F, Mackay D (1995) A global distribution model for persistent organic chemicals. Sci Total Environ 160/161: 211-232

Wania F, Mackay D (1999) Global chemical fate of alpha-hexachlorocyclohexane. 2. Use of a global distribution model for mass balancing, source apportionment, and trend predictions. Environ Toxicol Chem 18: 1400-1407

Wania F, Persson J, Di Guardo A, McLachlan MS (2000) The POPCYCLING-Baltic Model. A non-steady state multicompartment mass balance model of the fate of persistent organic pollutants in the Baltic Sea environment. NILU: OR 10/2000, Kjeller

Wania, F, Broman D, Axelman J, Näf C, Agrell C (2001) A multi-compartmental, multibasin fugacity model describing the fate of PCBs in the Baltic Sea. In: Wulff F, Larsson P, Rahm L (eds). A System Analysis of the Changing Baltic Sea. Springer, Heidelberg, pp 417-447

Wanninkhof R (1992) Relationship between wind speed and gas exchange over the ocean. J Geophys Res 97(C5): 7373-7382

Weigel S, Kuhlmann J, Hühnerfuss H (2002) Drugs and personal care products as ubiquitous pollutants: occurrence and distribution of chlofibric acid, caffeine and DEET in the North Sea. Sci Total Environ 295: 131-141

v. Westernhagen H, Dethlefsen V, Haarich M (2000) Temporal trends in malformations of pelagic fish emryos from the southern North Sea in relation to anthropogenic xenobiotics. ICES Annual Science Conference, CM 2000/S: 01

Whitman WG (1923) The two-film theory of gas absorption. Chem Metall Eng 29: 146-150

WHO (2003) Joint WHO/Convention Task Force on the Health Aspects of Air Pollution, Helath Risks of Persistent Organic Pollutants from Long-Range Transboundary Air Polution. WHO, Geneva

Wiesner MG, Haake B, Wirth H (1990) Organic facies of surface sediments in the North Sea. Org Geochem 15(4): 419-432

Willet KL, Ulrich EM, Hites RA (1998) Differential toxicity and environmental fates of hexachlorocyclohexane isomers. Environ Sci Technol 32: 2197-2207

WMO (1997) Report and Proceedings of the Workshop on the Assessment of EMEP Activities Concerning Heavy Metals and Persistent Organic Pollutants and their Further Development. Vol I and II. Varygina M, Soudine A (eds) WMO-GAW/EMEP/MSC-E Report 1/97, WMO, Geneva

Index

About the International Max Planck Research School for Maritime Affairs at the University of Hamburg

The International Max Planck Research School for Maritime Affairs at the University of Hamburg was established by the Max Planck Society for the Advancement of Science, in co-operation with the Max Planck Institute for Foreign Private Law and Private International Law (Hamburg), the Max Planck Institute for Comparative Foreign Public Law and International Law (Heidelberg), the Max Planck Institute for Meteorology (Hamburg) and the University of Hamburg. The School's research is focused on the legal, economic, and geophysical aspects of the use, protection, and organization of the oceans. Its researchers work in the fields of law, economics, and natural sciences. The School provides extensive research capacities as well as its own teaching curriculum. Currently, the School has 12 Directors who determine the general work of the School, act as supervisors for dissertations, elect applicants for the School's PhD-grants, and are the editors of this book series:

Prof. Dr. Dr. h.c. Jürgen Basedow is Director of the Max Planck Institute for Foreign Private Law and Private International Law; *Prof. Dr. Peter Ehlers* is the Director of the German Federal Maritime and Hydrographic Agency; *Prof. Dr. Dr. h.c. Hartmut Graßl* is Director of the Max Planck Institute for Meteorology; *Prof. Dr. Hans-Joachim Koch* is Managing Director of the Seminar of Environmental Law of the Faculty of Law at the University of Hamburg; *Prof. Dr. Rainer Lagoni* is Managing Director of the Institute of Maritime Law and the Law of the Sea at the University of Hamburg; *PD Dr. Gerhard Lammel* is Senior Scientist at the Max Planck Institute for Meteorology; *Prof. Dr. Ulrich Magnus* is Managing Director of the Seminar of Foreign Law and Private International Law at the University of Hamburg; *Prof. Dr. Peter Mankowski* is Director of the Seminar of Foreign and Private International Law at the University of Hamburg; *Prof. Dr. Marian Paschke* is Director of the Institute of Maritime Law and the Law of the Sea at the University of Hamburg; *Prof. Dr. Jürgen Sündermann* is Director at the Center for Marine and Climate Research at the University of Hamburg; *Prof. Dr. Richard Tol* is Director of the Research Unit Sustainability and Global Change at the University of Hamburg; *Prof. Dr. Dr. h.c. Rüdiger Wolfrum* is Director at the Max Planck Institute for Comparative Foreign Public Law and International Law and a judge at the International Tribunal for the Law of the Sea.

At present, *Prof. Dr. Dr. h.c. Jürgen Basedow* and *Prof. Dr. Ulrich Magnus* serve as speakers of the International Max Planck Research School for Maritime Affairs at the University of Hamburg.